REPLICATOR DYNAMICS WITH ALTERNATE GROWTH FUNCTIONS, DELAY, AND QUASIPERIODIC FORCING

A Dissertation

Presented to the Faculty of the Graduate School

of Cornell University

in Partial Fulfillment of the Requirements for the Degree of

Doctor of Philosophy

by

Elizabeth Wesson

May 2015

REPLICATOR DYNAMICS WITH ALTERNATE GROWTH FUNCTIONS, DELAY, AND QUASIPERIODIC FORCING

Elizabeth Wesson, Ph.D.

Cornell University 2015

Evolutionary dynamics combines game theory and nonlinear dynamics to model competition in biological and social situations. The replicator equation is a standard paradigm in evolutionary dynamics. The growth rate of each strategy is its excess fitness: the deviation of its fitness from the average. The game-theoretic aspect of the model lies in the choice of fitness function, which is determined by a payoff matrix. Two well-known replicator systems are the three-strategy Rock-Paper-Scissors game and the two-strategy Hawk-Dove game. In this work, we analyze the dynamics of replicator systems with three different types of modifications.

The first generalization of the replicator model is given by considering alternate growth functions. We find that in the Rock-Paper-Scissors game with a logistic growth function, there are several fixed points that do not exist in the standard replicator model. The system exhibits both periodic motion and convergence to attractors.

We also analyze replicator systems with delayed interactions between strategies. We consider a symmetric delay model, in which the fitness of each strategy is its expected payoff delayed by a time interval; and an asymmetric model, in which same-strategy terms appearing in the fitness of a given strategy are not delayed. In both cases, limit cycles arise that cannot occur in the usual replicator model.

Finally, we examine Rock-Paper-Scissors systems with quasiperiodic forcing of the payoff coefficients. This model may represent systems in which the competition is affected by cyclical processes on different time-scales. We find that the stability of the equilibrium state depends sensitively on the two forcing frequencies; in fact, the region of stability has fractal boundary.

BIOGRAPHICAL SKETCH

There is no independent evidence that Elizabeth Wesson exists.

This document is dedicated to perfecting its omelet-flipping technique.

ACKNOWLEDGEMENTS

This work would not have been possible without the guidance, help and patience of my advisor, Richard Rand.

Thanks, also, to the really improbable number of people whose contributions got me here and kept me going.

TABLE OF CONTENTS

LIST OF FIGURES

CHAPTER 1

INTRODUCTION: THE REPLICATOR EQUATION

Evolutionary game theory models the evolution of competing strategies within a population by combining the classical economic tools of game theory with differential equations [5]. The most common approach focuses on the relative frequencies of different strategies in a population using the replicator equation,

$$\dot{x}_i = x_i(f_i - \phi), \qquad i = 1, \ldots, n \tag{1.1}$$

where x_i is the frequency of (fraction of the population using) strategy i, $f_i(x_1, \ldots, x_n)$ is the fitness of strategy i, and $\phi = \sum f_i x_i$ is the average fitness across the population.

Hofbauer and Sigmund [5] have shown that the replicator equation can be derived from the Lotka-Volterra equation, the classic predator-prey model of species abundances (rather than frequencies). The n-strategy replicator equation is equivalent to the Lotka-Volterra system with $n - 1$ species. The derivation, however, requires a rescaling of time, and the correspondence between species and strategies is not one-to-one. See section 1.1.

Furthermore, it has been shown [14, 15] that the replicator equation can be derived from the exponential growth model

$$\dot{\xi}_i = \xi_i g_i, \qquad i = 1, \ldots, n \tag{1.2}$$

where ξ_i is the abundance of strategy i, and $g_i(\xi_1, \ldots, \xi_n)$ the fitness of strategy i. The equivalence simply uses the change of variables $x_i = \xi_i/p$ where p is the total population, with the assumption that the fitness functions depend only on the frequencies, and not on the populations directly. See section 1.2.

The game-theoretic component of the replicator equation lies in the choice of fitness functions. Take the payoff matrix $A = (a_{ij})$, where a_{ij} is the expected fitness gain for strategy i when it interacts with strategy j. Then the expected total fitness f_i is the expected payoff of strategy i when interacting with each strategy, weighted by the other strategies' frequencies:

$$f_i = (A \cdot \mathbf{x})_i. \tag{1.3}$$

where

$$\mathbf{x} = (x_1, \ldots, x_n). \tag{1.4}$$

In this work, we analyze the dynamics of two- and three-strategy replicator systems with three different types of generalizations.

The class of three-strategy systems considered here is Rock-Paper-Scissors (RPS) games. In RPS games, each strategy is neutral versus itself, has a positive expected payoff versus one of the other strategies, and a negative expected payoff against the third. They are characterized by payoff matrices of the form

$$A = \begin{pmatrix} 0 & -a_2 & b_3 \\ b_1 & 0 & -a_1 \\ -a_3 & b_2 & 0 \end{pmatrix} \tag{1.5}$$

where $a_1, \ldots, b_3$ are all positive.

The first generalization of the replicator model (Chapter 2) is given by considering alternate growth functions. We find that in the Rock-Paper-Scissors game with a logistic growth function, there are several fixed points that do not exist in the standard replicator model. The system exhibits both periodic motion and convergence to attractors.

We also analyze replicator systems with delayed interactions between strategies. We consider a symmetric delay model, in which the fitness of each strategy is its expected payoff delayed by a time interval; and an asymmetric model, in which same-strategy terms appearing in the fitness of a given strategy are not delayed. In Chapter 3, we analyze Rock-Paper-Scissors systems with symmetric delay. In Chapter 4, we analyze two-strategy systems under a linear homotopy between symmetric and asymmetric delay. In both cases, limit cycles arise that cannot occur in the usual replicator model.

Finally, we examine Rock-Paper-Scissors systems with quasiperiodic forcing of the payoff coefficients (Chapter 5). This model may represent systems in which the competition is affected by cyclical processes on different time-scales. We find that the stability of the equilibrium state depends sensitively on the two forcing frequencies; in fact, the region of stability has fractal boundary.

1.1 Derivation of replicator equation from Lotka-Volterra

We present the proof given by Hofbauer and Sigmund [5] that the n-strategy replicator equation

$$\dot{x}_i = x_i((A\mathbf{x})_i - \mathbf{x} \cdot A\mathbf{x}), \quad i = 1, \ldots, n \tag{1.6}$$

is orbitally equivalent to the $n-1$ species Lotka-Volterra equation

$$\dot{y}_i = y_i \left(r_i + \sum_{j=1}^{n-1} b_{ij} y_j \right), \quad i = 1, \ldots, n-1 \tag{1.7}$$

where $A = (a_{ij})$ is the payoff matrix, and where the coefficients in Eq. (1.7) are given by

$$r_i = a_{in} - a_{nn}, \quad b_{ij} = a_{ij} - a_{nj}. \tag{1.8}$$

That is, there is a differentiable, invertible map between the orbits of the former and the orbits of the latter.

It is reasonable that such an equivalence exists because the $n-1$ species Lotka-Volterra dynamics occur in $\mathbb{R}_+^{n-1}$, and the n-strategy replicator dynamics occur in the n-simplex, which is an $n-1$ dimensional manifold.

Proof:

First, define $y_n \equiv 1$, and consider the mapping $\mathbf{y} \mapsto \mathbf{x}$ given by

$$x_i = \frac{y_i}{\sum_{j=1}^{n} y_j}, \quad i = 1, \ldots, n \tag{1.9}$$

That is, $\mathbf{x}$ is a normalized version of the augmented $\mathbf{y}$ vector.

Notice that for any i, k

$$\frac{x_i}{x_k} = \frac{y_i}{y_k} \tag{1.10}$$

so in particular (since $y_n = 1$ identically)

$$y_i = \frac{y_i}{y_n} = \frac{x_i}{x_n}. \tag{1.11}$$

This gives an inverse mapping $\mathbf{x} \mapsto \mathbf{y}$.

Now, by the quotient rule (assuming $i \neq n$)

$$\frac{dy_i}{dt} = \frac{d}{dt}\left(\frac{x_i}{x_n}\right) = \frac{x_n \dot{x}_i - x_i \dot{x}_n}{x_n^2} \tag{1.12}$$

$$= \frac{x_n x_i((A\mathbf{x})_i - \mathbf{x} \cdot A\mathbf{x}) - x_i x_n((A\mathbf{x})_n - \mathbf{x} \cdot A\mathbf{x})}{x_n^2} \tag{1.13}$$

$$= \left(\frac{x_i}{x_n}\right)[(A\mathbf{x})_i - (A\mathbf{x})_n] \tag{1.14}$$

Using the identity $y_j = x_j/x_n$, this can be written as

$$\dot{y}_i = y_i \left(\sum_{j=1}^{n} (a_{ij} - a_{nj}) x_j \right) \tag{1.15}$$

$$= y_i \left(\sum_{j=1}^{n} (a_{ij} - a_{nj}) y_j x_n \right) \tag{1.16}$$

$$= y_i \left(r_i + \sum_{j=1}^{n-1} b_{ij} y_j \right) x_n \tag{1.17}$$

where in the last line we have written the $j = n$ term separately and used the hypothesis that $y_n = 1$.

It remains only to apply a change in velocity. Specifically, introduce a stretched time variable τ such that

$$d\tau = x_n dt \tag{1.18}$$

We know that $0 \leq x_n \leq 1$, so the rescaling of time is monotonic. Then we have

$$\frac{dy_i}{dt} = \frac{dy_i}{d\tau} x_n \tag{1.19}$$

so

$$\frac{dy_i}{d\tau} = y_i \left(r_i + \sum_{j=1}^{n-1} b_{ij} y_j \right), \quad i = 1, \ldots, n-1 \tag{1.20}$$

This shows that Eq. (1.20) is equivalent to Eq. (1.6) under the differentiable, invertible change of variables given by Eq. (1.9). Comparing this to Eq. (1.7), we see that the only difference is that (1.7) has a derivative with respect to t, while (1.20) has a derivative with respect to τ. Since τ is a monotonic rescaling of t, the orbits of the two differential equations are identical.

This shows that the n-strategy replicator equation is orbitally equivalent to the $n-1$ species Lotka-Volterra equation.

1.2 Derivation of the replicator equation

Consider an exponential model of population growth,

$$\dot{\xi}_i = \xi_i g_i \quad (i = 1, \ldots, n) \tag{1.21}$$

where ξ_i is a real-valued function that approximates the population of strategy i and $g_i(\xi_1, \ldots, \xi_n)$ is the fitness of that strategy. The replicator equation [14] results from equation (1.21) by changing variables from the populations ξ_i to the relative abundances, defined as $x_i \equiv \xi_i/p$ where p is the total population:

$$p(t) = \sum_i \xi_i(t). \tag{1.22}$$

We see that

$$\dot{p} = \sum_i \dot{\xi}_i = \sum_i \xi_i g_i \tag{1.23}$$

$$= p \sum_i \frac{\xi_i}{p} g_i = p \sum_i x_i g_i \tag{1.24}$$

$$= p\phi \tag{1.25}$$

where $\phi \equiv \sum_i x_i g_i$ is the average fitness of the whole population.

By the product rule,

$$\dot{x}_i = \frac{\dot{\xi}_i}{p} - \frac{\xi_i \dot{p}}{p^2} \tag{1.26}$$

$$= \frac{\xi_i}{p} g_i - \frac{\xi_i}{p} \frac{\dot{p}}{p} \tag{1.27}$$

$$= x_i \left(g_i - \phi \right). \tag{1.28}$$

Therefore

$$\sum_i \dot{x}_i = \sum_i x_i g_i - \phi \sum_i x_i \tag{1.29}$$

$$= \sum_i x_i g_i - \sum_j x_j g_j \sum_i x_i. \tag{1.30}$$

So, using the fact that

$$\sum_i x_i = \frac{\sum_i \xi_i}{p} = \frac{p}{p} \equiv 1 \tag{1.31}$$

equation (1.30) reduces to the identity

$$\sum_i \dot{x}_i = 0. \tag{1.32}$$

The fitness of a strategy is assumed to depend only on the relative abundance of each strategy in the overall population, since the model only seeks to capture the effect of competition between strategies, not any environmental or other factors. Therefore, we assume that g_i has the form

$$g_i(\xi_1, \ldots, \xi_n) = f_i\left(\frac{\xi_1}{p}, \ldots, \frac{\xi_n}{p}\right) = f_i(x_1, \ldots, x_n). \tag{1.33}$$

Under this assumption, equation (1.28) is the replicator equation,

$$\dot{x}_i = x_i(f_i - \phi), \tag{1.34}$$

where ϕ is now expressed entirely in terms of the x_i, as

$$\phi = \sum_i x_i f_i. \tag{1.35}$$

Mathematically, ϕ is a coupling term that introduces dependence on the abundance and fitness of other strategies.

CHAPTER 2

ROCK-PAPER-SCISSORS WITH ALTERNATE GROWTH FUNCTION

2.1 Introduction

Consider a biological or social system in which the rate of change of a given strategy's frequency is described by a natural growth function g, scaled by the excess fitness of that strategy.

In this chapter, we generalize the replicator model by replacing the base model $\dot{x}_i = x_i f_i$ by $\dot{x}_i = g(x_i) f_i$, where g is a natural growth function. The replicator equation for each strategy becomes

$$\dot{x}_i = g(x_i)(f_i - \phi), \tag{2.1}$$

where ϕ is now a modified average fitness, again chosen so that $\sum x_i = 1$.

The game-theoretic component of this model lies in the choice of fitness functions. Take the payoff matrix A, whose (i, j)-th entry is the expected reward for strategy i when it competes with strategy j. The fitness f_i of strategy i is then $(A \cdot x)_i$, where $x \in R^n$ is the vector of frequencies x_i. In this work, we use a payoff matrix representing a game analogous to rock-paper-scissors (RPS): there are three strategies, each of which has an advantage versus one other and a disadvantage versus the third. Each strategy is neutral versus itself.

Analysis of the resulting dynamical system is presented. We find that for the logistic model

$$g(x) = x - ax^2, \tag{2.2}$$

with appropriate choices of the parameter a, there are multiple fixed points of the system that do not exist in the usual model $g(x) = x$. We will show that when A is chosen so that the RPS game is zero-sum, there are 13 equilibria: one neutrally stable equilibrium with all three strategies surviving; three saddle points with all three strategies surviving; three saddles with only one surviving strategy; and three attracting and three repelling fixed points where two strategies survive. The system exhibits both periodic motion and convergence to attractors. We analyze the symmetries of this system, and its bifurcations as the entries of A vary.

This alternate formulation may be useful in modeling natural or social systems that are not adequately described by the usual replicator dynamics.

2.2 Derivation

Let us review the usual replicator dynamics. We have $f_i = f_i(x)$, where $f_i(x) = (A \cdot x)_i$, where A is the payoff matrix. The average payoff is thus $\phi = \sum_i x_i f_i$, and the change in frequency of strategy i is given by the product of the frequency x_i and its payoff relative to the average. In this model, all population-dependence of the effectiveness (hence growth rate) of strategy i is accounted for by f_i. However, we wish our fitness functions f_i to represent the game-theoretic payoff of individual-level competition. We therefore include some of the population dependence in a growth function $g(x_i)$; this represents the growth rate of the raw population using strategy i, in the absence of competition. Thus the expected population-level payoff of strategy i is $g(x_i) f_i$, and

the average population-level payoff is

$$\phi = \frac{\sum_i g(x_i) f_i}{\sum_i g(x_i)}. \tag{2.3}$$

We require that in this model, ϕ (and hence $\dot{x}$) is only defined for growth functions g such that the denominator does not vanish for any x in the region of interest. With that caveat, using this definition of ϕ, the replicator equation becomes

$$\dot{x}_i = g(x_i)(f_i - \phi), \ i = 1, \ldots, n. \tag{2.4}$$

We can verify that

$$\begin{aligned} \sum_i \dot{x}_i &= \sum_i g(x_i)(f_i - \phi) \\ &= \sum_i g(x_i) f_i - \sum_i g(x_i) \frac{\sum_i g(x_i) f_i}{\sum_i g(x_i)} \\ &= 0 \end{aligned} \tag{2.5}$$

so the total population over all strategies is constant, and it is valid to say that each x_i represents the *frequency* of strategy i. We will use the term *relative abundance* for x_i whenever there is ambiguity between x_i and the time-frequency of any periodic motion in the dynamics.

2.3 Rock-Paper-Scissors

We consider the game-theoretic case in which $n = 3$ and f_i is given by $f_i(x) = (A \cdot x)_i$, where A is the payoff matrix

$$A = \begin{pmatrix} 0 & -1 & +1 \\ +1 & 0 & -1 \\ -1 & +1 & 0 \end{pmatrix}, \tag{2.6}$$

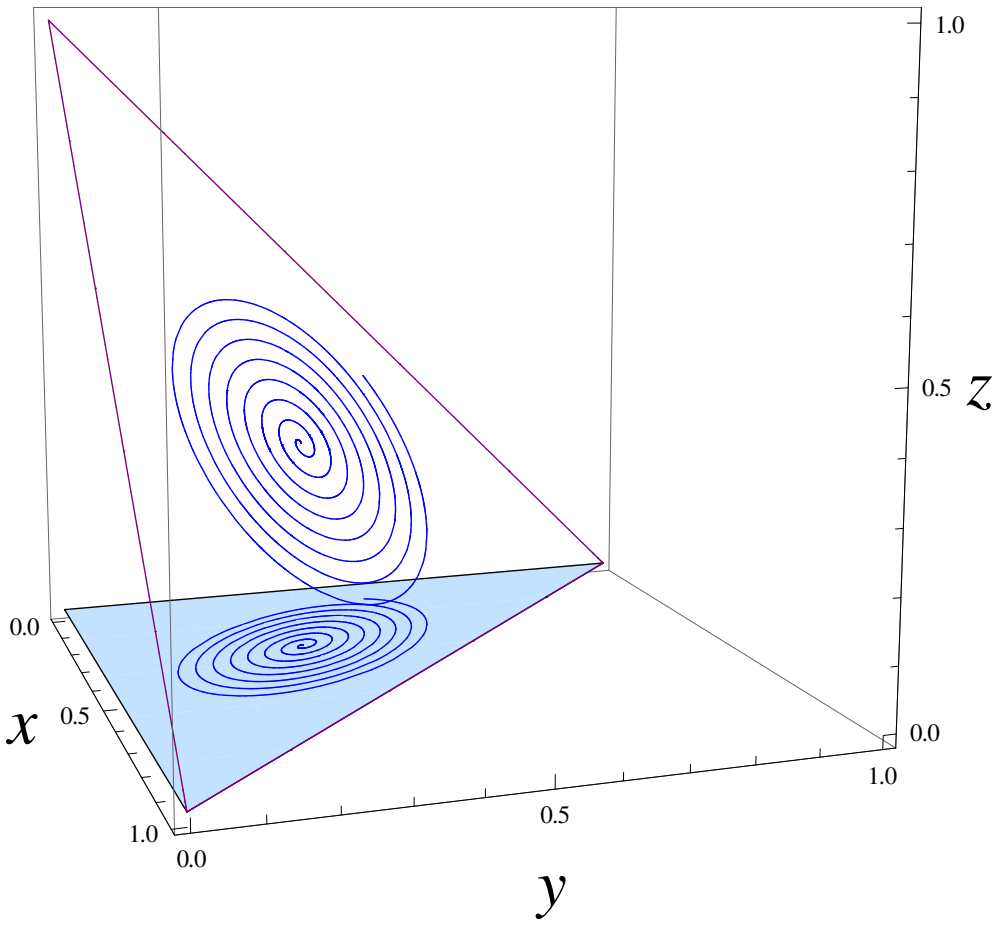

Figure 2.1: A curve in Σ and its projection in T.

representing a zero-sum rock-paper-scissors game. That is, writing (x_1, x_2, x_3) as (x, y, z),

$$f_1 = z - y, \quad f_2 = x - z, \quad f_3 = y - x. \tag{2.7}$$

We note that this model has been shown to be relevant to biological applications [8], [7], and to social interactions [11]. Note that the dynamics of the 3-strategy game takes place on the triangle in R^3 (in fact, the three-dimensional simplex)

$$\Sigma = \left\{(x, y, z) \in R^3 : x + y + z = 1 \text{ and } x, y, z \geq 0\right\}. \tag{2.8}$$

Therefore we can eliminate z using $z = 1 - x - y$. This reduces the problem

to two dimensions, so that (2.4) becomes

$$\dot{x} = \frac{g(x)\left((1-3y)\,g(1-x-y)+(2-3x-3y)\,g(y)\right)}{g(x)+g(y)+g(1-x-y)} \tag{2.9}$$

$$\dot{y} = -\frac{g(y)\left((1-3x)\,g(x)+(2-3x-3y)\,g(1-x-y)\right)}{g(x)+g(y)+g(1-x-y)} \tag{2.10}$$

where we have used ϕ as defined in Eqn (2.3). This vector field is defined on the projection of Σ onto the $x-y$ plane. We will refer to this region as

$$T = \{(x,y) : (x,y,1-x-y) \in \Sigma\}. \tag{2.11}$$

Note that since Σ, the region of interest for the three-dimensional flow, is confined to a plane in R^3, the projection down to T loses no information. See Fig. 2.1.

2.4 Choices of Growth Function

2.4.1 Taking $g(x_i) = x_i/(1+ax_i)$

First, consider the case where the growth function is given by $g(x_i) = \frac{x_i}{1+ax_i}$. This growth function increases monotonically in x_i, leading to dynamics that are qualitatively similar to the standard $g(x_i) = x_i$ case. We find that Eqns. (2.9) and (2.10) become

$$\dot{x} = \frac{-x(-1+x+2y)(-1+3ay(-1+x+y)}{-1+3a^2xy(-1+x+y)+2a(x^2+x(-1+y)+(-1+y)y))} \tag{2.12}$$

$$\dot{y} = \frac{y(-1+2x+y)(-1+3ax(-1+x+y))}{-1+3a^2xy(-1+x+y)+2a(x^2+x(-1+y)+(-1+y)y)} \tag{2.13}$$

Solving $\dot{x} = \dot{y} = 0$, we find that the equilibria are located at the corners of T,

$$(x,y) = (0,0), (0,1), (1,0)$$

and at its center,

$$(x, y) = \left(\frac{1}{3}, \frac{1}{3}\right).$$

Evaluating the Jacobian at each of these points and examining its eigenvalues, we find that the three corner points are saddles, with $\lambda_{1,2} = \pm 1$. The point $\left(\frac{1}{3}, \frac{1}{3}\right)$ is a linear center, with $\lambda_{1,2} = \pm\frac{i\sqrt{3}}{a+3}$. See Figs. 2.2 and 2.3.

As in the case of the standard replicator equation [7], when $g(x) = x/(1+ax)$, the linear center is surrounded by closed periodic orbits. (Although this claim is presented without proof, we will prove it in the next case, $g(x) = x - ax^2$. The proof in this case is largely identical.)

2.4.2 Taking $g\left(x_i\right) = x_i - ax_i^2$

The previous choice of $g\left(x_i\right)$ did not generate qualitatively different behavior from the usual replicator dynamics. However, it turns out that new behavior occurs when we use $g(x) = x - ax^2$ obtained by truncating the Maclaurin series

$$\frac{x}{1+ax} = x\sum_{n=0}^{\infty}(-ax)^n \tag{2.14}$$

after the x^2 term.

Thus we consider the case where the growth function is given by $g\left(x_i\right) = x_i - ax_i^2$. This represents the assumption that in the absence of competition, population x_i would experience logistic growth. In this case, Eqns. (2.9) and (2.10) become

$$\dot{x} = \frac{x\left(ax-1\right)\left(x+2y-1\right)\left(a\left(1+3y\left(y-1\right)+x\left(3y-1\right)\right)-1\right)}{a\left(x^2+y^2+\left(1-x-y\right)^2\right)-1} \tag{2.15}$$

$$\dot{y} = -\frac{y\left(ay-1\right)\left(y+2x-1\right)\left(a\left(1+3x\left(x-1\right)+y\left(3x-1\right)\right)-1\right)}{a\left(x^2+y^2+\left(1-x-y\right)^2\right)-1} \tag{2.16}$$

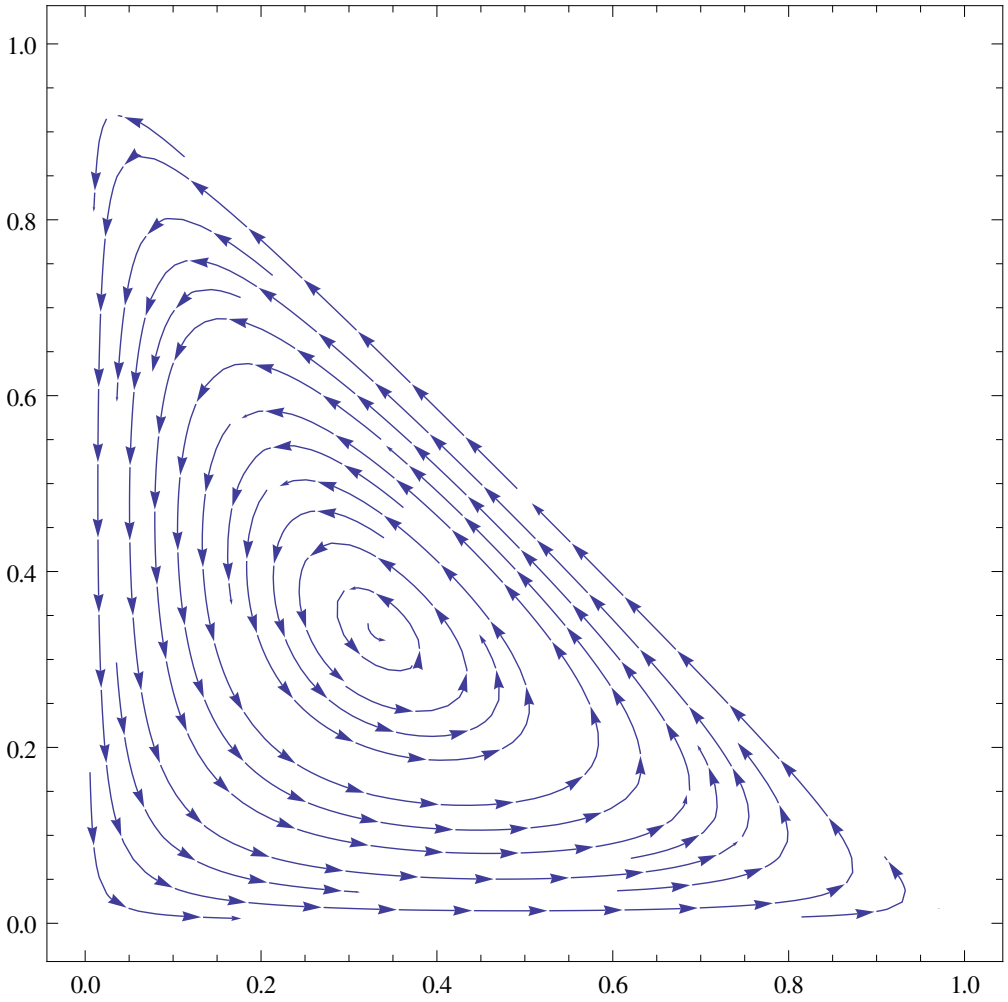

Figure 2.2: Vector field in T for the standard replicator equation $g(x) = x$. The horizontal axis is x and the vertical axis is y.

The denominators vanish when

$$x^2 + y^2 + (1 - x - y)^2 = \frac{1}{a}. \tag{2.17}$$

We reject values of a for which Eqn. (2.17) holds for any $(x, y) \in T$. This happens for $a \in [1, 3]$, so we stipulate that $0 \leq a < 1$ or $a > 3$. Geometrically, the vector field in T is undefined for values of a such that the sphere $x^2 + y^2 + z^2 = \frac{1}{a}$ intersects Σ, Eqn. (2.8).

This system has 13 equilibrium points:

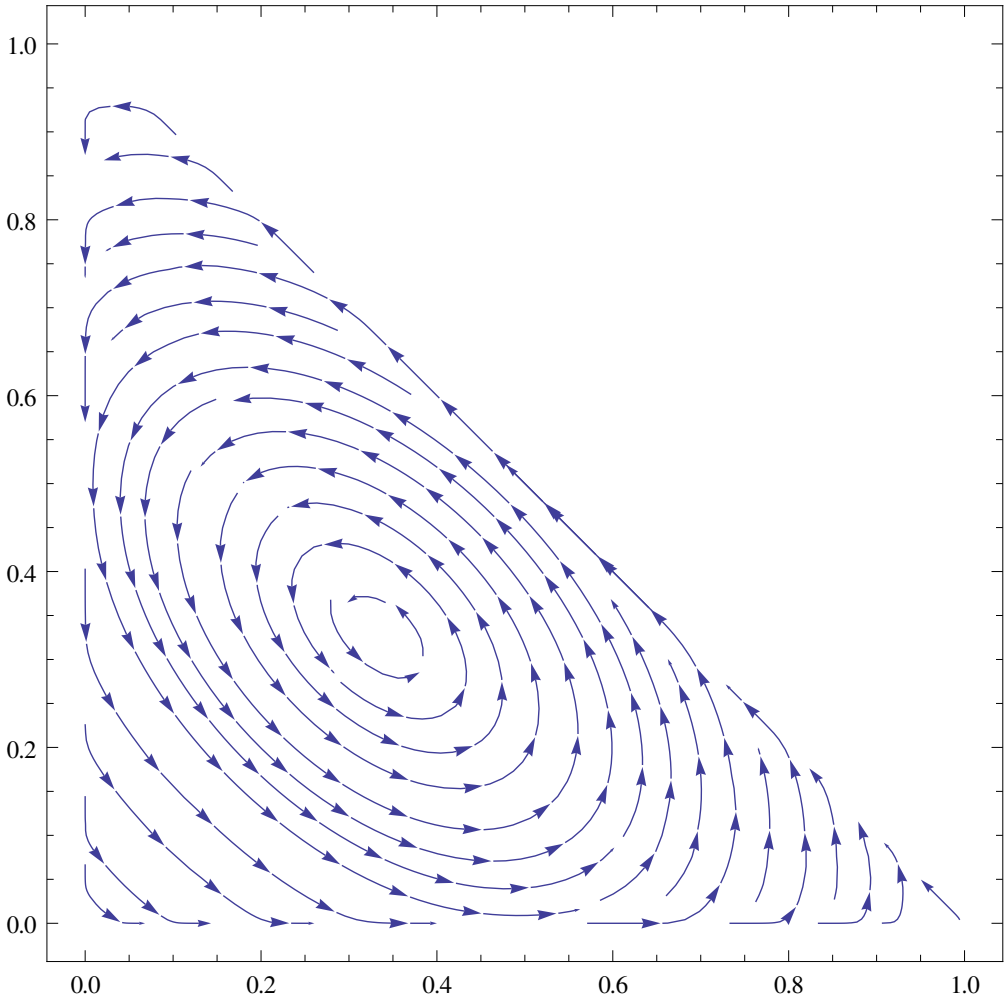

Figure 2.3: Vector field in T for $g(x) = x/(1 + ax)$ with $a = 100$. The axes are as above.

(i) The corners of T

$$(x, y) = (0, 0), (0, 1), (1, 0)$$

(ii) The center of T

$$(x, y) = \left(\frac{1}{3}, \frac{1}{3}\right)$$

(iii) Two points on each of the edges $x = 0$, $y = 0$ and $z = 0$

$$\begin{aligned}(x, y) &= \left(0, \frac{1}{a}\right), \left(0, \frac{a-1}{a}\right) \\ (x, y) &= \left(\frac{1}{a}, 0\right), \left(\frac{a-1}{a}, 0\right) \\ (x, y) &= \left(\frac{1}{a}, \frac{a-1}{a}\right), \left(\frac{a-1}{a}, \frac{1}{a}\right)\end{aligned}$$

(iv) Three points on lines that pass through the center of T

$$(x, y) = \left(\frac{1}{a}, \frac{1}{a}\right), \left(\frac{1}{a}, \frac{a-2}{a}\right), \left(\frac{a-2}{a}, \frac{1}{a}\right)$$

Figure 2.4 shows the location of the equilibria. For $0 \leq a < 1$, only the corners and the center point lie in T, Eqn. (2.11), and the dynamics are qualitatively similar to the Rock-Paper-Scissors game with standard replicator dynamics. Evaluating the Jacobian of $[\dot{x}, \dot{y}]$ at each equilibrium and computing the eigenvalues, we find that $\left(\frac{1}{3}, \frac{1}{3}\right)$ is a linear center and the corner points are saddles.

When $(x, y) = (\frac{1}{3}, \frac{1}{3})$,

$$J = \frac{a-3}{9}\begin{pmatrix} 1 & 2 \\ -2 & -1 \end{pmatrix} \Rightarrow \lambda_{1,2} = \frac{\pm i\,(a-3)}{3\sqrt{3}} \tag{2.18}$$

and when $(x, y) = (0, 0)$,

$$J = \begin{pmatrix} 1 & 0 \\ 0 & -1 \end{pmatrix} \Rightarrow \lambda_{1,2} = \pm 1. \tag{2.19}$$

The stability calculations for the other two corner points are similar. Figure 2.5 shows the vector field and equilibria for $a = \frac{1}{5}$.

For $a > 3$, the dynamics are more interesting. All 13 equilibria lie in T. By symmetry, the three equilibria which lie on lines through the center must be of

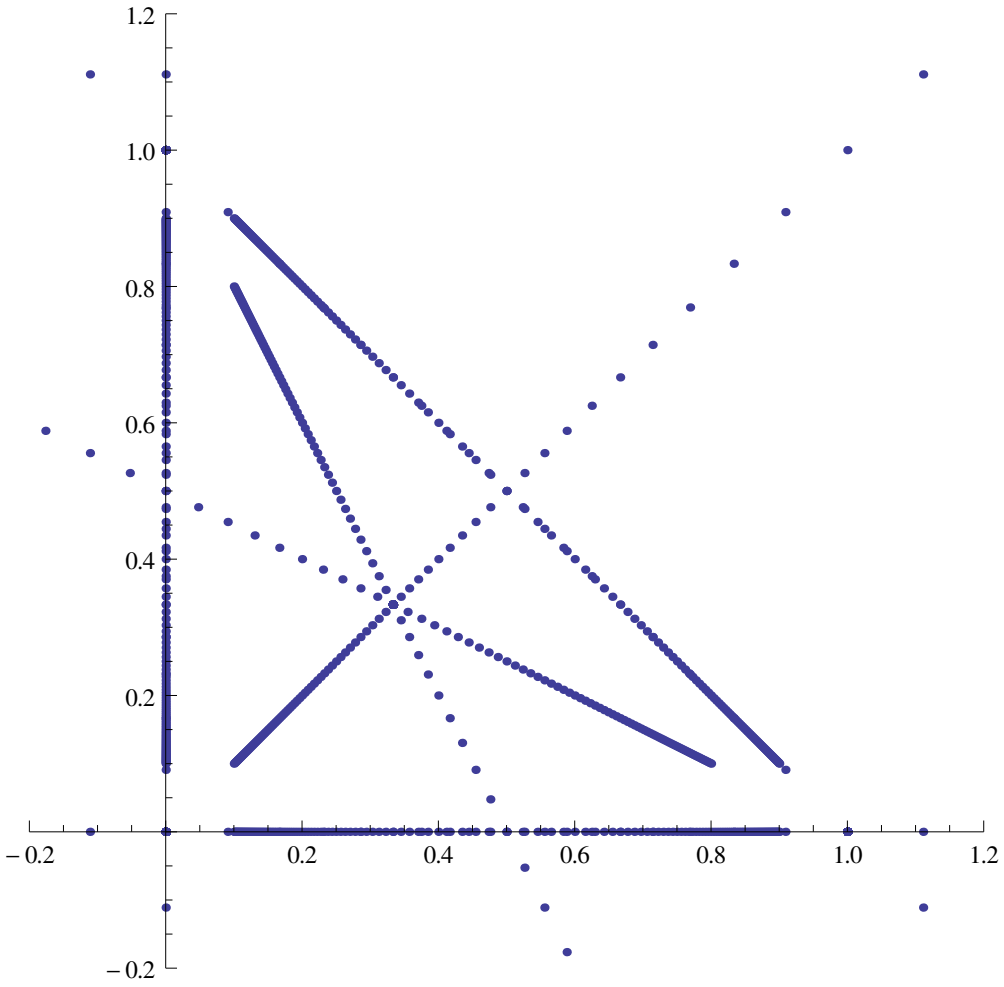

Figure 2.4: Location in the (x, y) plane of the 13 equilibria for $g(x) = x - ax^2$ as a varies from $a = 0.1$ to $a = 10$. As discussed in the text, for $a > 3$ all 13 equilibrium points lie in the region of interest T.

the same type; similarly, the two equilibria on the edge $x = 0$ must be of the

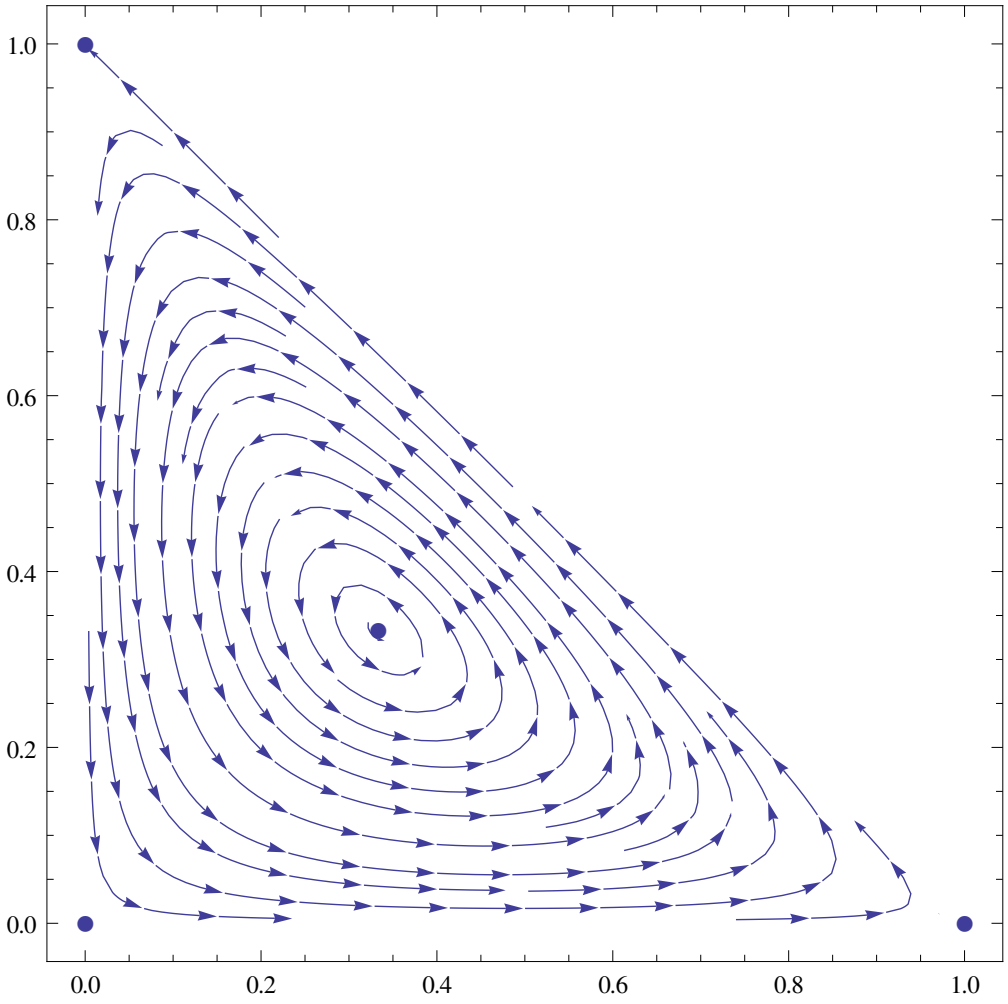

Figure 2.5: Vector field in T for $a = \frac{1}{5}$.

same types as their counterparts on the other two edges.

$$(x, y) = \left(\frac{1}{a}, \frac{1}{a}\right) \quad \Rightarrow \tag{2.20}$$

$$J = \begin{pmatrix} \frac{3}{a} - 1 & 0 \\ 0 & 1 - \frac{a}{3} \end{pmatrix} \Rightarrow \lambda_{1,2} = \pm\left(\frac{3}{a} - 1\right)$$

$$(x, y) = \left(0, \frac{1}{a}\right) \quad \Rightarrow \tag{2.21}$$

$$J = \begin{pmatrix} 1 - \frac{3}{a} & 0 \\ 0 & 1 \end{pmatrix} \Rightarrow \lambda_1 = 1, \lambda_2 = 1 - \frac{3}{a}$$

$$(x, y) = \left(0, 1 - \frac{1}{a}\right) \quad \Rightarrow \tag{2.22}$$

$$J = \begin{pmatrix} \frac{3}{a} - 1 & 0 \\ -\frac{3}{a} & -1 \end{pmatrix} \Rightarrow \lambda_1 = -1, \lambda_2 = \frac{3}{a} - 1.$$

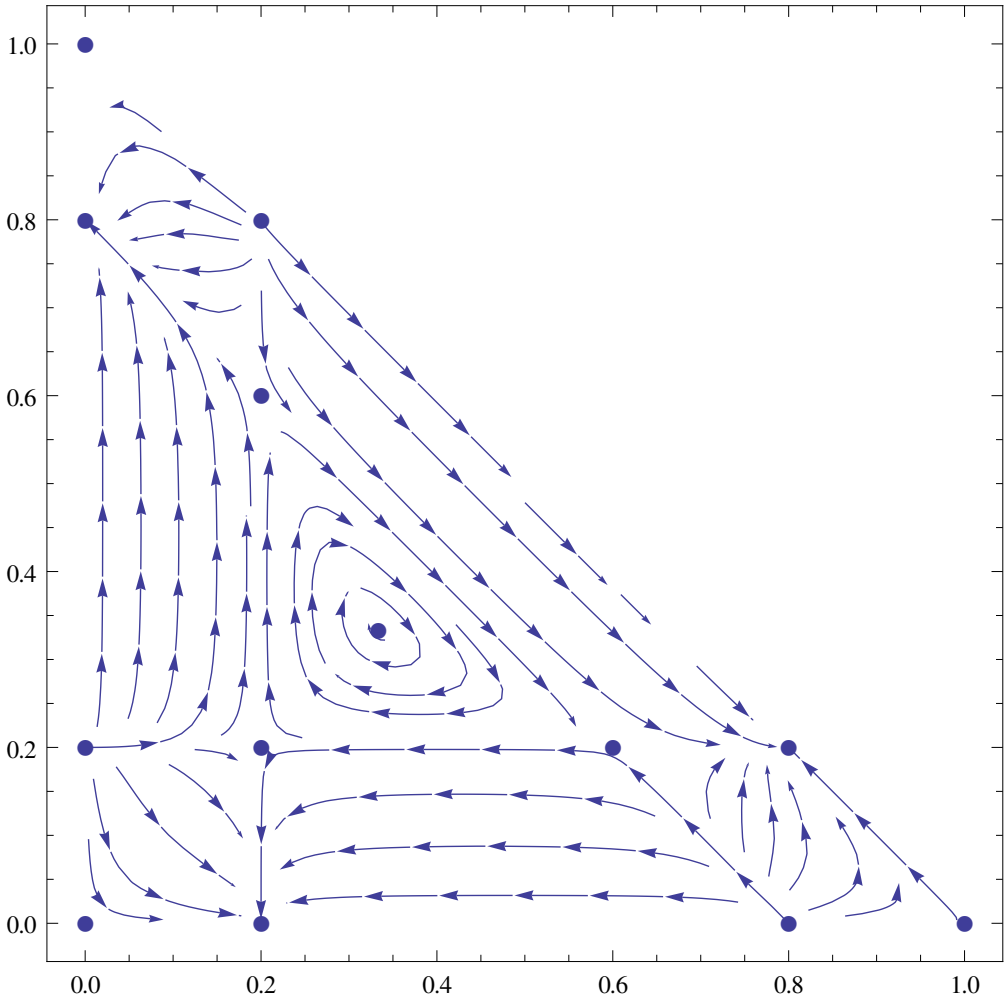

Figure 2.6: Vector field in T for $a = 5$.

Thus the interior equilibria are saddles, and there is a source and a sink on each edge.

Figures 2.6 and 2.7 exhibit another feature of this system: in addition to the boundaries of T, the lines $x = \frac{1}{a}$, $y = \frac{1}{a}$ and $x + y = 1 - \frac{1}{a}$ are also invariant, and for $a > 3$, portions of these lines fall within T. Substituting $x = \frac{1}{a}$ into Eqn.

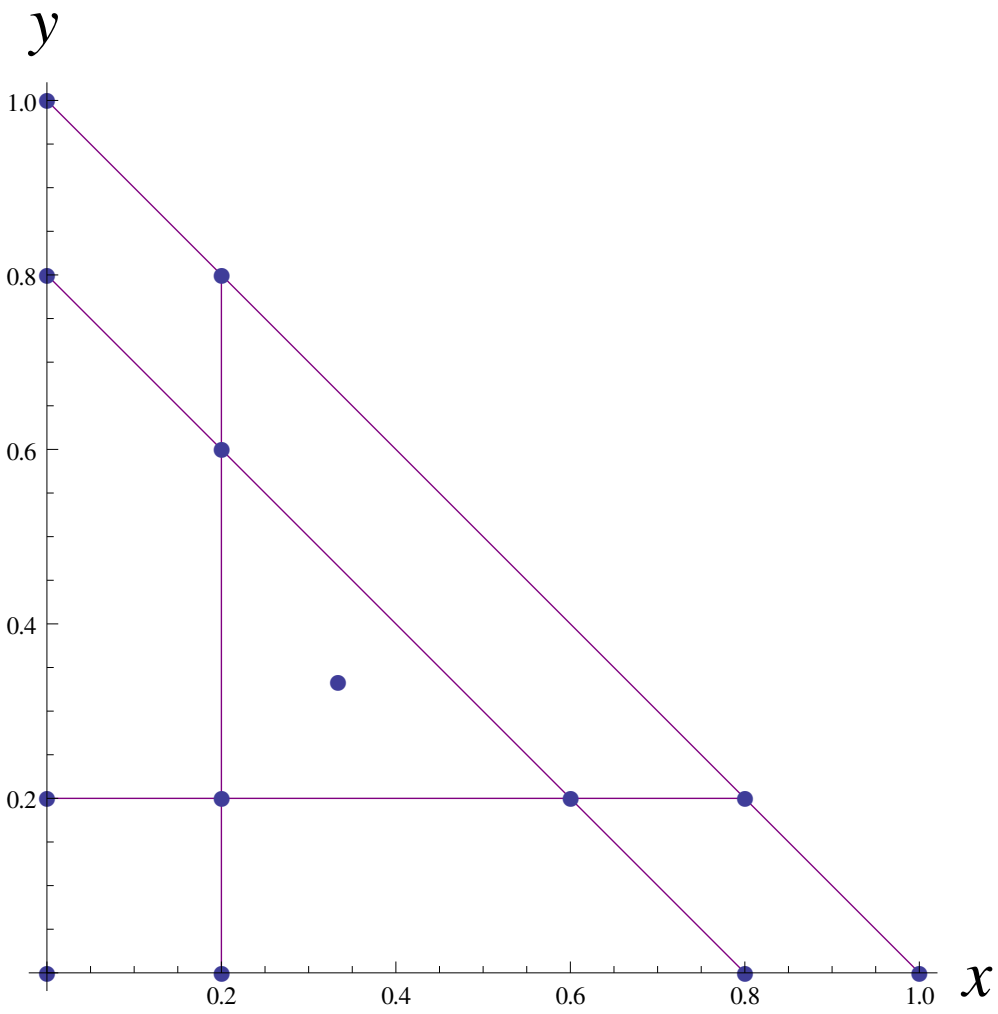

Figure 2.7: Equilibrium points and invariant lines of the system for $a = 5$.

(2.15), we obtain

$$\dot{x} = 0 \tag{2.23}$$

$$\dot{y} = \frac{(y - ay^2)\left(y + \frac{2}{a} - 1\right)\left(a\left(1 + \frac{3}{a}\left(\frac{1}{a} - 1\right) + y\left(\frac{3}{a} - 1\right)\right) - 1\right)}{a\left((\frac{1}{a})^2 + y^2 + \left(1 - \frac{1}{a} - y\right)^2\right) - 1}. \tag{2.24}$$

Similarly, taking $y = \frac{1}{a}$ gives $\dot{y} = 0$. To see that $x + y = 1 - \frac{1}{a}$ is an invariant

line, we take $y = 1 - x - \frac{1}{a}$, so that

$$\dot{x} = \frac{x\,(a-3)\,(1+a\,(x-1))\,(2+a\,(x-1))\,(ax-1)}{a\left(x^2+\left(1-x-\frac{1}{a}\right)^2+\left(\frac{1}{a}\right)^2\right)-1} \tag{2.25}$$

$$\dot{y} = -\frac{x\,(a-3)\,(1+a\,(x-1))\,(2+a\,(x-1))\,(ax-1)}{a\left(x^2+\left(1-x-\frac{1}{a}\right)^2+\left(\frac{1}{a}\right)^2\right)-1} \tag{2.26}$$

and $\dot{x} + \dot{y} = 0$.

Notice that there appear to be periodic orbits about the equilibrium $\left(\frac{1}{3}, \frac{1}{3}\right)$, moving in the opposite direction from before. We will examine this phenomenon more thoroughly in the next section.

2.5 Further examination of the $g\,(x_i) = x_i - ax_i^2$ case

We have observed that the $\left(\frac{1}{3}, \frac{1}{3}\right)$ equilibrium is a linear center, and the orbits about it appear to be periodic. To verify this, we show that there is a degenerate Hopf bifurcation in the more general system

$$\dot{x}_i = g\,(x_i)\,(f_i - \phi\,(x)) = g\,(x_i)\,((A \cdot x)_i - \phi\,(x)) \tag{2.27}$$

where the payoff matrix is

$$A = \begin{pmatrix} 0 & -a_2 & b_3 \\ b_1 & 0 & -a_1 \\ -a_3 & b_2 & 0 \end{pmatrix} \tag{2.28}$$

and $\phi\,(x)$ is defined as before. We substitute this choice of A into Eqn. (2.27), take the Jacobian, and find that when $(x, y, z) = \left(\frac{1}{3}, \frac{1}{3}, \frac{1}{3}\right)$ and $a_1 = \cdots = b_3 = 1$, the eigenvalues are

$$\lambda_{1,2} = \pm\frac{i(a-3)}{3\sqrt{3}}, \quad \lambda_3 = 0. \tag{2.29}$$

Thus there is a Hopf bifurcation at this point in the parameter space, as we might expect from the standard replicator equation [5].

To show that the Hopf bifurcation is in fact degenerate, we follow [2]. First we project the system into the (x, y) plane as before, and make the coordinate translation

$$(x, y) = (u + \frac{1}{3}, v + \frac{1}{3}) \tag{2.30}$$

to move the bifurcation to the origin. We then write the system as

$$\begin{pmatrix} \dot{u} \\ \dot{v} \end{pmatrix} = J \begin{pmatrix} u \\ v \end{pmatrix} + \begin{pmatrix} f(u, v) \\ g(u, v) \end{pmatrix} \tag{2.31}$$

Then we make a coordinate transformation $u = 2r$, $v = -r - s\sqrt{3}$. This gives the normal form

$$\begin{pmatrix} \dot{r} \\ \dot{s} \end{pmatrix} = \begin{pmatrix} 0 & -\omega \\ \omega & 0 \end{pmatrix} \begin{pmatrix} r \\ s \end{pmatrix} + \begin{pmatrix} h(r, s) \\ k(r, s) \end{pmatrix} \tag{2.32}$$

where $\omega = (a - 3)/3\sqrt{3}$, and h and k are not listed for brevity. Finally, we substitute the resulting nonlinear parts into the equation for the cubic stability coefficient (see [2] pp. 150-155)

$$\begin{aligned} c \;=\; & \frac{1}{16}[h_{rrr} + h_{rss} + k_{rrs} + k_{sss}] + \\ & \frac{1}{16\omega}[h_{rs}(h_{rr} + h_{ss}) - k_{rs}(k_{rr} + k_{ss}) - h_{rr}k_{rr} + h_{ss}k_{ss}] \end{aligned} \tag{2.33}$$

and find that $c = 0$. Thus the bifurcation is degenerate.

Generically, as the parameters $a_1, \ldots, b_3$ pass through the critical value $a_1 = \cdots = b_3 = 1$, the equilibrium point at $(x, y) = \left(\frac{1}{3}, \frac{1}{3}\right)$ changes from a stable focus to an unstable focus. In what follows we will show that this happens without the appearance of a traditional limit cycle. The family of periodic orbits associated with any Hopf bifurcation will be shown in this case to occur at the critical value, so that the space is filled with closed orbits.

2.5.1 Further symmetries

We have seen that the Hopf bifurcation is degenerate to at least third order. However, it is possible to show by a symmetry argument that the degeneracy extends to all orders, and the orbits inside the region bounded by the invariant lines are periodic.

Note that the flow in Fig. 2.6 appears conservative in the central region (i.e. all integral curves are closed). However, it is not conservative, as shown by the existence of attracting fixed points. The occurrence of periodic orbits is due to symmetry, not conservative dynamics, as we will now demonstrate.

To show this, we define $(\dot{x}, \dot{y}, \dot{z})$ using Eqn. (2.4) with the usual zero-sum RPS payoff matrix and $g(x) = x - ax^2$. We do not eliminate z, but instead define coordinates

$$\begin{pmatrix} u \\ v \\ w \end{pmatrix} = \begin{pmatrix} -\sqrt{\frac{2}{3}} & \frac{1}{\sqrt{6}} & \frac{1}{\sqrt{6}} \\ 0 & -\frac{1}{\sqrt{2}} & \frac{1}{\sqrt{2}} \\ \frac{1}{\sqrt{3}} & \frac{1}{\sqrt{3}} & \frac{1}{\sqrt{3}} \end{pmatrix} \begin{pmatrix} x \\ y \\ z \end{pmatrix}. \tag{2.34}$$

This is an orthogonal linear transformation such that the plane containing Σ is orthogonal to the w direction, as shown in Figs. 2.8 and 2.9. In these coordinates, the point $(x, y, z) = \left(\frac{1}{3}, \frac{1}{3}, \frac{1}{3}\right)$ is $(u, v, w) = \left(0, 0, \frac{1}{\sqrt{3}}\right)$, and $\dot{w} = 0$, so the dynamics can be analyzed in terms of u and v only with no loss of information or symmetry.

Next, we transform (u, v) into polar coordinates (r, θ) via

$$u = r\cos\theta, \quad v = r\sin\theta. \tag{2.35}$$

Applying the two successive coordinate changes Eqns. (2.34) and (2.35) to Eqn.

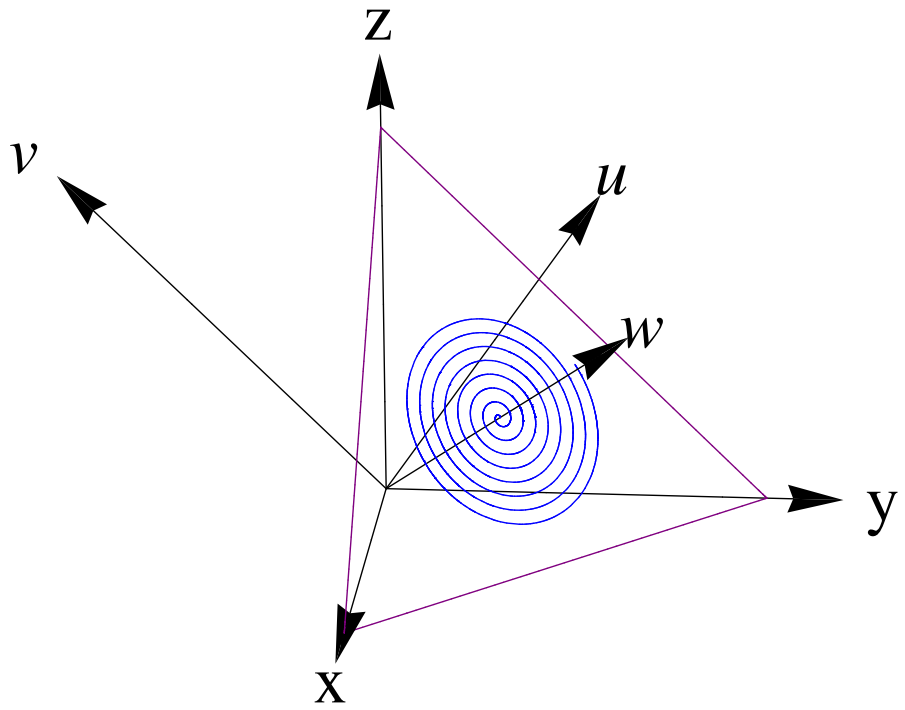

Figure 2.8: The unit vectors $x,\ y,\ z,\ u,\ v$ and w shown with a curve in Σ.

(2.27) and solving for $\dot{r}$ and $\dot{\theta}$, we obtain

$$\dot{r} = -\frac{r^2 \sin(3\theta)}{6\,(3ar^2 + a - 3)} \left(\sqrt{2}(a-3)(2a-3) + 3\sqrt{3}a^2 r^3 \cos(3\theta) \right) \tag{2.36}$$

$$\dot{\theta} = -\frac{1}{18\,(3ar^2 + a - 3)} \Big(9\sqrt{3}a^2 r^4 \cos^2(3\theta) + \sqrt{3}(a-3)(9ar^2 + 2a - 6) + 3r\sqrt{2}(2a-3)(3ar^2 + a - 3)\cos(3\theta) \Big) \tag{2.37}$$

Since θ appears only in terms of $\cos(3\theta)$ and $\sin(3\theta)$, we see that the vector field is periodic in θ with period $\frac{2\pi}{3}$. Figures 2.10 and 2.11 show the boundaries of Σ and the vector field in the (θ, r) plane.

Finally we show that the central region of Σ is filled with periodic orbits.

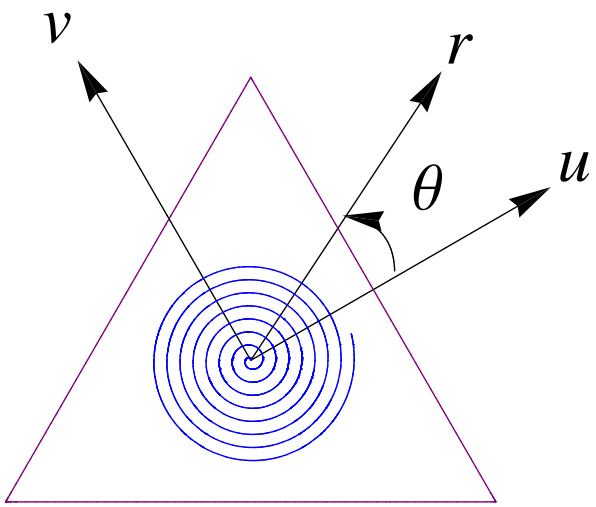

Figure 2.9: Polar coordinates (r, θ) on Σ. The w direction is out of the page.

Notice that $\dot{r}$ is odd, and $\dot{\theta}$ is even, considered as functions of θ. So, if we let

$$\psi = -\theta, \quad \tau = -t \tag{2.38}$$

then

$$\left.\frac{dr}{d\tau}\right|_{(r,\psi)} = \left.\frac{dr}{d(-t)}\right|_{(r,-\theta)} = \left.\frac{dr}{dt}\right|_{(r,\theta)} \tag{2.39}$$

$$\left.\frac{d\psi}{d\tau}\right|_{(r,\psi)} = \left.\frac{d(-\theta)}{d(-t)}\right|_{(r,-\theta)} = \left.\frac{d\theta}{dt}\right|_{(r,\theta)}. \tag{2.40}$$

Thus if there is a trajectory (Trajectory A) that starts at $(r, \theta) = (r_0, 0)$ at $t = 0$ and goes through $(r, \theta) = \left(r_1, \frac{2\pi}{3}\right)$ at $t = t_1$, then there is a matching trajectory (Trajectory B) that starts at $(r, \psi) = (r_0, 0)$ at $\tau = 0$ and goes through $(r, \psi) = \left(r_1, \frac{2\pi}{3}\right)$ at $\tau = t_1$.

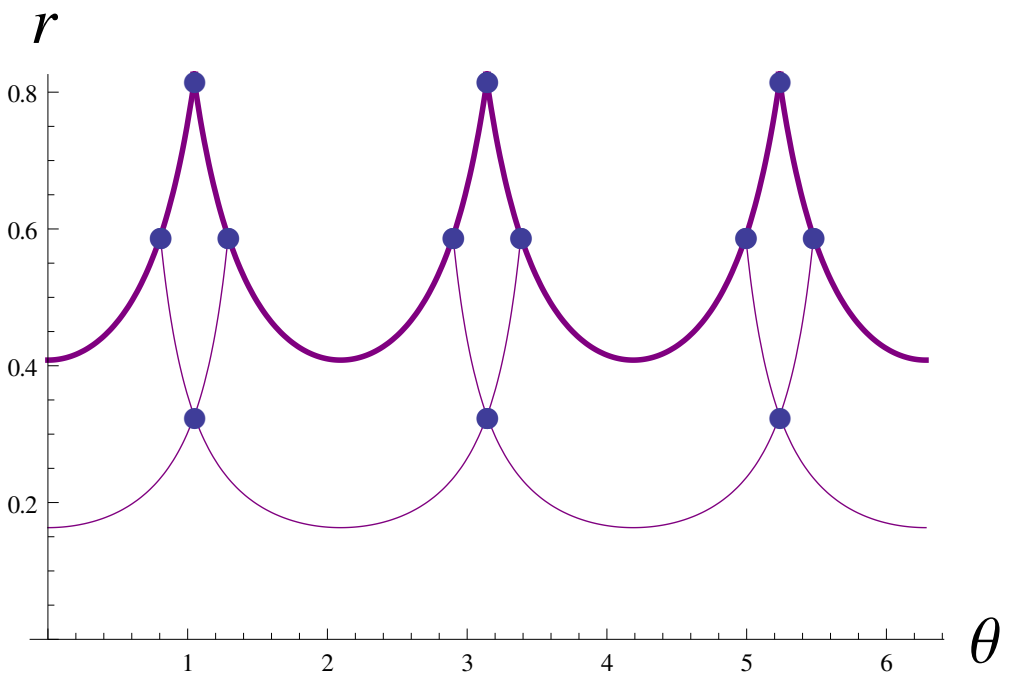

Figure 2.10: Boundary of Σ, invariant lines, and equilibrium points for $a = 5$, in the (θ, r) plane.

By the definitions of ψ and τ, Trajectory B in terms of θ starts at $(r, \theta) = \left(r_1, -\frac{2\pi}{3}\right)$ at $t = -t_1$ and goes through $(r, \theta) = (r_0, 0)$ at $t = 0$. (A schematic of these trajectories is shown in Fig. 2.12.)

Since $\dot{r}$ and $\dot{\theta}$ are autonomous (hence invariant under translations in time) and $\frac{2\pi}{3}$-periodic in θ, there is a trajectory (Trajectory C) that starts at $(r, \theta) = (r_1, 0)$ at $t = 0$ and goes through $(r, \theta) = (r_0, \frac{2\pi}{3})$ at $t = t_1$.

In order for this to occur, if $r_0 \neq r_1$, Trajectory A and Trajectory C must cross. This cannot happen since $\dot{r}$ and $\dot{\theta}$ are well-defined functions. Therefore $r_0 = r_1$, and we see that all trajectories that pass through both $\theta = 0$ and $\theta = \frac{2\pi}{3}$ are in fact closed orbits.

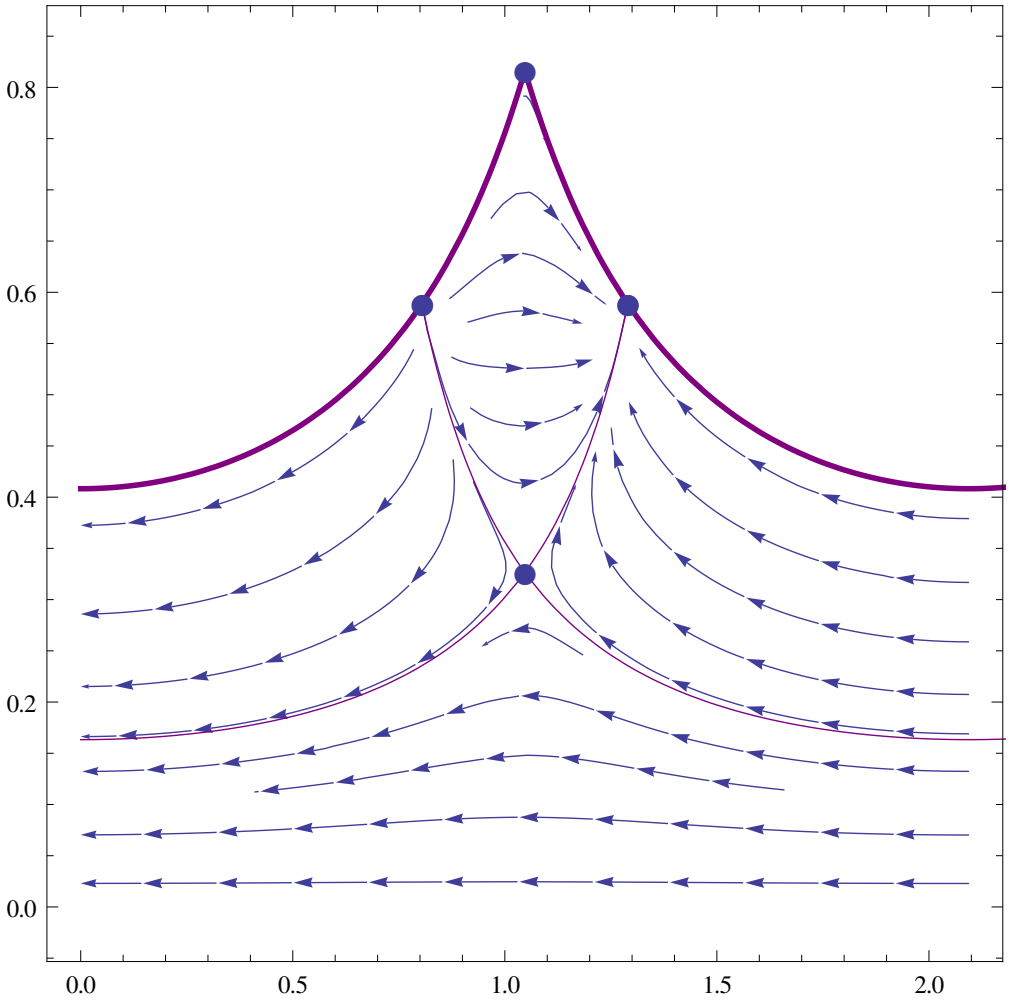

Figure 2.11: Vector field in (θ, r) plane for $0 < \theta < \frac{2\pi}{3}$ and $a = 5$. Boundaries of Σ and invariant lines shown.

2.6 Conclusion

We have investigated the dynamics of certain systems of the form

$$\dot{x}_i = g\left(x_i\right)\left(f_i - \phi\right)$$

where $f_i(x) = (A \cdot x)_i$. For $g(x) = x - ax^2$, and the zero-sum RPS choice of A, we find that the system has several fixed points that do not exist in the usual replicator model. It exhibits both periodic motion and convergence to attractors.

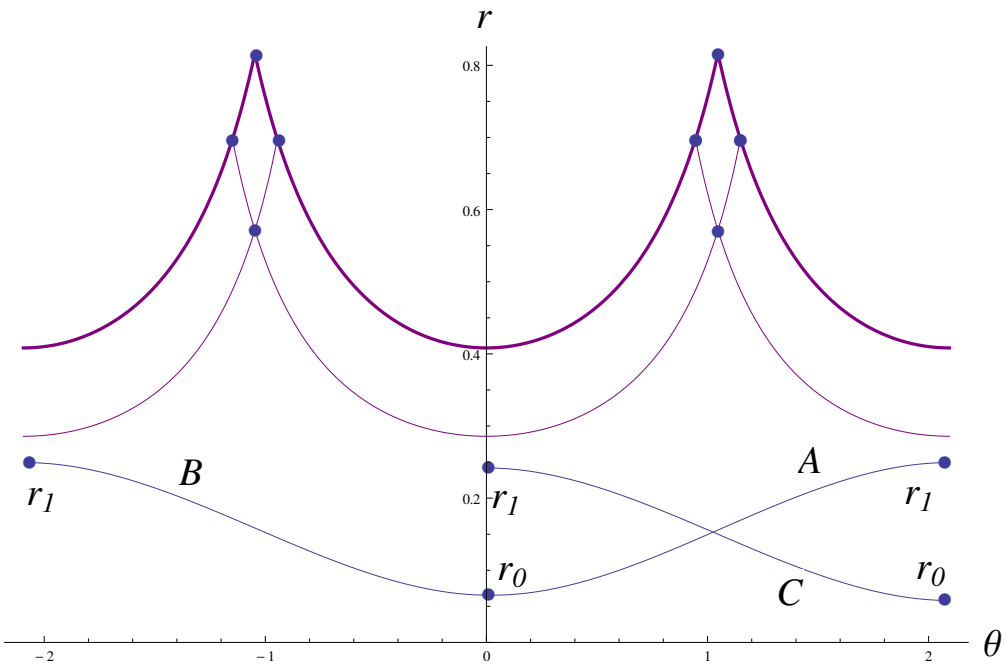

Figure 2.12: If $r_0 \neq r_1$, then Trajectory A and Trajectory C must cross.

This alternate formulation may be instructive in modeling natural or social systems that are not adequately described by the usual replicator dynamics. In particular, this model may apply to systems that exhibit both monotonic and periodic responses depending on initial conditions.

CHAPTER 3

ROCK-PAPER-SCISSORS WITH DELAY

3.1 Introduction

In the standard replicator equation, interactions are assumed to occur instantaneously: the fitness of a given strategy depends on the frequency of each strategy at the given moment. In many real-world contexts, however, the fitness consequences of interactions are not immediate, but instead experience some amount of delay. In this chapter, we explore the consequences of such delay. Specifically, we consider the Rock-Paper-Scissors replicator system, generalized to models in which the fitnesses are functions of the strategy frequencies delayed by a time interval T.

In this chapter, we consider systems in which the fitness of each strategy depends only on the expected payoffs at time $t - T$, as in [6, 16]. If we write $\bar{x}_i \equiv x_i(t - T)$ and define

$$\bar{\mathbf{x}} \equiv (\bar{x}_1, \ldots, \bar{x}_n) \tag{3.1}$$

then the total expected payoff – i.e. the fitness – for strategy i is given by

$$f_i = (A \cdot \bar{\mathbf{x}})_i. \tag{3.2}$$

The use of delayed fitness functions makes the replicator equation into the delay differential equation (DDE)

$$\dot{x}_i = x_i(f_i - \phi) \tag{3.3}$$

where

$$\phi = \sum_i x_i f_i = \sum_i x_i (A \cdot \bar{\mathbf{x}})_i. \tag{3.4}$$

As a system of ODEs, the standard replicator equation is an $(n-1)$ - dimensional problem, since $n-1$ of the x_i are required to specify a point in phase space, in view of the fact that $\sum x_i = 1$. The delayed replicator equation, by contrast, is an infinite-dimensional problem [1] whose solution is a flow on the space of functions on the interval $[-T, 0)$.

A concrete interpretation of this model is that it represents a *social-type* time delay [6]. There is a large, finite pool of players, each of whom uses a particular strategy at any given time. The population is well-mixed, and one-on-one contests between players happen continously. Each player continually decides whether to switch teams, based on the latest information they have about the expected payoff of each strategy. This information is delayed by an interval T.

Previous works on replicator systems with delay [6, 16] have examined two-strategy systems which have a stable interior equilibrium point (i.e. both strategies coexist) when there is no delay. It has been shown that for such systems, there is a critical delay T_c at which the interior equilibrium x^* changes stability; for delay greater than T_c solutions oscillate about x^*.

In this work, we prove a similar result for RPS systems. Moreover, we use nonlinear methods to analyze the resulting limit cycles' amplitude and frequency.

3.2 Three-strategy games: Rock-Paper-Scissors

3.2.1 Derivation

Recall the form of the replicator equation (3.3) with delayed fitness functions (3.4),

$$\dot{x}_i = x_i(f_i - \phi) \tag{3.5}$$

where $f_i = (A \cdot \bar{\mathbf{x}})_i$ and

$$\phi = \sum_i x_i f_i = \sum_i x_i (A \cdot \bar{\mathbf{x}})_i. \tag{3.6}$$

where the bar indicates delay.

We analyze a subset of the space of three-strategy delayed evolutionary games: those known as Rock-Paper-Scissors (RPS) games. RPS games have three strategies, each of which is neutral vs. itself, and has a positive expected payoff vs. one of the other strategies and a negative expected payoff vs. the remaining strategy. The payoff matrix A thus has the form

$$A = \begin{pmatrix} 0 & -b_2 & a_1 \\ a_2 & 0 & -b_3 \\ -b_1 & a_3 & 0 \end{pmatrix} \tag{3.7}$$

where the a_i and b_i are all positive. For ease of notation, write $(x_1, x_2, x_3) = (x, y, z)$. Then

$$\dot{x} = x(a_1\bar{z} - b_2\bar{y} - \phi) \tag{3.8}$$

$$\dot{y} = y(a_2\bar{x} - b_3\bar{z} - \phi) \tag{3.9}$$

$$\dot{z} = z(a_3\bar{y} - b_1\bar{x} - \phi) \tag{3.10}$$

where

$$\phi = x(a_1\bar{z} - b_2\bar{y}) + y(a_2\bar{x} - b_3\bar{z}) + z(a_3\bar{y} - b_1\bar{x}). \tag{3.11}$$

Now, since x, y, z are the relative abundances of the three strategies, the region of interest is the three-dimensional simplex in $\mathbb{R}^3$

$$\Sigma \equiv \{(x, y, z) \in \mathbb{R}^3 : x + y + z = 1 \text{ and } x, y, z \geq 0\}. \tag{3.12}$$

Therefore we can eliminate z using $z = 1 - x - y$. The region of interest is then S, the projection of Σ into the $x - y$ plane:

$$S \equiv \{(x, y) \in \mathbb{R}^2 : (x, y, 1 - x - y) \in \Sigma\} \tag{3.13}$$

See Figure 3.1.

Equations (3.8) and (3.9) become

$$\dot{x} = x(a_1(1 - \bar{x} - \bar{y}) - b_2\bar{y} - \phi) \tag{3.14}$$

$$\dot{y} = y(a_2\bar{x} - b_3(1 - \bar{x} - \bar{y}) - \phi) \tag{3.15}$$

where

$$\begin{aligned}\phi = {} & x(a_1(1 - \bar{x} - \bar{y}) - b_2\bar{y}) + y(a_2\bar{x} - b_3(1 - \bar{x} - \bar{y})) \\ & + (1 - x - y)(a_3\bar{y} - b_1\bar{x}).\end{aligned} \tag{3.16}$$

3.2.2 Stability of Equilibria

The system (3.14)-(3.15) has seven equilibria: the corners of the triangle S,

$$(x, y) = (0, 0), \quad (x, y) = (0, 1), \quad (x, y) = (1, 0) \tag{3.17}$$

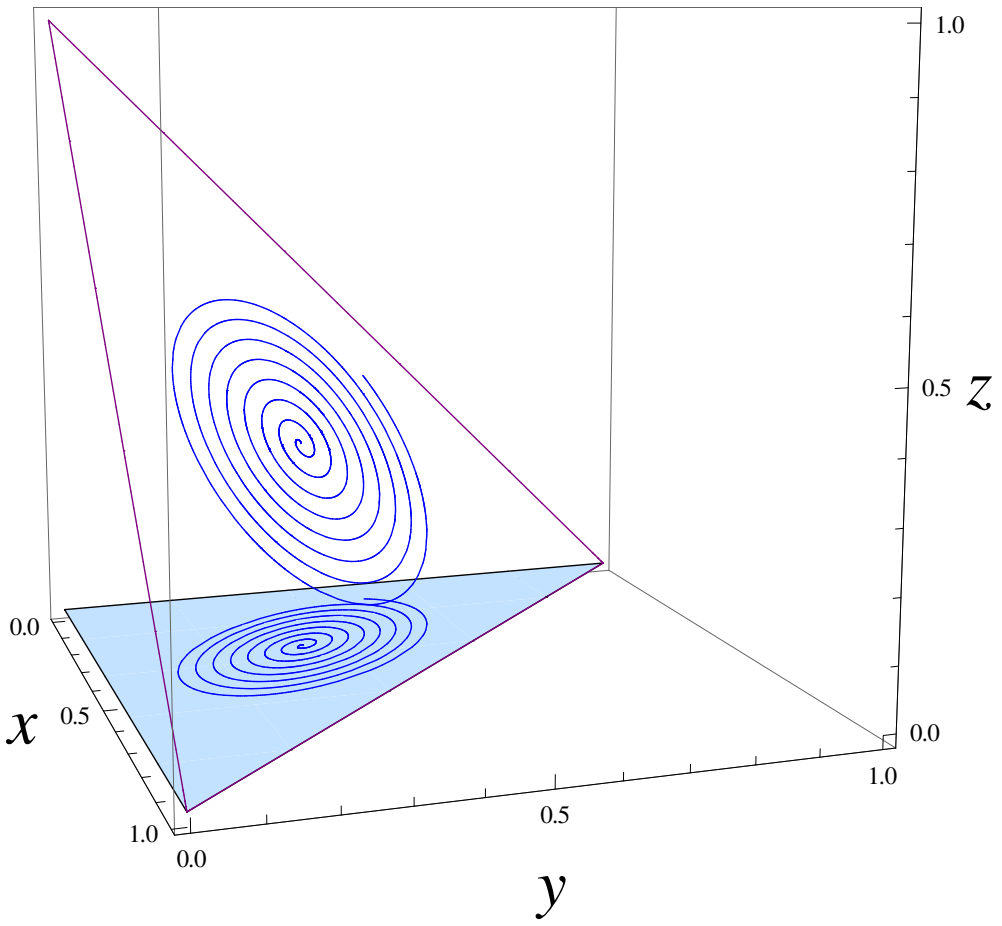

Figure 3.1: A curve in Σ and its projection in S

one point in the interior of S,

$$(x,y) = \left(\frac{b_3\left(a_3+b_2\right)+a_1a_3}{a_1\left(a_2+a_3+b_1\right)+a_2\left(a_3+b_2\right)+b_3\left(a_3+b_1+b_2\right)+b_1b_2}, \frac{a_1\left(a_2+b_1\right)+b_1b_3}{a_1\left(a_2+a_3+b_1\right)+a_2\left(a_3+b_2\right)+b_3\left(a_3+b_1+b_2\right)+b_1b_2} \right) \tag{3.18}$$

and three other points:

$$(x,y) = \left(0, \frac{b_3}{b_3-a_3}\right), \tag{3.19}$$

$$(x,y) = \left(\frac{a_1}{a_1-b_1}, 0\right), \tag{3.20}$$

$$(x,y) = \left(\frac{b_2}{b_2-a_2}, \frac{a_2}{a_2-b_2}\right). \tag{3.21}$$

Note that since the payoff coefficients $a_1, \ldots, b_3$ are positive, the non-zero coordinate(s) of the last three equilibria are either negative or greater than 1. In either case, these points lie outside of S and we will not consider them further.

We linearize about the three corner equilibrium points to determine their stability. In all three cases, the linearization is independent of the delayed variables $\bar{x}$ and $\bar{y}$; that is, the linearized system about each corner point is an ordinary differential equation. Therefore, the stability of each corner point is determined by the eigenvalues of the Jacobian.

At the point $(x, y) = (0, 0)$, the eigenvalues and eigenvectors of the Jacobian are

$$\lambda_1 = a_1, \quad \mathbf{v}_1 = [1, 0] \tag{3.22}$$

$$\lambda_2 = -b_3, \quad \mathbf{v}_2 = [0, 1]. \tag{3.23}$$

Similarly, at the point $(x, y) = (1, 0)$, the eigenvalues and eigenvectors of the Jacobian are

$$\lambda_1 = a_2, \quad \mathbf{v}_1 = [-1, 1] \tag{3.24}$$

$$\lambda_2 = -b_1, \quad \mathbf{v}_2 = [1, 0]. \tag{3.25}$$

Finally, at the point $(x, y) = (0, 1)$, the eigenvalues and eigenvectors of the Jacobian are

$$\lambda_1 = a_3, \quad \mathbf{v}_1 = [0, 1] \tag{3.26}$$

$$\lambda_2 = -b_2, \quad \mathbf{v}_2 = [-1, 1]. \tag{3.27}$$

Therefore, as in the non-delayed RPS system [1], each corner of S is a saddle point, and its eigenvectors lie along the two edges of S adjacent to it. (Since the

lines containing the edges of S are invariant, these lines are in fact the stable and unstable manifolds of the three corner equilibria.)

Next, consider the interior equilibrium (3.18). Let (x^*, y^*) be the coordinates of the equilibrium point. It is known [7] that in the case of no delay ($T = 0$), this point is globally stable if

$$\det A = a_1 a_2 a_3 - b_1 b_2 b_3 > 0. \tag{3.28}$$

All trajectories starting from interior points of S converge to (x^*, y^*). Similarly, if $T = 0$ and $\det A < 0$, the equilibrium point is unstable and all trajectories starting from other points converge to the boundary of S. If $T = 0$ and $\det A = 0$, then S is filled with periodic orbits.

If $T > 0$, however, then in contrast to the corner equilibria, the linearization about (x^*, y^*) depends only on the *delayed* variables, and it is reasonable to expect that its stability will depend on the delay T. So, we analyze the system for a Hopf bifurcation, taking T as the bifurcation parameter.

Define the translated variables u and v via

$$u = x - x^*, \quad v = y - y^*. \tag{3.29}$$

Then the linearization about $(u, v) = (0, 0)$ is

$$\begin{pmatrix} \dot{u} \\ \dot{v} \end{pmatrix} = \begin{pmatrix} \alpha & \beta \\ \gamma & \delta \end{pmatrix} \begin{pmatrix} \bar{u} \\ \bar{v} \end{pmatrix} \equiv J \begin{pmatrix} \bar{u} \\ \bar{v} \end{pmatrix} \tag{3.30}$$

where the entries $(\alpha, \beta, \gamma, \delta)$ of the matrix J are rational functions of the payoff

coefficients $a_1, \ldots, b_3$. These are given by

$$\alpha = x^* \left((a_1 - b_1)(x^* - 1) - (a_2 + b_1 + b_3)y^*\right) \tag{3.31}$$

$$\beta = x^* \left((a_1 + a_3 + b_2)(x^* - 1) + (a_3 - b_3)y^*\right) \tag{3.32}$$

$$\gamma = y^* \left((a_1 - b_1)x^* - (a_2 + b_1 + b_3)(y^* - 1)\right) \tag{3.33}$$

$$\delta = y^* \left((a_1 + a_3 + b_2)x^* + (a_3 - b_3)(y^* - 1)\right) \tag{3.34}$$

where x^* and y^* are the coordinates of the interior equilibrium point, given in Equation (3.18).

Set $u = re^{\lambda t}$ and $v = se^{\lambda t}$ to obtain the characteristic equations

$$\lambda r = e^{-\lambda T}(\alpha r + \beta s) \tag{3.35}$$

$$\lambda s = e^{-\lambda T}(\gamma r + \delta s). \tag{3.36}$$

Rearranging, we obtain

$$\begin{pmatrix} \lambda - \alpha e^{-\lambda T} & -\beta e^{-\lambda T} \\ -\gamma e^{-\lambda T} & \lambda - \delta e^{\lambda T} \end{pmatrix} \begin{pmatrix} r \\ s \end{pmatrix} = \begin{pmatrix} 0 \\ 0 \end{pmatrix}. \tag{3.37}$$

For brevity, write

$$M \equiv \begin{pmatrix} \lambda - \alpha e^{-\lambda T} & -\beta e^{-\lambda T} \\ -\gamma e^{-\lambda T} & \lambda - \delta e^{\lambda T} \end{pmatrix}. \tag{3.38}$$

Then for a nontrivial solution to Equation (3.37), we require

$$\det M = 0. \tag{3.39}$$

This occurs when

$$\beta\gamma = \left(\alpha - \lambda e^{\lambda T}\right)\left(\delta - \lambda e^{\lambda T}\right). \tag{3.40}$$

At the critical value of delay for a Hopf bifurcation, the eigenvalues are pure imaginary. So, we set $T = T_0$ and $\lambda = i\omega_0$. Substituting this into Equation (3.40)

and separating the real and imaginary parts, we obtain

$$\beta\gamma = -\alpha\delta - \omega_0^2 \cos(2\omega_0 T_0) + (\alpha + \delta)\sin(\omega_0 T_0) \tag{3.41}$$

$$0 = \omega_0 \cos(\omega_0 T_0)(\alpha + \delta + 2\omega_0 \sin(\omega_0 T_0)). \tag{3.42}$$

In terms of the matrix J, these equations are

$$\det J = \omega_0^2 \cos(2\omega_0 T_0) - (\mathsf{tr}\ J)\sin(\omega_0 T_0) \tag{3.43}$$

$$0 = \omega_0 \cos(\omega_0 T_0)(\mathsf{tr}\ J + 2\omega_0 \sin(\omega_0 T_0)). \tag{3.44}$$

Solving these equations for $\det J$ and $\mathsf{tr}\ J$, we get

$$\det J = \omega_0^2, \quad \mathsf{tr}\ J = -2\omega_0 \sin(\omega_0 T_0). \tag{3.45}$$

Thus, ω_0 and T_0 are given by

$$\omega_0 = \sqrt{\det J}, \quad T_0 = \frac{-1}{\sqrt{\det J}} \sin^{-1}\left(\frac{\mathsf{tr}\ J}{2\sqrt{\det J}}\right). \tag{3.46}$$

We have found the critical delay and frequency associated with a Hopf bifurcation. In the next subsection, we use Lindstedt's method to approximate the form of the limit cycle that is born in this bifurcation.

3.2.3 Approximation of Limit Cycle

Recall that we have the system

$$\dot{x} = x(a_1(1 - \bar{x} - \bar{y}) - b_2\bar{y} - \phi) \tag{3.47}$$

$$\dot{y} = y(a_2\bar{x} - b_3(1 - \bar{x} - \bar{y}) - \phi) \tag{3.48}$$

where

$$\begin{aligned}\phi = {} & x(a_1(1 - \bar{x} - \bar{y}) - b_2\bar{y}) + y(a_2\bar{x} - b_3(1 - \bar{x} - \bar{y})) \\ & + (1 - x - y)(a_3\bar{y} - b_1\bar{x})\end{aligned} \tag{3.49}$$

with the interior equilibrium point

$$(x^*, y^*) = \left(\frac{b_3 (a_3 + b_2) + a_1 a_3}{a_1 (a_2 + a_3 + b_1) + a_2 (a_3 + b_2) + b_3 (a_3 + b_1 + b_2) + b_1 b_2}, \right.$$
$$\left. \frac{a_1 (a_2 + b_1) + b_1 b_3}{a_1 (a_2 + a_3 + b_1) + a_2 (a_3 + b_2) + b_3 (a_3 + b_1 + b_2) + b_1 b_2} \right). \quad (3.50)$$

We have introduced the translated coordinates u and v, defined by

$$u = x - x^*, \quad v = y - y^* \quad (3.51)$$

and we have determined in Equation (3.46) the critical delay T_0 and frequency ω_0 associated with a Hopf bifurcation of the point $(u, v) = (0, 0)$.

Substituting in u and v, the system (3.47)-(3.48) can be written as

$$\dot{u} = \alpha \bar{u} + \beta \bar{v} + c_1 u\bar{u} + c_2 u\bar{v} + c_3 v\bar{u} + c_4 v\bar{v}$$
$$+ d_1 u^2 \bar{u} + d_2 u^2 \bar{v} + d_3 uv\bar{u} + d_4 uv\bar{v} \quad (3.52)$$
$$\dot{v} = \gamma \bar{u} + \delta \bar{v} + h_1 u\bar{u} + h_2 u\bar{v} + h_3 v\bar{u} + h_4 v\bar{v}$$
$$+ j_1 v^2 \bar{u} + j_2 v^2 \bar{v} + j_3 uv\bar{u} + j_4 uv\bar{v} \quad (3.53)$$

where $\alpha, \beta, \gamma, \delta$ are as in the linearization Equation (3.30). The other coefficients $c_1, \ldots, j_4$ are also rational functions of the payoff coefficients $a_1, \ldots, b_3$. These

are given by

$$c_1 = (a_1 - b_1)(2x^* - 1) - (a_2 + b_1 + b_3)y^* \tag{3.54}$$

$$c_2 = (a_1 + a_3 + b_2)(2x^* - 1) + (a_3 - b_3)y^* \tag{3.55}$$

$$c_3 = -(a_2 + b_1 + b_3)x^* \tag{3.56}$$

$$c_4 = (a_3 - b_3)x^* \tag{3.57}$$

$$d_1 = a_1 - b_1 \tag{3.58}$$

$$d_2 = a_1 + a_3 + b_2 \tag{3.59}$$

$$d_3 = -(a_2 + b_1 + b_3) \tag{3.60}$$

$$d_4 = a_3 - b_3 \tag{3.61}$$

$$h_1 = (a_1 - b_1)y^* \tag{3.62}$$

$$h_2 = (a_1 + a_3 + b_2)y^* \tag{3.63}$$

$$h_3 = (a_1 - b_1)x^* - (a_2 + b_1 + b_3)(2y^* - 1) \tag{3.64}$$

$$h_4 = (a_1 + a_3 + b_2)x^* - (a_3 - b_3)(2y^* - 1) \tag{3.65}$$

$$j_1 = -(a_2 + b_1 + b_3) \tag{3.66}$$

$$j_2 = a_3 - b_3 \tag{3.67}$$

$$j_3 = a_1 - b_1 \tag{3.68}$$

$$j_4 = a_1 + a_3 + b_2. \tag{3.69}$$

Now we use Lindstedt's method to approximate the form of the limit cycle generated by this bifurcation.

We are looking for periodic solutions with delay close to T_0 and frequency

close to ω_0. First, we rescale time via $\tau = \omega t$, so

$$\dot{u} = \frac{du}{dt} = \frac{du}{d\tau}\frac{d\tau}{dt} = \omega\frac{du}{d\tau} \equiv \omega u' \tag{3.70}$$

$$\dot{v} = \frac{dv}{dt} = \frac{dv}{d\tau}\frac{d\tau}{dt} = \omega\frac{dv}{d\tau} \equiv \omega v' \tag{3.71}$$

and, considering u and v to be functions of τ,

$$\bar{u} = u(\tau - \omega T), \quad \bar{v} = v(\tau - \omega T). \tag{3.72}$$

Next, expand the delay and frequency in ϵ:

$$T = T_0 + \epsilon^2\mu_1 + \epsilon^3\mu_2 \tag{3.73}$$

$$\omega = \omega_0 + \epsilon^2 k_1 + \epsilon^3 k_2 \tag{3.74}$$

Note that there is no $O(\epsilon^1)$ term in T or ω because of the presence of quadratic terms in Equations (3.52) and (3.53). Removal of secular terms at the appropriate order of ϵ will require any $O(\epsilon^1)$ terms in Equations (3.73) and (3.74) to vanish.

We expand the functions u and v similarly:

$$u = \epsilon u_0 + \epsilon^2 u_1 + \epsilon^3 u_2 \tag{3.75}$$

$$v = \epsilon v_0 + \epsilon^2 v_1 + \epsilon^3 v_2. \tag{3.76}$$

Then, we substitute the expanded functions and parameters into Equations (3.52) and (3.53) and collect like orders of ϵ. This includes expanding $\bar{u}$ and $\bar{v}$

in Taylor series:

$$\begin{aligned}
\bar{u} &= u(\tau - \omega T) \\
&= \epsilon u_0(\tau - \omega_0 T_0) + \epsilon^2 u_1(\tau - \omega_0 T_0) \\
&\quad + \epsilon^3 \left(u_2(\tau - \omega_0 T_0) - (T_0 k_1 + \omega_0 \mu_1) u_0'(\tau - \omega_0 T_0)\right) + \dots \qquad (3.77) \\
\bar{v} &= v(\tau - \omega T) \\
&= \epsilon v_0(\tau - \omega_0 T_0) + \epsilon^2 v_1(\tau - \omega_0 T_0) \\
&\quad + \epsilon^3 \left(v_2(\tau - \omega_0 T_0) - (T_0 k_1 + \omega_0 \mu_1) v_0'(\tau - \omega_0 T_0)\right) + \dots \qquad (3.78)
\end{aligned}$$

Since the only remaining delayed terms are of the form $u(\tau - \omega_0 T_0)$ or $v(\tau - \omega_0 T_0)$, we introduce the notation

$$\tilde{u} \equiv u(\tau - \omega_0 T_0), \qquad \tilde{v} \equiv v(\tau - \omega_0 T_0). \qquad (3.79)$$

The resulting equations are

$$\begin{aligned}
O(\epsilon^1): \quad & \omega_0 u_0' = \alpha \tilde{u}_0 + \beta \tilde{v}_0 && (3.80) \\
& \omega_0 v_0' = \gamma \tilde{u}_0 + \delta \tilde{v}_0 && (3.81) \\
O(\epsilon^2): \quad & \omega_0 u_1' = \alpha \tilde{u}_1 + \beta \tilde{v}_1 + \tilde{u}_0(c_1 u_0 + c_3 v_0) + \tilde{v}_0(c_2 u_0 + c_4 v_0) && (3.82) \\
& \omega_0 v_1' = \gamma \tilde{u}_1 + \delta \tilde{v}_1 + \tilde{u}_0(h_1 u_0 + h_3 v_0) + \tilde{v}_0(h_2 u_0 + h_4 v_0) && (3.83) \\
O(\epsilon^3): \quad & \omega_0 u_2' = \alpha \tilde{u}_2 + \beta \tilde{v}_2 + \tilde{u}_1(c_1 u_0 + c_3 v_0) + \tilde{v}_1(c_2 u_0 + c_4 v_0) \\
& \qquad + \tilde{u}_0(c_1 u_1 + c_3 v_1 + d_1 u_0^2 + d_3 u_0 v_0) \\
& \qquad + \tilde{v}_0(c_2 u_1 + c_4 v_1 + d_2 u_0^2 + d_4 u_0 v_0) \\
& \qquad - k_1 u_0' - \alpha(T_0 k_1 + \omega_0 \mu_1)\tilde{u}_0' - \beta(T_0 k_1 + \omega_0 \mu_1)\tilde{v}_0' && (3.84) \\
& \omega_0 v_2' = \gamma \tilde{u}_2 + \delta \tilde{v}_2 + \tilde{u}_1(h_1 u_0 + h_3 v_0) + \tilde{v}_1(h_2 u_0 + h_4 v_0) \\
& \qquad + \tilde{u}_0(h_1 u_1 + h_3 v_1 + j_1 v_0^2 + j_3 u_0 v_0) \\
& \qquad + \tilde{v}_0(h_2 u_1 + h_4 v_1 + j_2 v_0^2 + j_4 u_0 v_0) \\
& \qquad - k_1 v_0' - \gamma(T_0 k_1 + \omega_0 \mu_1)\tilde{u}_0' - \delta(T_0 k_1 + \omega_0 \mu_1)\tilde{v}_0'. && (3.85)
\end{aligned}$$

We must solve the equations for each order of ϵ successively, substituting in the results from the lower-order equations as we proceed.

Solve for u_0 and v_0

As seen above, the ϵ^1 equations are linear:

$$\omega_0 u_0' = \alpha\tilde{u}_0 + \beta\tilde{v}_0 \tag{3.80}$$

$$\omega_0 v_0' = \gamma\tilde{u}_0 + \delta\tilde{v}_0. \tag{3.81}$$

Up to a phase shift, the solution has the form

$$u_0 = A_0 \sin\tau \tag{3.86}$$

$$v_0 = A_0(r\sin\tau + s\cos\tau) \tag{3.87}$$

for some constants r and s. We substitute these solutions into Equations (3.80) and (3.81) and use the angle-sum identities to obtain

$$\begin{aligned}\omega_0\cos\tau = {} & (s\beta\cos(\omega_0 T_0) - (\alpha + r\beta)\sin(\omega_0 T_0))\cos\tau \\ & + (s\beta\sin(\omega_0 T_0) + (\alpha + r\beta)\cos(\omega_0 T_0))\sin\tau \end{aligned} \tag{3.88}$$

$$\begin{aligned}\omega_0(r\cos\tau - s\sin\tau) = {} & (s\delta\cos(\omega_0 T_0) - (\gamma + r\delta)\sin(\omega_0 T_0))\cos\tau \\ & + (s\delta\sin(\omega_0 T_0) + (\gamma + r\delta)\cos(\omega_0 T_0))\sin\tau. \end{aligned} \tag{3.89}$$

Setting the coefficients of $\cos\tau$ and $\sin\tau$ equal to 0 in both equations gives us

$$r = \frac{\delta - \alpha}{2\beta}, \quad s = \frac{\sqrt{-4\beta\gamma - (\alpha - \delta)^2}}{2\beta}. \tag{3.90}$$

Thus

$$u_0 = A_0 \sin\tau \tag{3.91}$$

$$v_0 = A_0\frac{1}{2\beta}\left((\delta - \alpha)\sin\tau + \sqrt{-4\beta\gamma - (\alpha - \delta)^2}\cos\tau\right). \tag{3.92}$$

(Note that the coefficient of $\cos\tau$ above is real for the values of $\alpha, \beta, \gamma, \delta$ given in Appendix B.)

Solve for u_1 and v_1

Next we solve for u_1 and v_1 using the solutions for u_0 and v_0 above. Recall that they satisfy the equations

$$\omega_0 u_1' = \alpha\tilde{u}_1 + \beta\tilde{v}_1 + \tilde{u}_0(c_1u_0 + c_3v_0) + \tilde{v}_0(c_2u_0 + c_4v_0) \tag{3.82}$$

$$\omega_0 v_1' = \gamma\tilde{u}_1 + \delta\tilde{v}_1 + \tilde{u}_0(h_1u_0 + h_3v_0) + \tilde{v}_0(h_2u_0 + h_4v_0). \tag{3.83}$$

Using Equations (3.91) and (3.92), and the values of the various coefficients given in Appendix B, these become

$$\omega_0 u_1' = \alpha\tilde{u}_1 + \beta\tilde{v}_1 + A_0^2\left(B_1\sin 2\tau + B_2\cos 2\tau\right) \tag{3.93}$$

$$\omega_0 v_1' = \gamma\tilde{u}_1 + \delta\tilde{v}_1 + A_0^2\left(B_3\sin 2\tau + B_4\cos 2\tau\right). \tag{3.94}$$

The constant coefficients $B_1, \ldots, B_4$ are given in by

$$\begin{aligned} B_1 = \frac{1}{2}\big[&s\left(2c_4r + c_2 + c_3\right)\cos(\omega_0T_0) \\ &- \left(c_4(r-s)(r+s) + \left(c_2+c_3\right)r + c_1\right)\sin(\omega_0T_0)\big] \end{aligned} \tag{3.95}$$

$$\begin{aligned} B_2 = \frac{1}{2}\big[&-s\left(2c_4r + c_2 + c_3\right)\sin(\omega_0T_0) \\ &- \left(c_4(r-s)(r+s) + \left(c_2+c_3\right)r + c_1\right)\cos(\omega_0T_0)\big] \end{aligned} \tag{3.96}$$

$$\begin{aligned} B_3 = \frac{1}{2}\big[&s\left(2h_4r + h_2 + h_3\right)\cos(\omega_0T_0) \\ &- \left(h_4(r-s)(r+s) + \left(h_2+h_3\right)r + h_1\right)\sin(\omega_0T_0)\big] \end{aligned} \tag{3.97}$$

$$\begin{aligned} B_4 = \frac{1}{2}\big[&-s\left(2h_4r + h_2 + h_3\right)\sin(\omega_0T_0) \\ &- \left(h_4(r-s)(r+s) + \left(h_2+h_3\right)r + h_1\right)\cos(\omega_0T_0)\big] \end{aligned} \tag{3.98}$$

where r and s are as in Equation (3.90).

Note that there are no resonant terms to eliminate, and the homogeneous solutions are unnecessary because they will have the same form as u_0 and v_0.

Thus we expect solutions of the form

$$u_1 = A_0^2(r_1 \sin 2\tau + s_1 \cos 2\tau) \tag{3.99}$$

$$v_1 = A_0^2(r_2 \sin 2\tau + s_2 \cos 2\tau). \tag{3.100}$$

Substituting into Equations (3.93)-(3.94) gives

$$\begin{aligned}
&[B_2 - \sin(2T_0\omega_0)(\alpha r_1 + \beta r_2) - 2r_1\omega_0 + \cos(2T_0\omega_0)(\alpha s_1 + \beta s_2)] \cos 2\tau \\
&+ [B_1 + \cos(2T_0\omega_0)(\alpha r_1 + \beta r_2) + \sin(2T_0\omega_0)(\alpha s_1 + \beta s_2) + 2s_1\omega_0] \sin 2\tau \\
&\quad = 0
\end{aligned} \tag{3.101}$$

$$\begin{aligned}
&[B_4 - \sin(2T_0\omega_0)(\gamma r_1 + \delta r_2) - 2r_2\omega_0 + \cos(2T_0\omega_0)(\gamma s_1 + \delta s_2)] \cos 2\tau \\
&+ [B_3 + \cos(2T_0\omega_0)(\gamma r_1 + \delta r_2) + \sin(2T_0\omega_0)(\gamma s_1 + \delta s_2) + 2s_2\omega_0] \sin 2\tau \\
&\quad = 0.
\end{aligned} \tag{3.102}$$

We set the coefficients of $\sin 2\tau$ and $\cos 2\tau$ equal to 0. This gives four linear equations in r_1, r_2, s_1, and s_2, which can be solved easily:

$$\begin{pmatrix} r_1 \\ r_2 \\ s_1 \\ s_2 \end{pmatrix} = C^{-1} \begin{pmatrix} B_1 \\ B_2 \\ B_3 \\ B_4 \end{pmatrix} \tag{3.103}$$

where

$$C = \begin{pmatrix} \alpha \cos & \beta \cos & 2\omega_0 + \alpha \sin & \beta \sin \\ -2\omega_0 - \alpha \sin & -\beta \sin & \alpha \cos & \beta \cos \\ \gamma \cos & \delta \cos & \gamma \sin & 2\omega_0 + \delta \sin \\ -\gamma \sin & -2\omega_0 - \delta \sin & \gamma \cos & \delta \cos \end{pmatrix} \tag{3.104}$$

where the argument of each $\sin$ and $\cos$ is $2\omega_0 T_0$. However, the expressions for $r_1, \ldots, s_2$ are cumbersome and are omitted here for brevity.

Use the u_2 and v_2 equations to find A_0 and k_1 in terms of μ_1

As in the previous steps, we substitute the solutions found above for u_0, v_0, u_1 and v_1 into the equations satisfied by u_2 and v_2. Recall that

$$\begin{aligned}\omega_0 u_2' &= \alpha\tilde{u}_2 + \beta\tilde{v}_2 + \tilde{u}_1(c_1u_0 + c_3v_0) + \tilde{v}_1(c_2u_0 + c_4v_0) \\ &\quad + \tilde{u}_0(c_1u_1 + c_3v_1 + d_1u_0^2 + d_3u_0v_0) \\ &\quad + \tilde{v}_0(c_2u_1 + c_4v_1 + d_2u_0^2 + d_4u_0v_0) \\ &\quad - k_1u_0' - \alpha(T_0k_1 + \omega_0\mu_1)\tilde{u}_0' - \beta(T_0k_1 + \omega_0\mu_1)\tilde{v}_0' \qquad (3.84) \\ \omega_0 v_2' &= \gamma\tilde{u}_2 + \delta\tilde{v}_2 + \tilde{u}_1(h_1u_0 + h_3v_0) + \tilde{v}_1(h_2u_0 + h_4v_0) \\ &\quad + \tilde{u}_0(h_1u_1 + h_3v_1 + j_1v_0^2 + j_3u_0v_0) \\ &\quad + \tilde{v}_0(h_2u_1 + h_4v_1 + j_2v_0^2 + j_4u_0v_0) \\ &\quad - k_1v_0' - \gamma(T_0k_1 + \omega_0\mu_1)\tilde{u}_0' - \delta(T_0k_1 + \omega_0\mu_1)\tilde{v}_0'. \qquad (3.85)\end{aligned}$$

Using Equations (3.91), (3.92), (3.99) and (3.100), these become

$$\omega_0 u_2' = \alpha\tilde{u}_2 + \beta\tilde{v}_2 + K_1\cos\tau + K_2\sin\tau + L_1\cos 3\tau + L_2\sin 3\tau \qquad (3.105)$$

$$\omega_0 v_2' = \gamma\tilde{u}_2 + \delta\tilde{v}_2 + K_3\cos\tau + K_4\sin\tau + L_3\cos 3\tau + L_4\sin 3\tau. \qquad (3.106)$$

The coefficients $K_1, \ldots, L_4$ are omitted for brevity.

The $\sin 3\tau$ and $\cos 3\tau$ terms are non-resonant, so the L_i will not give any information about A_0 or k_1. The $\sin\tau$ and $\cos\tau$ terms are resonant, so we use the method detailed in the next subsection to eliminate secular terms. The existence of a periodic solution to Equations (3.105) and (3.106) requires

$$K_3 = \frac{K_1(\delta - \alpha) - K_2\sqrt{-(\alpha - \delta)^2 - 4\beta\gamma}}{2\beta} \qquad (3.107)$$

$$K_4 = \frac{K_1\sqrt{-(\alpha - \delta)^2 - 4\beta\gamma} + K_2(\delta - \alpha)}{2\beta}. \qquad (3.108)$$

We find that the K_i have the form

$$K_i = A_0(q_{i1}A_0^2 + q_{i2}k_1 + q_{i3}\mu_1). \tag{3.109}$$

Substituting (3.109) into Equations (3.107) and (3.108) gives two simultaneous equations on A_0, k_1 and μ_1. We solve these for A_0 and k_1 in terms of μ_1.

As expected, A_0 is proportional to $\sqrt{\mu_1}$. If the proportionality constant is real, the limit cycle exists for $\mu_1 > 0$, and its stability is the same as that of the interior equilibrium (x^*, y^*) when $T = 0$.

Removal of secular terms in Lindstedt's method with delay

Consider a system of differential delay equations of the form

$$\omega\frac{du}{dt} = \alpha\bar{u} + \beta\bar{v} + K_1 \sin t + K_2 \cos t \tag{3.110}$$

$$\omega\frac{dv}{dt} = \gamma\bar{u} + \delta\bar{v} + K_3 \sin t + K_4 \cos t. \tag{3.111}$$

where $\bar{u} = u(t - \omega T)$ and $\bar{v} = v(t - \omega T)$, and where ω and T are such that the associated homogeneous problem,

$$\omega\frac{du}{dt} = \alpha\bar{u} + \beta\bar{v} \tag{3.112}$$

$$\omega\frac{dv}{dt} = \gamma\bar{u} + \delta\bar{v} \tag{3.113}$$

admits solutions of the form $\sin t$ and $\cos t$, or equivalently e^{it}.

Substituting $u = re^{it}$ and $v = se^{it}$ into Equations (3.112) and (3.113), we obtain the characteristic equations

$$ir\omega = e^{-i\omega T}(\alpha r + \beta s) \tag{3.114}$$

$$is\omega = e^{-i\omega T}(\gamma r + \delta s). \tag{3.115}$$

Rearranging, these become

$$\begin{pmatrix} \alpha e^{-i\omega T} - i\omega & \beta e^{-i\omega T} \\ \gamma e^{-i\omega T} & \delta e^{-i\omega T} - i\omega \end{pmatrix} \begin{pmatrix} r \\ s \end{pmatrix} = \begin{pmatrix} 0 \\ 0 \end{pmatrix}. \tag{3.116}$$

Define

$$R \equiv \begin{pmatrix} \alpha e^{-i\omega T} - i\omega & \beta e^{-i\omega T} \\ \gamma e^{-i\omega T} & \delta e^{-i\omega T} - i\omega \end{pmatrix}. \tag{3.117}$$

A nontrivial solution for r and s requires that $\det R = 0$. Separating the real and imaginary parts, this means that

$$Re(\det R) = \cos(2\omega T)(\alpha\delta - \beta\gamma) - \omega((\alpha + \delta)\sin(\omega T) + \omega) = 0 \tag{3.118}$$

$$Im(\det R) = -\cos(\omega T)(\sin(\omega T)(2\alpha\delta - 2\beta\gamma) + \omega(\alpha + \delta)) = 0. \tag{3.119}$$

Equation (3.119) tells us that

$$\sin(\omega T) = \frac{\omega(\alpha + \delta)}{2(\beta\gamma - \alpha\delta)}. \tag{3.120}$$

(We neglect the alternate possibility that $\cos(\omega T) = 0$.) Then, we substitute this back into Equation (3.118) to obtain

$$\omega^2 = \alpha\delta - \beta\gamma. \tag{3.121}$$

Under the conditions (3.120) and (3.121), the solutions to Equations (3.110) and (3.111) will in general have secular terms:

$$u = m_1 \cos t + m_2 \sin t + n_1 t \cos t + n_2 t \sin t \tag{3.122}$$

$$v = m_3 \cos t + m_4 \sin t + n_3 t \cos t + n_4 t \sin t. \tag{3.123}$$

We wish to derive conditions on the K_i in Equations (3.110) and (3.111) such that the n_i are all equal to 0.

We substitute the solutions (3.122) and (3.123) into Equations (3.110) and (3.111), and set the coefficients of $\sin t$, $\cos t$, $t \sin t$ and $t \cos t$ separately equal to 0 in both equations.

The coefficients of $\sin t$ and $\cos t$ give us a system of linear equations on the m_i and n_i, of the form

$$M \cdot \mathbf{m} + N \cdot \mathbf{n} = -\mathbf{k} \tag{3.124}$$

where $\mathbf{m} = (m_1, \ldots, m_4)^T$, $\mathbf{n} = (n_1, \ldots, n_4)^T$, and $\mathbf{k} = (K_1, \ldots, K_4)^T$.

Similarly, the coefficients of $t \sin t$ and $t \cos t$ give us a system of linear equations on the n_i, of the form

$$S \cdot \mathbf{n} = \mathbf{0}. \tag{3.125}$$

By row-reducing in Mathematica, we find that both M and S have rank 2. To eliminate the n_i, we proceed as follows:

- Without loss of generality, set $m_3 = m_4 = 0$.
- Solve any two independent rows of Equation (3.125) for n_3 and n_4 in terms of n_1 and n_2. The result is

$$n_3 = \frac{n_2 \omega \cos(\omega T) - n_1(\alpha + \omega \sin(\omega T))}{\beta} \tag{3.126}$$

$$n_4 = -\frac{n_1 \omega \cos(\omega T) + n_2(\alpha + \omega \sin(\omega T))}{\beta} \tag{3.127}$$

- Substitute these expressions for n_3 and n_4 into Equation (3.124). This is now a *full-rank* linear system of equations on m_1, m_2, n_1 and n_2. Solve this system to obtain expressions for m_1, m_2, n_1 and n_2 in terms of the K_i.
- Substitute the expressions for n_1 and n_2 from the previous step into Equations (3.126) and (3.127). Now we have all the n_i in terms of the K_i.

- Set the n_i expressions equal to 0. This gives a rank-2 system of equations on the K_i, so it is possible to solve for K_3 and K_4 in terms of K_1 and K_2. The result is

$$K_3 = \frac{\gamma(K_1(\alpha + \omega\sin(\omega T)) + K_2\omega\cos(\omega T))}{\alpha^2 + 2\alpha\omega\sin(\omega T) + \omega^2} \tag{3.128}$$

$$K_4 = \frac{\gamma(K_2(\alpha + \omega\sin(\omega T)) - K_1\omega\cos(\omega T))}{\alpha^2 + 2\alpha\omega\sin(\omega T) + \omega^2}. \tag{3.129}$$

  Using Equations (3.120) and (3.121), these reduce to

$$K_3 = \frac{K_1(\delta - \alpha) - K_2\sqrt{-(\alpha - \delta)^2 - 4\beta\gamma}}{2\beta} \tag{3.130}$$

$$K_4 = \frac{K_1\sqrt{-(\alpha - \delta)^2 - 4\beta\gamma} + K_2(\delta - \alpha)}{2\beta}. \tag{3.131}$$

If Equations (3.130) and (3.131) hold, then there are solutions of Equations (3.110) and (3.111) with no secular terms.

3.2.4 Example

Consider the RPS system

$$\dot{x}_i = x_i(f_i - \phi) \tag{3.132}$$

where $f_i = (A \cdot \bar{\mathbf{x}})_i$ and

$$\phi = \sum_i x_i f_i = \sum_i x_i (A \cdot \bar{\mathbf{x}})_i \tag{3.133}$$

with

$$A = \begin{pmatrix} 0 & -1 & 2 \\ 1 & 0 & -1 \\ -1 & 1 & 0 \end{pmatrix}. \tag{3.134}$$

Following Section 2.2, we see that in this case, $\det A = 1$, so the interior equilibrium point $(x^*, y^*) = (\frac{1}{3}, \frac{5}{12})$ is stable when $T = 0$. The critical delay and frequency are

$$\omega_0 = \frac{1}{2}\sqrt{\frac{5}{3}} \approx 0.64550, \qquad T_0 = 2\sqrt{\frac{3}{5}} \sin^{-1}\left(\frac{1}{4\sqrt{15}}\right) \approx 0.10007. \tag{3.135}$$

Using the method of Sections 2.3.1 and 2.3.2, we find that

$$u_0 = A_0 \sin\tau \tag{3.136}$$

$$v_0 = A_0(-0.671875 \sin\tau - 0.72467 \cos\tau) \tag{3.137}$$

and

$$u_1 = A_0^2(0.235279 \sin 2\tau - 0.430682 \cos 2\tau) \tag{3.138}$$

$$v_1 = A_0^2(0.203199 \sin 2\tau - 0.0397297 \cos 2\tau). \tag{3.139}$$

Then, as in Section 2.3.3,

$$\omega_0 u_2' = \alpha\tilde{u}_2 + \beta\tilde{v}_2 + K_1 \cos\tau + K_2 \sin\tau + L_1 \cos 3\tau + L_2 \sin 3\tau \tag{3.140}$$

$$\omega_0 v_2' = \gamma\tilde{u}_2 + \delta\tilde{v}_2 + K_3 \cos\tau + K_4 \sin\tau + L_3 \cos 3\tau + L_4 \sin 3\tau. \tag{3.141}$$

where

$$\alpha = -\frac{23}{36}, \quad \beta = -\frac{8}{9}, \quad \gamma = \frac{125}{144}, \quad \delta = \frac{5}{9} \tag{3.142}$$

and

$$K_1 = A_0^2(-0.957018A_0^2 - k_1) \tag{3.143}$$

$$K_2 = A_0^2(-0.146492A_0^2 + 0.0645946k_1 + 0.416667\mu_1) \tag{3.144}$$

$$K_3 = A_0^2(0.573076A_0^2 + 0.625065k_1 - 0.301946\mu_1) \tag{3.145}$$

$$K_4 = A_0^2(-0.472711A_0^2 - 0.768069k_1 - 0.279948\mu_1). \tag{3.146}$$

Therefore, using Equations (3.107) and (3.108), the condition to eliminate secular terms is

$$A_0 = 2.26293\sqrt{\mu_1}, \qquad k_1 = -4.46834\mu_1. \tag{3.147}$$

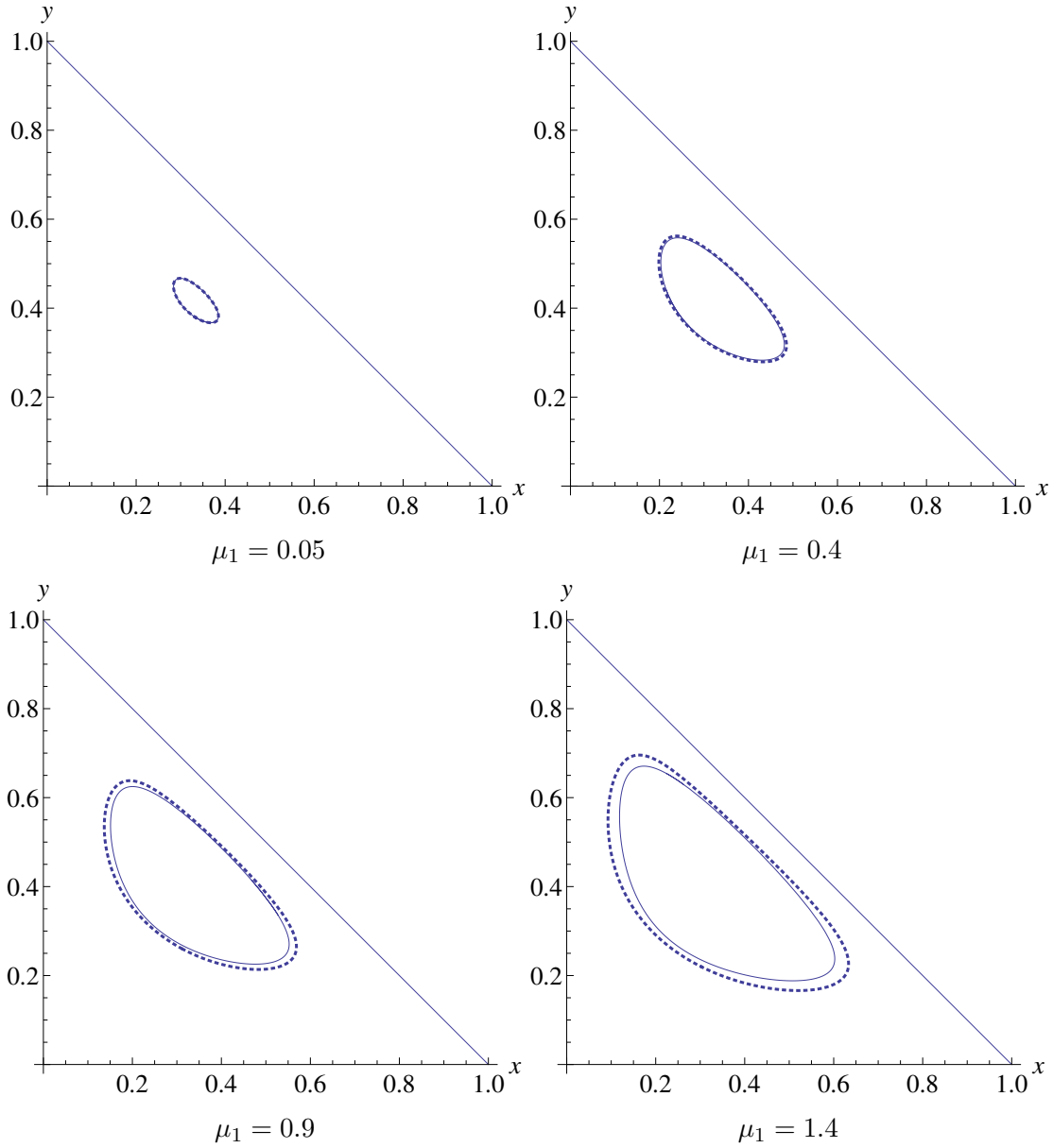

Figure 3.2: Limit cycle given by Lindstedt (dotted) and numerical integration (solid) for $\epsilon = 0.1$ and varying values of μ_1. Recall that $T = T_0 + \epsilon^2 \mu_1$.

This means that the limit cycle exists when $\mu_1 > 0$, so the bifurcation is supercritical and the limit cycle is stable.

To evaluate the results of Lindstedt's method qualitatively, we compute the

average radius of the limit cycle (i.e. the radius of the circle with the same enclosed area). For the limit cycle predicted by Lindstedt's method, this is simply

$$r_{\text{Lind}} = \left[\frac{\omega}{2\pi} \int_0^{2\pi/\omega} \left(u(t)^2 + v(t)^2 \right) dt \right]^{1/2} \tag{3.148}$$

where u and v are as in Equations (3.136)-(3.139). Recall that $\tau = \omega t$ where $\omega = \omega_0 + \epsilon^2 k_1$, where ω_0 is given by Equation (3.135) and k_1 by Equation (3.147).

We compare this to the average radius of the approximate limit cycle given by numerical integration. To find this, we integrate the original system given in Equations (3.132)-(3.134), using NDSOLVE in Mathematica. This is a versatile method that can handle ordinary, partial, or delay differential equations, and which adaptively chooses from among several solving routines. For 40 values of μ_1 between -0.5 and 1.5, we integrated the system up to $t = 3000$, with the assumption that the solutions were constant for $t < 0$. We found that for $t > 2900$, the numerical solutions were nearly periodic: in all cases tested, the peak-to-peak times of the first cycle after $t = 2900$ and the last cycle before $t = 3000$ differed by less than one part in 10^{-7}. This gave the desired approximation to the limit cycle.

Thus, the average radius for the numerical limit cycle is

$$r_{\text{numer}} = \left[\frac{1}{p(\mu_1)} \int_{t_0}^{t_0 + p(\mu_1)} \left((x(t) - x^*)^2 + (y(t) - y^*)^2 \right) dt \right]^{1/2} \tag{3.149}$$

where $p(\mu_1)$ is the period of the limit cycle, obtained using FINDROOT in Mathematica, and t_0 is chosen large enough that the numerical solutions are close to the limit cycle.

We compare the average radius given by Lindstedt's method to that found by numerical integration, and observe from Figure 3.3 that the two methods are in relatively good agreement for small μ_1.

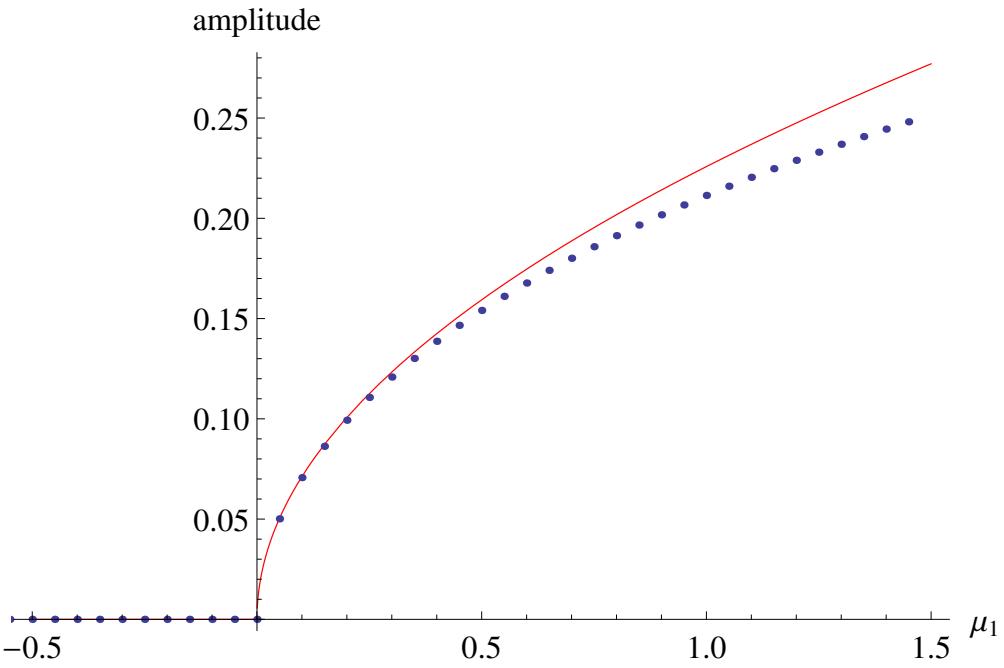

Figure 3.3: Average radius of the limit cycle given by Lindstedt (solid) and numerical integration (dotted) for $\epsilon = 0.1$ as a function of μ_1

Conclusion

We have investigated the dynamics of Rock-Paper-Scissors systems of the form

$$\dot{x}_i = x_i(f_i - \phi), \tag{3.150}$$

where $f_i = (A \cdot \bar{\mathbf{x}})_i$ is the (delayed) fitness of strategy i.

It is known that limit cycles cannot occur in non-delayed rock-paper-scissors systems; the phase space is filled with either decreasing, increasing, or neutral oscillations, depending on the determinant of the payoff matrix A.

In this work, we have shown using nonlinear methods that, by introducing a social-type delay in the fitnesses of the strategies, it is possible to find rock-paper-scissors systems which exhibit non-degenerate Hopf bifurcations and limit cycles. We have analyzed the resulting limit cycles using Lindstedt's

method, finding an approximation of their frequency and amplitude. We have demonstrated a choice of parameters for which a Rock-Paper-Scissors system undergoes a supercritical Hopf bifurcation and exhibits a stable limit cycle. For this choice of parameters, the prediction of Lindstedt's method is found to agree with numerical integration for T close to T_0.

This generalization of the replicator model may be useful in modeling natural or social systems in which each player has a delayed estimate of the expected payoff of each strategy.

CHAPTER 4

TWO-STRATEGY GAMES WITH DELAY

4.1 Introduction

In the previous chapter, we investigated a replicator system in which the fitness functions depended only on the delayed expected payoffs. In this chapter, we consider a range of models in which not all interactions are equally subject to delay. Specifically, we consider the two-strategy replicator system, generalized to models in which the fitnesses are functions of the strategy frequencies delayed by a time interval T.

For ease of notation, write

$$A = \begin{pmatrix} a & b \\ c & d \end{pmatrix} \tag{4.1}$$

and

$$\mathbf{x} = (x_1, x_2) = (x, y). \tag{4.2}$$

Two-strategy games with delay have previously been investigated by Yi and Zuwang [16] and Miekisz [6]. These previous works considered cases that have an equilibrium in which the two strategies coexist, and obtained conditions for the instability of this interior equilibrium when all interactions are subject to delay. They did not, however, analyze the bifurcations that occur at the change of stability.

In the present paper, we extend this work in two ways. First, we include nonlinear terms, which allows us to analyze the Hopf bifurcations that occur

in these systems and their associated limit cycles. Second, we consider models in which not all interactions are equally subject to delay: interactions between agents with different strategies may be more likely to be delayed than interactions between agents with the same strategy. Specifically, we consider a range of models indexed by a homotopy parameter γ that determines the relative weights of delayed and non-delayed terms in the fitness functions.

At one extreme is the case considered previously [16, 6], in which all interactions are delayed by T time units. We refer to this as the **full** delay model: If we write $\bar{x}_i \equiv x_i(t-T)$ and define

$$\bar{\mathbf{x}} \equiv (\bar{x}, \bar{y}) \tag{4.3}$$

then the total expected payoff – i.e. the fitness – for strategy i is given by

$$f_i = (A \cdot \bar{\mathbf{x}})_i. \tag{4.4}$$

That is,

$$f_1 = a\bar{x} + b\bar{y}, \quad f_2 = c\bar{x} + d\bar{y}. \tag{4.5}$$

Thus each agent's payoff at the current moment depends on the frequencies of each strategy T time units ago (i.e. the expected payoff of that agent's strategy T time units ago). This could represent a situation in which human learners preferentially imitate those with higher payoffs, but information about the payoff of each strategy is delayed by T; or a situation in which organisms evolving in a well-mixed population consume resources produced by other organisms to determine their fitness, and resources take T time to diffuse between one organism and the next.

At the other end of the spectrum, only interactions between agents with different strategies are delayed, while interactions between agents with the same

strategy are instantaneous. We refer to this as the **off-diagonal** delay model. In this case, if we define

$$\bar{\mathbf{x}}^1 \equiv (x, \bar{y}), \quad \bar{\mathbf{x}}^2 \equiv (\bar{x}, y) \tag{4.6}$$

then the fitness for strategy i is given by

$$f_i = (A \cdot \bar{\mathbf{x}}^i)_i. \tag{4.7}$$

That is,

$$f_1 = ax + b\bar{y}, \quad f_2 = c\bar{x} + dy. \tag{4.8}$$

Note that in this model, the fitness cannot be considered an expected payoff, as $\bar{\mathbf{x}}^i$ is not a unit vector. This model may be interpreted as the result of a certain form of assortment: human learners have immediate information about the payoff consequences of interactions with those having their own strategy, but information about the outcome of interactions with people using the other strategy is delayed by T; or resources produced by the other type of organism take T time units to diffuse whereas resources produced by organisms of one's own type are immediately available (perhaps because of spatial co-localization of agents of the same type).

In general, we can bridge the two extreme models by introducing a linear homotopy between them: we define

$$\bar{\mathbf{x}}^i_\gamma \equiv \gamma \bar{\mathbf{x}}^i + (1-\gamma)\bar{\mathbf{x}} \tag{4.9}$$

and consider the fitness functions

$$f_i = (A \cdot \bar{\mathbf{x}}^i_\gamma)_i. \tag{4.10}$$

That is,

$$f_1 = a(\gamma x + (1-\gamma)\bar{x}) + b\bar{y}, \quad f_2 = c\bar{x} + d(\gamma y + (1-\gamma)\bar{y}). \tag{4.11}$$

When $\gamma = 0$, we are in the full-delay case; when $\gamma = 1$ we are in the off-diagonal delay case. For values of γ between 0 and 1, the system may be considered as a stochastic combination of the two: interactions with agents using the other strategy are always delayed by T, but interactions with agents using one's own strategy are instanteous with probability γ and delayed with probability $1 - \gamma$.

For any value of γ, the use of delayed frequencies in the fitness functions makes the replicator equation into the delay differential equation (DDE)

$$\dot{x}_i = x_i(f_i - \phi) \tag{4.12}$$

where f_i is given in (4.11), and

$$\phi = \sum_i x_i f_i = x f_1 + y f_2. \tag{4.13}$$

As a system of ODEs, the standard replicator equation is an $(n - 1)$ - dimensional problem, because $\sum x_i = 1$. This means $n-1$ of the x_i are required to specify a point in phase space. In particular, the non-delayed two-strategy replicator system reduces to a single autonomous ODE. The delayed two-strategy replicator equation reduces to a single autonomous DDE which, by contrast, is an infinite-dimensional system [1] whose solution is a flow on the space of functions on the interval $[-T, 0)$.

4.2 Derivation

We will analyze the replicator equation (4.12) without specifying the homotopy parameter γ – that is, the fitness is given by (4.11). The full delay and off-diagonal delay models correspond to the special cases $\gamma = 0$ and $\gamma = 1$,

respectively. Then

$$\dot{x} = x(f_1 - \phi) \quad \text{and} \quad \dot{y} = y(f_2 - \phi) \tag{4.14}$$

where

$$f_1 = a(\gamma x + (1-\gamma)\bar{x}) + b\bar{y} \quad \text{and} \quad f_2 = c\bar{x} + d(\gamma y + (1-\gamma)\bar{y}), \tag{4.15}$$

which means

$$\begin{aligned} \phi &= x f_1 + y f_2 \\ &= x\left[a(\gamma x + (1-\gamma)\bar{x}) + b\bar{y}\right] + y\left[c\bar{x} + d(\gamma y + (1-\gamma)\bar{y})\right]. \end{aligned} \tag{4.16}$$

Substituting in these values, and writing $y = 1 - x$, the system is reduced to the single delay differential equation

$$\dot{x} = x(1-x)\left[b - d + (a - b - c + d)\bar{x} + (a+d)(x - \bar{x})\gamma\right]. \tag{4.17}$$

At this point, we note that the number of parameters may be reduced by defining p, q, r as follows:

$$p \equiv a - c \tag{4.18}$$

$$q \equiv d - b \tag{4.19}$$

$$r \equiv a + d = \text{tr } A. \tag{4.20}$$

Then equation (4.17) becomes

$$\dot{x} = x(1-x)(p\bar{x} + q(\bar{x} - 1) + \gamma r(x - \bar{x})). \tag{4.21}$$

4.3 Analysis

The equilibrium points of equation (4.21) satisfy $\dot{x} = 0$ and $\bar{x} = x$. There are three equilibria:

$$x = 0, \quad x = 1, \quad x = \frac{q}{p+q}. \tag{4.22}$$

The first two are the endpoints of the interval of physical relevance, since we require that $x \in [0, 1]$. The third lies in the interval $(0, 1)$ if and only if p and q have the same sign. We will assume that this is the case. Notice that the equilibria do not depend on the homotopy parameter γ. We examine the stability of the three points.

Taylor expanding about $x = 0$ and $x = 1$, respectively, we obtain the linearized systems

$$\dot{x} = -qx \qquad \text{about } x = 0 \tag{4.23}$$

$$(x-1)^{\cdot} = -p(x-1) \qquad \text{about } x = 1 \tag{4.24}$$

These two linearizations do not depend on $\bar{x}$, so the stability of the endpoints depends only on the payoff coefficients and not on the delay. The two endpoints have the same stability, since by assumption p and q have the same sign. If $p, q > 0$, we find that both endpoints are stable; if $p, q < 0$, then both endpoints are unstable.

Now consider the third equilibrium. To determine its stability, we set

$$z = x - \frac{q}{p+q}. \tag{4.25}$$

In terms of z, equation (4.21) is

$$\dot{z} = -\frac{(p(z-1)+qz)(z(p+q)+q)(\bar{z}(p+q-\gamma r)+\gamma r z)}{(p+q)^2} \tag{4.26}$$

We linearize about $z = 0$ to get

$$\dot{z} = \frac{pq(\bar{z}(p+q-\gamma r)+\gamma r z)}{(p+q)^2}. \tag{4.27}$$

First, note that if delay $T = 0$, the linearization reduces to

$$\dot{z} = \frac{pqz}{p+q}. \tag{4.28}$$

Under the assumption that p and q have the same sign, we see that the stability of the point $z = 0$ is opposite that of the endpoints. If $p, q > 0$, we find that the point $z = 0$ is unstable when $T = 0$; if $p, q < 0$, then it is stable.

In general, however, the linearization (4.27) has a non-zero $\bar{z}$ term, so it is reasonable to expect that the stability will depend on the delay T. Given that, we analyze the system for a Hopf bifurcation, taking T as the bifurcation parameter.

Set $z = e^{\lambda t}$ (and $\bar{z} = e^{\lambda(t-T)}$) in equation (4.27) to obtain the characteristic equation

$$\lambda = \frac{pq\, e^{-\lambda T}\left(p+q+\gamma r\left(e^{\lambda T}-1\right)\right)}{(p+q)^2}. \tag{4.29}$$

At the critical value of delay for a Hopf bifurcation, the eigenvalues are pure imaginary, so we take $T = T_c$ and $\lambda = i\omega$. Substituting this into the characteristic equation and taking the real and imaginary parts, we obtain

$$\cos \omega T_c = -\frac{\gamma p^2 q^2 r(p+q-\gamma r)}{(\gamma pqr)^2 + \omega^2 (p+q)^4} \tag{4.30}$$

$$\sin \omega T_c = -\frac{pq\omega(p+q)^2(p+q-\gamma r)}{(\gamma pqr)^2 + \omega^2 (p+q)^4}. \tag{4.31}$$

Squaring these equations and adding them, we can solve for the critical frequency ω:

$$\omega = pq\sqrt{\frac{p+q-2\gamma r}{(p+q)^3}}. \tag{4.32}$$

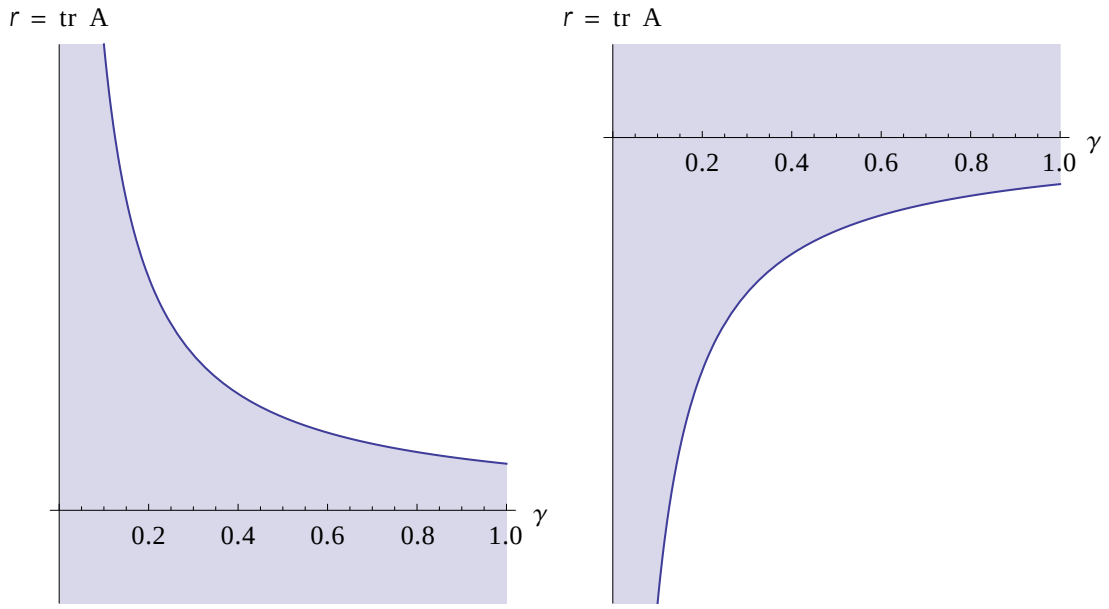

Figure 4.1: The Hopf bifurcation occurs in systems lying in the shaded regions, i.e. below the curve $p + q = 2\gamma r$ if $p + q > 0$ (left) and above the curve $p + q = 2\gamma r$ if $p + q < 0$ (right).

It can be shown that the frequency is real and non-zero if and only if (in addition to p and q having the same sign) $p + q - 2\gamma r$ has the same sign as $p + q$. That is,

$$\{p, q < 0\,,\; p + q < 2\gamma r\} \quad \text{or} \quad \{p, q > 0\,,\; p + q > 2\gamma r\}\,. \tag{4.33}$$

Thus (4.33) is a necessary condition for a Hopf bifurcation to exist. See Figure 4.1. We will assume that this condition is satisfied.

Notice that in the full delay case $\gamma = 0$, (4.33) is trivially satisfied whenever p and q have the same sign. That is, the Hopf occurs for any payoff matrix such that the equilibrium point lies in the interval of relevance. In this case, (4.32) reduces to

$$\omega = \frac{pq}{|p + q|}. \tag{4.34}$$

For any nonzero value of γ, however, there exist payoff matrices for which the equilibrium point lies in the interval of relevance, but $|r|$ is large enough that

(4.33) does not hold and the Hopf does not exist.

Now, substituting (4.32) back into (4.30), we obtain the critical delay T_c:

$$T_c = \cos^{-1}\left(\frac{-\gamma r}{p+q-\gamma r}\right)\frac{1}{pq}\sqrt{\frac{(p+q)^3}{p+q-2\gamma r}}. \tag{4.35}$$

This result agrees with the values of T_c and ω given by Rand and Verdugo [9]. We also apply the results of [9] to obtain an approximation for the amplitude of the limit cycle generated by the Hopf bifurcation. See the next subsection. Equation (4.26) can be written as

$$\dot{z} = \alpha z + \beta\bar{z} + a_1 z^2 + a_2 z\bar{z} + a_3\bar{z}^2 + b_1 z^3 + b_2 z^2\bar{z} + b_3 z\bar{z}^2 + b_4\bar{z}^3 \tag{4.36}$$

where

$$\alpha = \frac{\gamma pqr}{(p+q)^2} \tag{4.37}$$

$$\beta = \frac{pq(p+q-\gamma r)}{(p+q)^2} \tag{4.38}$$

$$a_1 = \frac{\gamma r(p-q)}{p+q} \tag{4.39}$$

$$a_2 = \frac{(p-q)(p+q-\gamma r)}{p+q} \tag{4.40}$$

$$b_1 = -r\gamma, \tag{4.41}$$

$$b_2 = -p-q+\gamma r \tag{4.42}$$

$$a_3 = b_3 = b_4 = 0. \tag{4.43}$$

If $T = T_c + \mu$, the amplitude R is given by

$$R = \sqrt{\mu P/Q} \tag{4.44}$$

where

$$P = -\frac{4p^7q^7(5(p+q)-9\gamma r)(p+q-2\gamma r)(p+q-\gamma r)^3}{(p+q)^{12}} \tag{4.45}$$

$$\begin{aligned} Q = &-\frac{p^4q^4\sqrt{\frac{p+q-2\gamma r}{(p+q)^3}}(p+q-\gamma r)^3}{(p+q)^8}\left[\left(p^2-q^2\right)^2(p+q-3\gamma r)\sqrt{\frac{p+q-2\gamma r}{(p+q)^3}}\right. \\ &+\left[-3\gamma r\left(2p^2-pq+2q^2\right)(p+q)+\left(3p^2-pq+3q^2\right)(p+q)^2\right. \\ &\left.\left.+3\gamma^2r^2(p-q)^2\right]\cos^{-1}\left(-\frac{\gamma r}{p+q-\gamma r}\right)\right]. \end{aligned} \tag{4.46}$$

When $\gamma = 0$, this reduces to

$$P = -\frac{20p^7q^7}{(p+q)^7} \tag{4.47}$$

$$Q = -\frac{p^4q^4\left(\pi\left(3p^2-pq+3q^2\right)|p+q|+2(p+q)(p-q)^2\right)}{2(p+q)^5}. \tag{4.48}$$

Since R is real, μ must have the same sign as P/Q. This determines whether the Hopf bifurcation is sub- or supercritical. In particular, if the point $z = 0$ is stable for delay $T < T_c$ and $\mu > 0$, then the limit cycle is stable and the bifurcation is supercritical. We will treat an example of this type in the next section.

4.3.1 Hopf bifurcation formula for first-order DDEs

We present the formula for the radius of a limit cycle that is born in a Hopf bifurcation in a first-order constant-coefficient differential delay equation, derived by Rand and Verdugo [9].

Consider a differential delay equation (DDE)

$$\frac{dx}{dt} = \alpha x + \beta\bar{x} + a_1x^2 + a_2x\bar{x} + a_3\bar{x}^2 + b_1x^3 + b_2x^2\bar{x} + b_3x\bar{x}^2 + b_4\bar{x}^3 \tag{4.49}$$

where $x = x(t)$ and $\bar{x} = x(t - T)$. The associated linear DDE is

$$\frac{dx}{dt} = \alpha x + \beta \bar{x}. \tag{4.50}$$

Assume that equation (4.49) has a critical delay T_c for which it has a pair of pure imaginary eigenvalues $\pm\omega i$ corresponding to the solution

$$x = c_1 \cos \omega t + c_2 \sin \omega t. \tag{4.51}$$

Then for values of delay T close to T_c,

$$T = T_c + \mu \tag{4.52}$$

the nonlinear equation (4.49) will in general exhibit a periodic solution that can be approximated by

$$x = R \cos \omega t \tag{4.53}$$

where the amplitude R satisfies

$$R^2 = \mu P/Q \tag{4.54}$$

where

$$P = 4\beta^3(4\alpha - 5\beta)(\beta - \alpha)(\alpha + \beta)^2 \tag{4.55}$$

$$\begin{aligned}
Q =& 5b_2T_c\beta^6 + 15b_4T_c\beta^6 + 15b_1\beta^5 + 5b_3\beta^5 - 4a_1^2T_c\beta^5 - 3a_2^2T_c\beta^5 \\
&- 22a_3^2T_c\beta^5 - 7a_1a_2T_c\beta^5 - 14a_1a_3T_c\beta^5 - 7a_2a_3T_c\beta^5 - 15\alpha b_1T_c\beta^5 \\
&+ \alpha b_2T_c\beta^5 - 15\alpha b_3T_c\beta^5 + 3\alpha b_4T_c\beta^5 - 18a_1^2\beta^4 - a_2^2\beta^4 - 4a_3^2\beta^4 \\
&- 9a_1a_2\beta^4 - 18a_1a_3\beta^4 - 9a_2a_3\beta^4 + 3\alpha b_1\beta^4 - 15\alpha b_2\beta^4 + \alpha b_3\beta^4 \\
&- 15\alpha b_4\beta^4 + 18\alpha a_1^2T_c\beta^4 + 7\alpha a_2^2T_c\beta^4 + 12\alpha a_3^2T_c\beta^4 + 19\alpha a_1a_2T_c\beta^4 \\
&+ 30\alpha a_1a_3T_c\beta^4 + 37\alpha a_2a_3T_c\beta^4 - 3\alpha^2b_1T_c\beta^4 + 6\alpha^2b_2T_c\beta^4 \\
&- 3\alpha^2b_3T_c\beta^4 - 12\alpha^2b_4T_c\beta^4 + 12\alpha a_1^2\beta^3 + 11\alpha a_2^2\beta^3 + 26\alpha a_3^2\beta^3 \\
&+ 33\alpha a_1a_2\beta^3 + 30\alpha a_1a_3\beta^3 + 19\alpha a_2a_3\beta^3 - 12\alpha^2b_1\beta^3 - 3\alpha^2b_2\beta^3 \\
&+ 6\alpha^2b_3\beta^3 - 3\alpha^2b_4\beta^3 - 8\alpha^2a_1^2T_c\beta^3 - 12\alpha^2a_2^2T_c\beta^3 + 4\alpha^2a_3^2T_c\beta^3 \\
&- 26\alpha^2a_1a_2T_c\beta^3 - 16\alpha^2a_1a_3T_c\beta^3 - 20\alpha^2a_2a_3T_c\beta^3 + 12\alpha^3b_1T_c\beta^3 \\
&+ 2\alpha^3b_2T_c\beta^3 + 12\alpha^3b_3T_c\beta^3 - 14\alpha^2a_2^2\beta^2 - 8\alpha^2a_3^2\beta^2 - 18\alpha^2a_1a_2\beta^2 \\
&- 12\alpha^2a_1a_3\beta^2 - 32\alpha^2a_2a_3\beta^2 + 12\alpha^3b_2\beta^2 + 2\alpha^3b_3\beta^2 + 12\alpha^3b_4\beta^2 \\
&+ 8\alpha^3a_2^2T_c\beta^2 + 8\alpha^3a_1a_2T_c\beta^2 - 4\alpha^3a_2a_3T_c\beta^2 - 8\alpha^4b_2T_c\beta^2 \\
&+ 4\alpha^3a_2^2\beta - 8\alpha^3a_3^2\beta + 8\alpha^3a_2a_3\beta - 8\alpha^4b_3\beta + 8\alpha^4a_2a_3
\end{aligned} \tag{4.56}$$

The critical delay T_c and frequency ω may be expressed in terms of α and β by considering the linear equation (4.50). Substituting equation (4.53) into (4.50) and setting the coefficients of $\sin\omega t$ and $\cos\omega t$ equal to zero gives

$$\beta\sin\omega T_c = -\omega, \quad \beta\cos\omega T_c = -\alpha. \tag{4.57}$$

Squaring and adding these, and substituting the result back in, yields

$$\omega = \sqrt{\beta^2 - \alpha^2} \tag{4.58}$$

and

$$T_c = \frac{\cos^{-1}(-\alpha/\beta)}{\sqrt{\beta^2 - \alpha^2}}. \tag{4.59}$$

4.4 Example: Hawk-Dove games

As an example, consider the hawk-dove system described by Nowak [7]. There are two strategies competing for a resource with benefit b: "hawks," who will escalate fights against other players, and "doves," who will retreat from fights. So, if a hawk meets a dove, the hawk always wins, receiving benefit b, while the dove receives nothing. If two doves meet, each is equally likely to win the resource, so the expected payoff is $b/2$. If two hawks meet, they fight over the resource; each expects to gain benefit $b/2$ and incur a cost of injury $c/2$, for an expected payoff of $\frac{b-c}{2}$. Therefore the game is represented by the payoff matrix

$$A = \begin{pmatrix} \frac{b-c}{2} & b \\ 0 & \frac{b}{2} \end{pmatrix} \tag{4.60}$$

where b and c are positive numbers. (Note that b, c in equation (4.60) are not the same as b, c in equation (4.1).)

In this case, we have

$$p = \frac{b-c}{2}, \quad q = -\frac{b}{2}, \quad r = b - \frac{c}{2} \tag{4.61}$$

and equation (4.21) becomes

$$\dot{x} = \frac{1}{2}x(x-1)(c\bar{x} - b + \gamma(2b-c)(\bar{x} - x)). \tag{4.62}$$

The equilibria of the system are

$$x = 0, \quad x = 1, \quad x = \frac{b}{c}. \tag{4.63}$$

The condition for the third equilibrium to lie in the interval of physical relevance $(0, 1)$, which is that p and q must have the same sign, reduces to

$$0 < b < c. \tag{4.64}$$

Notice that this means there is an equilibrium point where both x and y are nonzero (i.e. both strategies coexist), if and only if the expected payoff $\frac{1}{2}(b - c)$ for a hawk versus another hawk is negative.

If we let

$$z = x - \frac{b}{c} \tag{4.65}$$

then the linearization about $z = 0$ is

$$\dot{z} = \frac{b(b-c)(c\bar{z} - (c-2b)(\bar{z} - z)\gamma)}{2c^2}. \tag{4.66}$$

In the case of no delay ($T = 0$ and $\bar{z} = z$) this becomes

$$\dot{z} = \frac{b(b-c)z}{2c}. \tag{4.67}$$

Therefore, if (4.64) holds – that is, if the third equilibrium lies in the interval of relevance – then the point $z = 0$ is stable for $T = 0$, for any value of γ.

If there is a Hopf bifurcation, its critical frequency (4.32) is

$$\omega = \frac{b(c-b)}{2c^{3/2}}\sqrt{4b\gamma - 2\gamma c + c}. \tag{4.68}$$

From (4.33), we see that the condition for ω to be real – i.e. for the point $z = 0$ to have a Hopf bifurcation – is

$$(2\gamma - 1)c < 4\gamma b. \tag{4.69}$$

If $\gamma \leq 1/2$, then (4.69) is trivially true, so ω is real for all hawk-dove games such that (4.64) holds. If $\gamma > 1/2$, however, ω is real only if

$$c < \frac{4b\gamma}{2\gamma - 1}. \tag{4.70}$$

It is instructive to define a new parameter k, such that

$$c = kb. \tag{4.71}$$

Intuitively, k is the *cost per unit of benefit* that the hawks are willing to incur. We can enforce conditions (4.64) and (4.69) by stipulating that $k > 1$, and if $\gamma > 1/2$,

$$k < \frac{4\gamma}{2\gamma - 1}. \tag{4.72}$$

Then in terms of b and k, the frequency ω is

$$\omega = \frac{b(k-1)\sqrt{4\gamma - 2\gamma k + k}}{2k^{3/2}} \tag{4.73}$$

The critical delay (4.35) is

$$T_c = \frac{2c^{3/2}}{b(c-b)\sqrt{4b\gamma - 2\gamma c + c}} \cos^{-1}\left(1 - \frac{c}{2b\gamma - \gamma c + c}\right) \tag{4.74}$$

$$= \frac{2k^{3/2}}{b(k-1)\sqrt{4\gamma - 2\gamma k + k}} \cos^{-1}\left(\frac{k}{(\gamma-1)k - 2\gamma} + 1\right). \tag{4.75}$$

and the amplitude of the limit cycle that is born in this bifurcation is given by equations (4.44)-(4.46):

$$R = \sqrt{\mu P/Q} \tag{4.76}$$

where $\mu = T - T_c$. The ratio P/Q can be written in terms of b and k as

$$\begin{aligned}\frac{P}{Q} = &\left[2bk^{-5/2}(k-1)^3(2\gamma(k-2)-k)(9\gamma(k-2)-5k)\right] \Big/ \\ &\Big[\sqrt{k}(k-2)^2\left(-k^2 - 6\gamma^2(k-2)^2 + 5\gamma(k-2)k\right) + \\ &\sqrt{4\gamma - 2\gamma k + k}\left(k^2(k(3k-7)+7) + 3\gamma^2(k-2)^4 - \right. \\ &\left. 3\gamma k(k(2k-5)+5)(k-2)\right)\cos^{-1}\left(\frac{k}{(\gamma-1)k - 2\gamma} + 1\right)\Big]\end{aligned} \tag{4.77}$$

In the full delay case ($\gamma = 0$) the critical frequency and delay become

$$\omega = \frac{b(k-1)}{2k} \tag{4.78}$$

and

$$T_c = \frac{\pi k}{b(k-1)} \tag{4.79}$$

and the ratio P/Q reduces to

$$\frac{P}{Q} = \frac{20b(k-1)^3}{k^3\left(\pi(k(3k-7)+7) - 2(k-2)^2\right)}. \tag{4.80}$$

In the off-diagonal case ($\gamma = 1$) these values are

$$\omega = \frac{b\sqrt{4-k}(k-1)}{2k^{3/2}} \tag{4.81}$$

and

$$T_c = \frac{2k^{3/2}\cos^{-1}\left(1-\frac{k}{2}\right)}{b\sqrt{4-k}(k-1)} \tag{4.82}$$

and

$$\frac{P}{Q} = \frac{-2b\sqrt{4-k}(k-1)^3(2k-9)k^{-5/2}}{(k-3)\sqrt{-(k-4)k}(k-2)^2 + (24-(k-3)k(2k-11))\cos^{-1}\left(1-\frac{k}{2}\right)} \tag{4.83}$$

Note that in terms of b and k, for all values of γ

$$\omega \propto b, \quad T_c \propto \frac{1}{b}, \quad \frac{P}{Q} \propto b. \tag{4.84}$$

Therefore, we can divide each of these quantities by the appropriate power of b to obtain normalized versions that depend only on the parameter k.

Observe (Figures 4.2, 4.3, 4.4) that when $k = 2$, ω, T_c and P/Q do not change as γ varies. In fact, for $k = 2$ they reduce to

$$\omega = \frac{b}{4}, \quad T_c = \frac{2\pi}{b}, \quad P/Q = \frac{b}{2\pi}. \tag{4.85}$$

This is to be expected, since for this value of k the hawk-dove replicator equation (4.62) does not depend on γ. It reduces to

$$\dot{x} = \frac{1}{2}b(x-1)x(2\bar{x}-1). \tag{4.86}$$

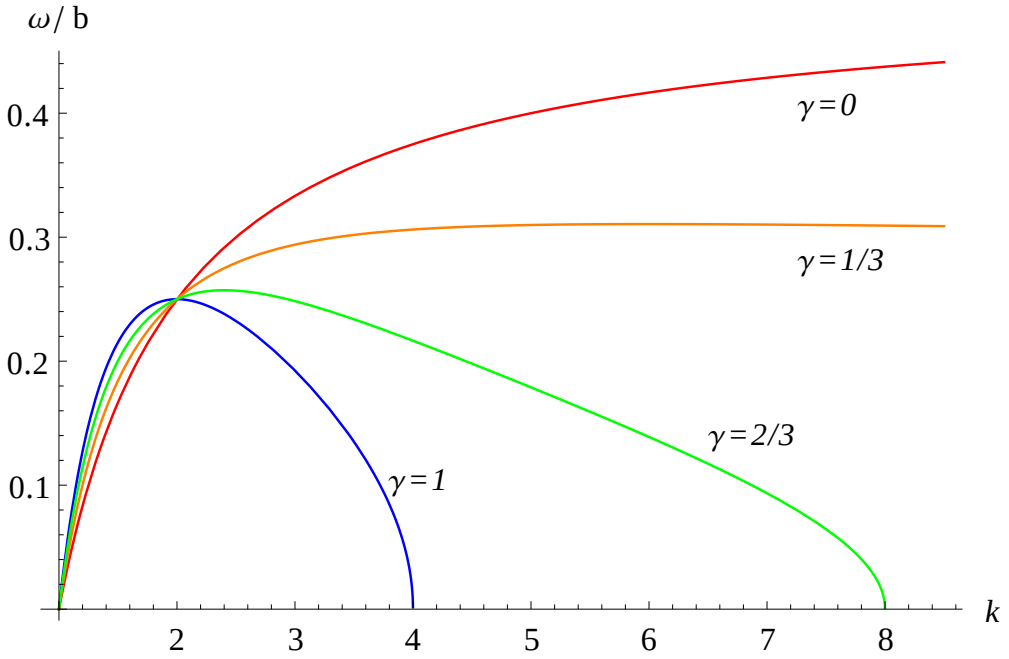

Figure 4.2: Normalized frequency ω/b, at the Hopf bifurcation in the hawk-dove system, as a function of $k = c/b$. Red: full type delay ($\gamma = 0$). Blue: off-diagonal delay ($\gamma = 1$). Orange: $\gamma = 1/3$. Green: $\gamma = 2/3$.

We see by plotting the normalized version of (4.77) (Figure 4.4) that $P/Q > 0$, so for the amplitude R to be real, μ must also be positive. Thus the Hopf bifurcation is supercritical, and the limit cycle is stable.

Finally, we compare the results of this perturbation method to those obtained by continuation in DDE-Biftool for the particular case $b = 1$ and $c = k = 3$, for $\gamma = 0$, $\gamma = 1/3$, $\gamma = 2/3$, and $\gamma = 1$. (The latter method is outlined by Heckman, [3].) Note that the amplitude given by DDE-Biftool is the full width of the limit cycle, twice the amplitude predicted by Lindstedt's method, which is the average displacement from the equilibrium point. We observe from Figure 4.5 that for all tested values of γ the results of the two methods are in good agreement for values of T reasonably close to T_c.

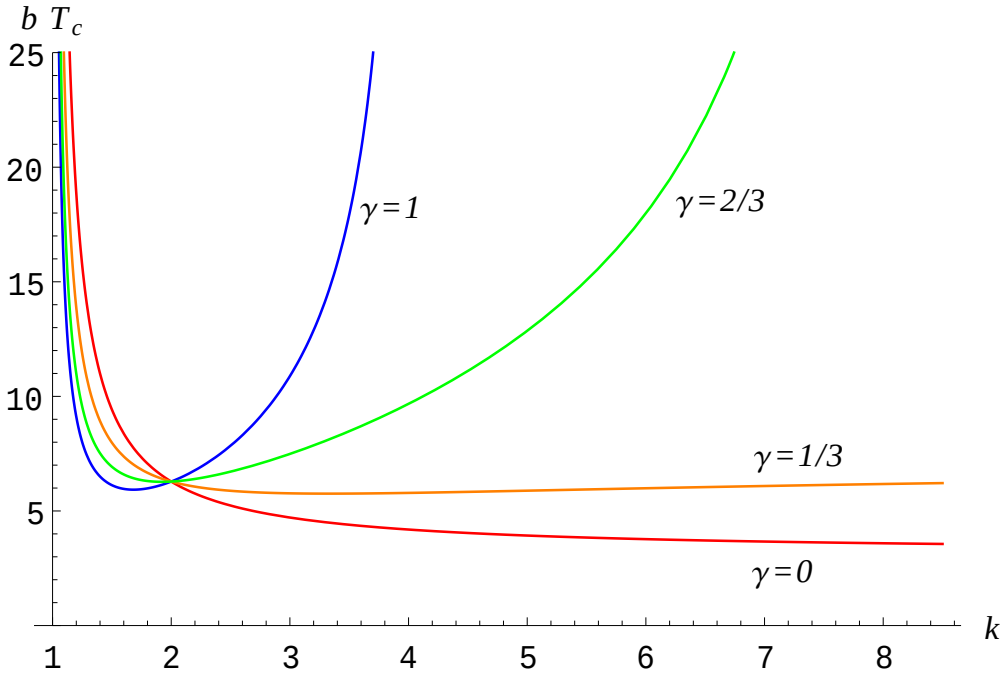

Figure 4.3: Normalized critical delay bT_c, for the Hopf, as a function of $k = c/b$. Red: full type delay ($\gamma = 0$). Blue: off-diagonal delay ($\gamma = 1$). Orange: $\gamma = 1/3$. Green: $\gamma = 2/3$.

Conclusion

We have investigated the dynamics of two-strategy replicator systems with delay. We have considered a range of models indexed by a homotopy parameter γ, which determines the relative weights of delayed and non-delayed terms when determining the fitness arising from interactions with agents having the same strategy. (Interactions between agents with different strategies are always delayed). At one extreme ($\gamma = 0$) the model describes a full-type delay in which the fitness of each strategy is the delayed expected payoff of that strategy. At the other extreme ($\gamma = 1$) only the opposite-strategy terms in each fitness function are delayed.

It is well known that periodic motions cannot occur in non-delayed two-

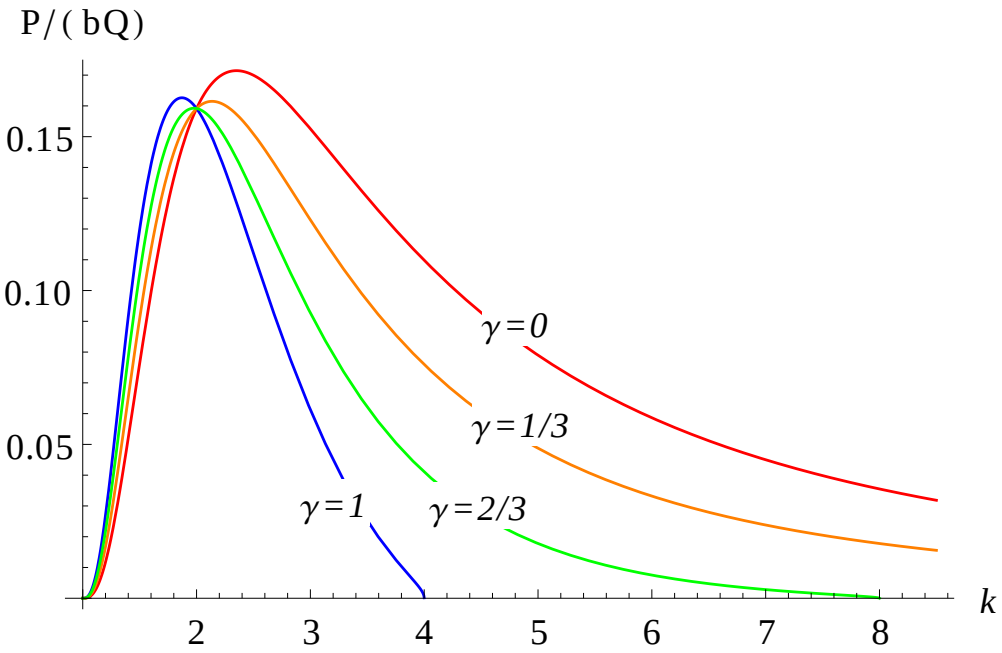

Figure 4.4: Normalized growth coefficient $\frac{P}{bQ}$, for the Hopf, as a function of $k = c/b$. Red: full type delay ($\gamma = 0$). Blue: off-diagonal delay ($\gamma = 1$). Orange: $\gamma = 1/3$. Green: $\gamma = 2/3$.

strategy replicator systems, since the phase space is one-dimensional. The introduction of delay makes the system into a DDE, so the phase space is infinite-dimensional.

In this work, we have shown that, for all values of γ, there exist two-strategy games for which non-degenerate Hopf bifurcations and limit cycles occur. In the full delay case ($\gamma = 0$) Hopf bifurcations occur for all two-strategy games. For $\gamma > 0$, there exist two-strategy games for which there is no Hopf bifurcation.

In particular, we have demonstrated a range of parameters for which Hawk-Dove systems with delayed competition exhibit stable limit cycles which are born in Hopf bifurcations. We have used Lindstedt's method to approximate the amplitude of the limit cycles, and we have shown that this approximation agrees with the results of numerical continuation.

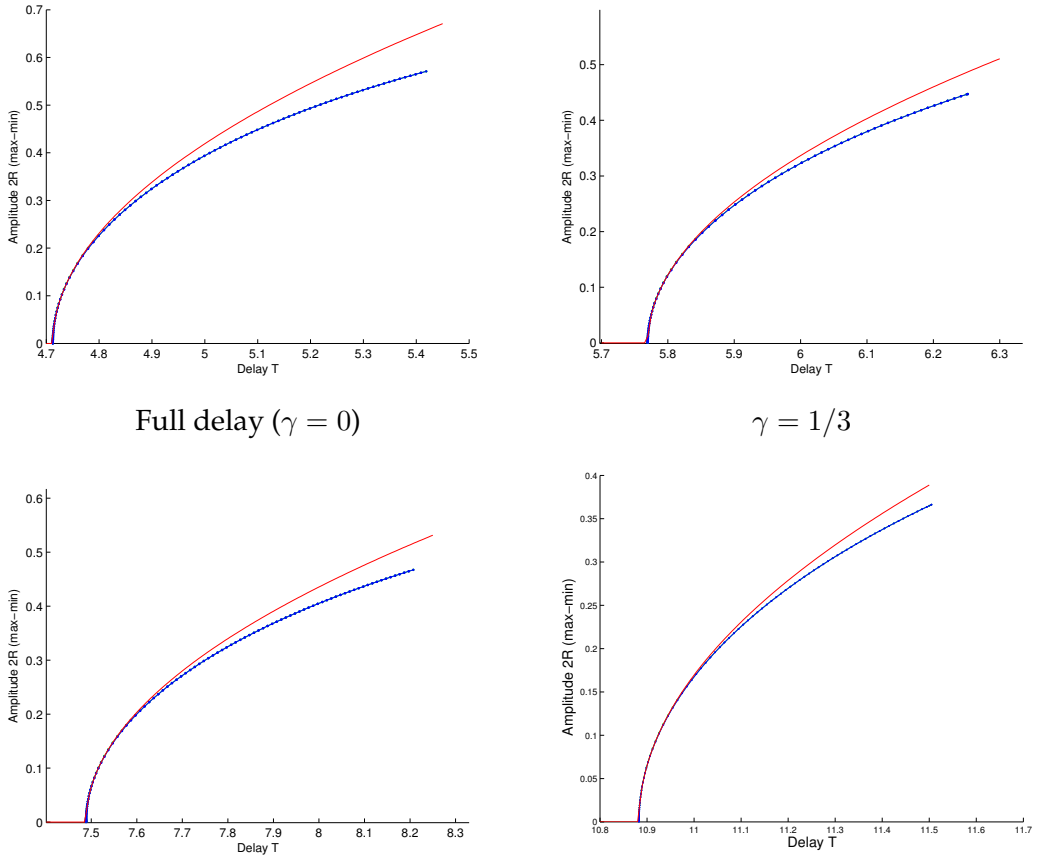

Figure 4.5: Amplitude of limit cycle vs. T in the hawk-dove system with $b = 1$, $c = k = 3$ given by Lindstedt (upper curve, red) and continuation in DDE-Biftool (lower curve, blue), for various values of γ.

This generalization of the replicator equation may be useful in modeling a range of scenarios, given the ubiquity and heterogeneity of delay in real-world applications. It is often the case that people have more accurate and up to date information about those who are more similar to themselves, and that organisms which have the same phenotype are located closer to each other. Thus it may well be that delay plays a bigger role in interactions between agents with different strategies than agents with the same strategy. The framework we introduce here demonstrates the important consequences such heterogeneous delays

can have on the system's evolutionary dynamics.

CHAPTER 5

ROCK-PAPER-SCISSORS WITH QUASIPERIODIC FORCING

5.1 Introduction

In this chapter, we generalize the replicator model to systems in which the payoff coefficients are quasiperiodic functions of time. Previous work by Ruelas and Rand [11, 12] investigated the Rock-Paper-Scissors replicator dynamics problem with periodic forcing of the payoff coefficients. We also consider a forced Rock-Paper-Scissors system. The quasiperiodically forced replicator model may find applications in biological or social systems where competition is affected by cyclical processes on different scales, such as days/years or weeks/years.

5.2 The model

5.2.1 Rock-Paper-Scissors games with quasiperiodic forcing

Rock-Paper-Scissors (RPS) games are a class of three-strategy evolutionary games in which each strategy is neutral vs. itself, and has a positive expected payoff vs. one of the other strategies and a negative expected payoff vs. the remaining strategy. The payoff matrix is thus

$$A = \begin{pmatrix} 0 & -b_2 & a_1 \\ a_2 & 0 & -b_3 \\ -b_1 & a_3 & 0 \end{pmatrix}. \tag{5.1}$$

We perturb off of the canonical case, $a_1 = \cdots = b_3 = 1$, by taking

$$A = \begin{pmatrix} 0 & -1 - F(t) & 1 + F(t) \\ 1 & 0 & -1 \\ -1 & 1 & 0 \end{pmatrix} \tag{5.2}$$

where the forcing function F is given by

$$F(t) = \epsilon((1 - \delta)\cos\omega_1 t + \delta\cos\omega_2 t). \tag{5.3}$$

For ease of notation, write $(x_1, x_2, x_3) = (x, y, z)$. The dynamics occur in the simplex

$$S \equiv \{(x, y, z) \in \mathbb{R} \,|\, x, y, z \in [0, 1]\} \tag{5.4}$$

but since x, y, z are the frequencies of the three strategies, and hence $x+y+z = 1$, we can eliminate z using $z = 1 - x - y$. Therefore, the region of interest is T, the projection of S into the $x - y$ plane:

$$T \equiv \{(x, y) \in \mathbb{R} \,|\, x, y, x + y \in [0, 1]\}. \tag{5.5}$$

See Figure 5.1. Thus the replicator equation becomes

$$\dot{x} = -x(x + 2y - 1)(1 + (x - 1)F(t)) \tag{5.6}$$

$$\dot{y} = y(2x + y - 1 - x(x + 2y - 1)F(t)) \tag{5.7}$$

Note that $\dot{x} = 0$ when $x = 0$, $\dot{y} = 0$ when $y = 0$, and

$$\dot{x} + \dot{y} = (x + y - 1)(xF(t)(x + 2y - 1) - x + y) \tag{5.8}$$

so that $\dot{x} + \dot{y} = 0$ when $x + y = 1$, which means that $x + y = 1$ is an invariant manifold. This shows that the boundary of T is invariant, so trajectories cannot escape the region of interest.

It is known [7] that in the unperturbed case ($\epsilon = 0$) there is an equilibrium point at $(x, y) = (\frac{1}{3}, \frac{1}{3})$, and the interior of T is filled with periodic orbits. We see from equations (5.6)-(5.7) that this interior equilibrium point persists when $\epsilon \neq 0$. Numerical integration suggests that the Lyapunov stability of motions around the equilibrium point depends sensitively on the values of ω_1 and ω_2. See Figure 5.2. We investigate the stability of the interior equilibrium using Floquet theory and harmonic balance, as well as by numerical methods.

5.2.2 Linearization

To study the linear stability of the equilibrium point, we set $x = u + \frac{1}{3}$, $y = v + \frac{1}{3}$, substitute these into (5.6)-(5.7) and linearize, to obtain

$$\dot{u} = -\frac{1}{9}(u + 2v)(3 + 2F(t)) \tag{5.9}$$

$$\dot{v} = \frac{1}{9}(F(t)(u + 2v) + 3(2u + v)). \tag{5.10}$$

The linearized system (5.9)-(5.10) can also be written [10] as a single second-order equation on u, by differentiating (5.9) and substituting in expressions for $\dot{v}$ from (5.10) and v from (5.9). This gives us

$$g(t)\ddot{u} - \dot{g}(t)\dot{u} - \frac{1}{9}g^2(t)u = 0 \tag{5.11}$$

where

$$g(t) = -3 - 2F(t) = -3 - 2\epsilon((1 - \delta)\cos\omega_1 t + \delta\cos\omega_2 t). \tag{5.12}$$

Now that we have a linear system with coefficients that are functions of time, we use Floquet theory to determine the stability of the origin.

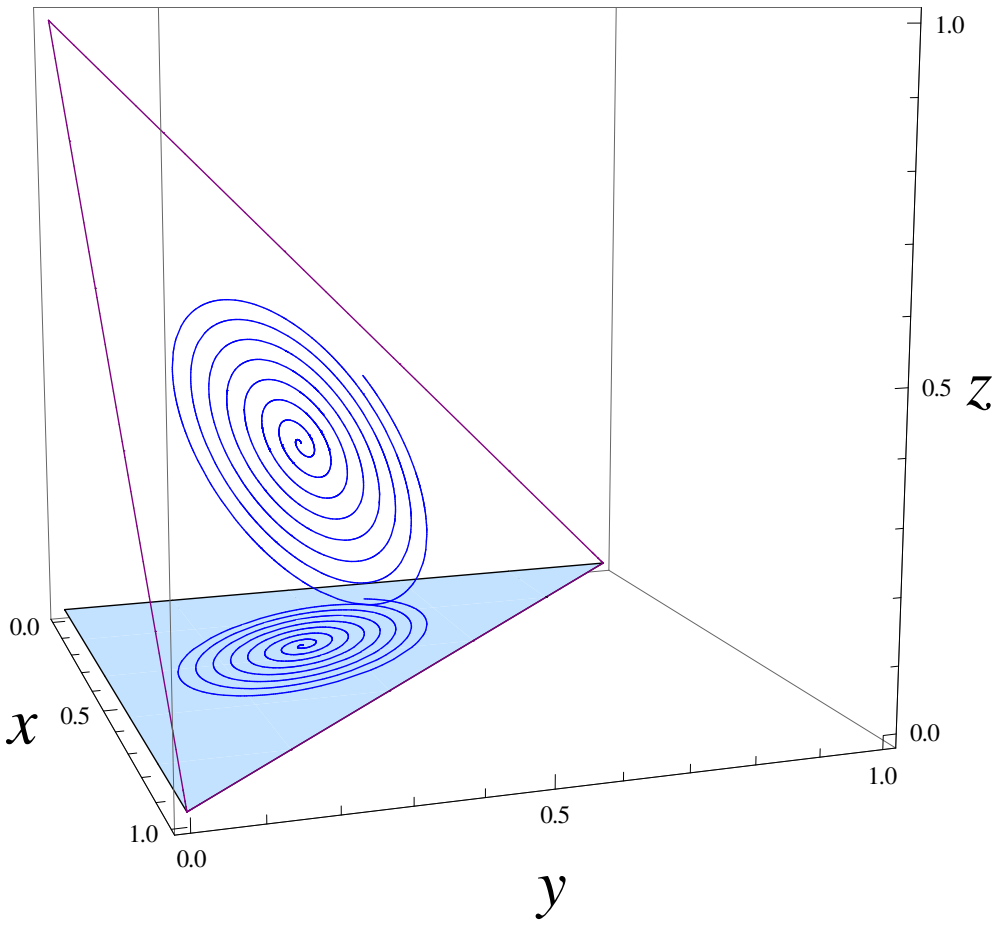

Figure 5.1: A curve in S and its projection in T

5.3 Floquet theory

Floquet theory is concerned with systems of differential equations of the form

$$\frac{dx}{dt} = M(t)x, \quad M(t+T) = M(t). \tag{5.13}$$

We have the system (5.9)-(5.10), which can be written as

$$\begin{bmatrix} \dot{u} \\ \dot{v} \end{bmatrix} = \frac{1}{9} \begin{bmatrix} g(t) & 2g(t) \\ \frac{1}{2}(9 - g(t)) & -g(t) \end{bmatrix} \begin{bmatrix} u \\ v \end{bmatrix} \equiv B(t) \begin{bmatrix} u \\ v \end{bmatrix} \tag{5.14}$$

where $g(t)$ is as in (5.12).

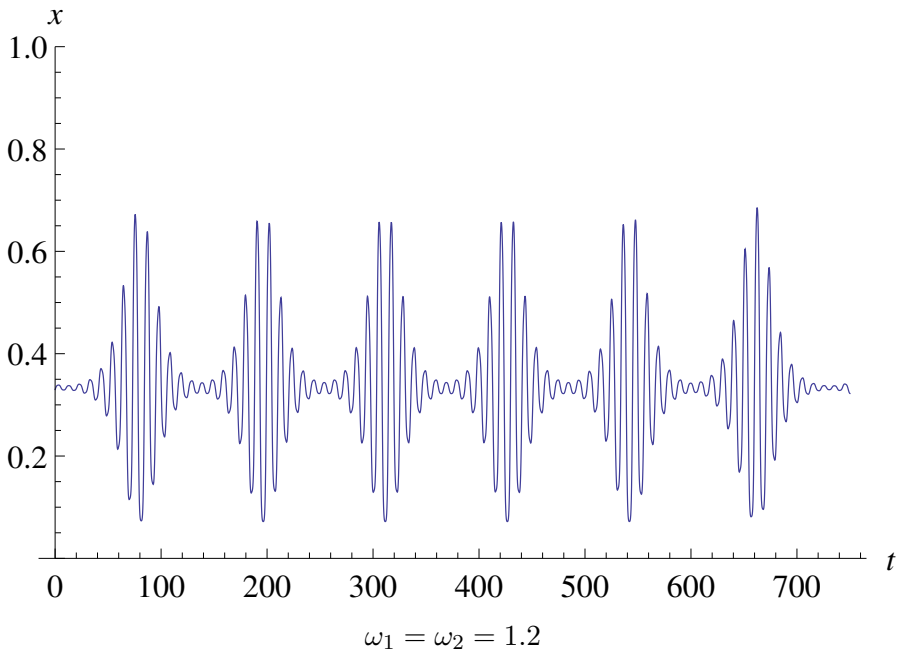

$\omega_1 = \omega_2 = 1.2$

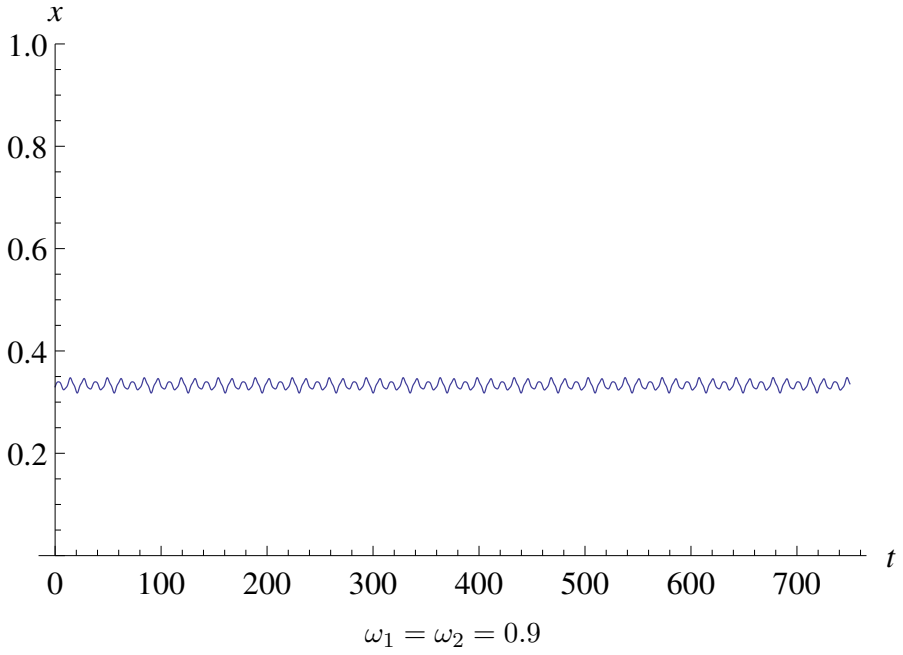

$\omega_1 = \omega_2 = 0.9$

Figure 5.2: Numerical solutions for $x(t)$ with identical initial conditions $x(0) = y(0) = 0.33$ and parameters $\epsilon = 0.9, \delta = 0.6$, but with different ω_1, ω_2

In general, $B(t)$ is not periodic, since ω_1 and ω_2 are rationally independent. However, the set of points for which ω_1 and ω_2 are rationally dependent is dense in the $\omega_1 - \omega_2$ plane, and solutions of (5.14) must vary continuously with ω_1 and ω_2. This means that for any $d > 0$ and finite time interval $[0, M]$, there exists some $r(d, M)$ such that if the distance between two choices of (ω_1, ω_2) is less than r, then the distance between the corresponding solutions of (5.14) is less than d for all $t \in [0, M]$.

We consider an empirical notion of stability: given a maximum time M, we choose a threshold value k. If solutions of (5.14) for a particular choice of (ω_1, ω_2) expand by more than a factor of k in the time interval $[0, M]$, we consider the point (ω_1, ω_2) to be unstable. By the above continuity argument, if a rationally related choice of (ω_1, ω_2) is unstable under this definition, then so are all sufficiently close points (ω_1', ω_2'). (Note that the radius of the ball of unstable points around (ω_1, ω_2) depends on the amount by which the solution's expansion exceeds the threshold k.)

Therefore, for this empirical notion of stability, it is reasonable to consider only the case that $F(t)$, and hence $g(t)$ and $B(t)$, are in fact periodic.

Assume that $\omega_2 = \frac{a}{b}\omega_1$ in lowest terms, where a and b are relatively prime integers. Then we can make the change of variables $\tau = \omega_1 t$, so $\omega_2 t = \frac{a}{b}\tau$. Since a and b are relatively prime, we see that F, and hence g and B, have period $T = 2\pi b$ in τ. Thus (5.14) becomes

$$\begin{bmatrix} u' \\ v' \end{bmatrix} = \frac{1}{\omega_1} B(\tau) \begin{bmatrix} u \\ v \end{bmatrix}, \quad B(\tau + 2\pi b) = B(\tau) \tag{5.15}$$

where u' indicates $du/d\tau$. This has the same form as (5.13), so we can apply the results of Floquet theory.

Suppose that there is a fundamental solution matrix of (5.15),

$$X(\tau) = \begin{bmatrix} u_1(\tau) & u_2(\tau) \\ v_1(\tau) & v_2(\tau) \end{bmatrix} \tag{5.16}$$

where

$$\begin{bmatrix} u_1(0) \\ v_1(0) \end{bmatrix} = \begin{bmatrix} 1 \\ 0 \end{bmatrix}, \quad \begin{bmatrix} u_2(0) \\ v_2(0) \end{bmatrix} = \begin{bmatrix} 0 \\ 1 \end{bmatrix}. \tag{5.17}$$

Then the Floquet matrix is $C = X(T) = X(2\pi b)$, and stability is determined by the eigenvalues of C:

$$\lambda^2 - (\text{tr}C)\lambda + \det C = 0. \tag{5.18}$$

We can show [8] that $\det C = 1$, as follows. Define the Wronskian

$$W(\tau) = \det X(\tau) = u_1(\tau)v_2(\tau) - u_2(\tau)v_1(\tau). \tag{5.19}$$

Notice that $W(0) = \det X(0) = 1$. Then taking the time derivative of W and using (5.15) gives

$$\begin{aligned} \frac{dW}{d\tau} &= u_1'(\tau)v_2(\tau) + u_1(\tau)v_2'(\tau) - u_2'(\tau)v_1(\tau) - u_2(\tau)v_1'(\tau) \\ &= \frac{1}{9\omega_1}\Bigg(g(\tau)(u_1 + 2v_1)v_2 + \frac{1}{2}u_1(9u_2 - (u_2 + 2v_2)g(\tau)) \\ &\quad -g(\tau)(u_2 + 2v_2)v_1 - \frac{1}{2}u_2(9u_1 - (u_1 + 2v_1)g(\tau))\Bigg) = 0. \end{aligned} \tag{5.20}$$

This shows that $W(\tau) = 1$ for all τ, and in particular $W(T) = \det C = 1$. Therefore,

$$\lambda = \frac{\text{tr}C \pm \sqrt{\text{tr}C^2 - 4}}{2} \tag{5.21}$$

which means [8] that the transition between stable and unstable solutions occurs when $|\text{tr}C| = 2$, and this corresponds to periodic solutions of period $T = 2\pi b$ or $2T = 4\pi b$.

Given the period of the solutions on the transition curves in the $\omega_1 - \omega_2$ plane, we use harmonic balance to approximate those transition curves.

5.4 Harmonic balance

We seek solutions to (5.11) of period $4\pi b$ in τ:

$$u = \sum_{k=0}^{\infty} \alpha_k \cos\left(\frac{k\tau}{2b}\right) + \beta_k \sin\left(\frac{k\tau}{2b}\right). \tag{5.22}$$

Since $\omega_2 = \frac{a}{b}\omega_1$ where a and b are relatively prime, any integer k can be written as $na + mb$ for some integers n and m [17, 4]. That is, there is a one-to-one correspondence between integers k and ordered pairs (m, n). We can therefore write the solution as

$$u = \sum_{m=0}^{\infty} \sum_{n=-\infty}^{\infty} \alpha_{mn} \cos\left(\frac{ma+nb}{2b}\tau\right) + \beta_{mn} \sin\left(\frac{ma+nb}{2b}\tau\right) \tag{5.23}$$

$$= \sum_{m=0}^{\infty} \sum_{n=-\infty}^{\infty} \alpha_{mn} \cos\left(\frac{m\omega_2+n\omega_1}{2}t\right) + \beta_{mn} \sin\left(\frac{m\omega_2+n\omega_1}{2}t\right). \tag{5.24}$$

We substitute a truncated version of (5.24) into (5.11), expand the trigonometric functions and collect like terms. This results in cosine terms whose coefficients are functions of the α_{mn}, and sine terms whose coefficients are functions of the β_{mn}. Let the coefficient matrices of these two sets of terms be Q and R, respectively. In order for a nontrivial solution to exist, the determinants of both coefficient matrices must vanish [8]. We solve the equations $\det Q = 0$ and $\det R = 0$ for relations between ω_1 and ω_2. This gives the approximate transition curves seen in Figure 5.3.

It has been shown [11, 10] that in a periodically forced RPS system (i.e. $\delta = 0$ in our model) there are tongues of instability emerging from $\omega_1 = 2/n\sqrt{3}$ in the $\omega_1 - \epsilon$ plane. Our harmonic balance analysis is consistent with this: we observe bands of instability around $\omega_1 = 2/\sqrt{3}$ and $\omega_2 = 2/\sqrt{3}$, which get broader as ϵ increases. We also see narrower regions of instability along the lines $n\omega_1 + m\omega_2 = 2/\sqrt{3}$, for each n, m used in the truncated solution (5.24).

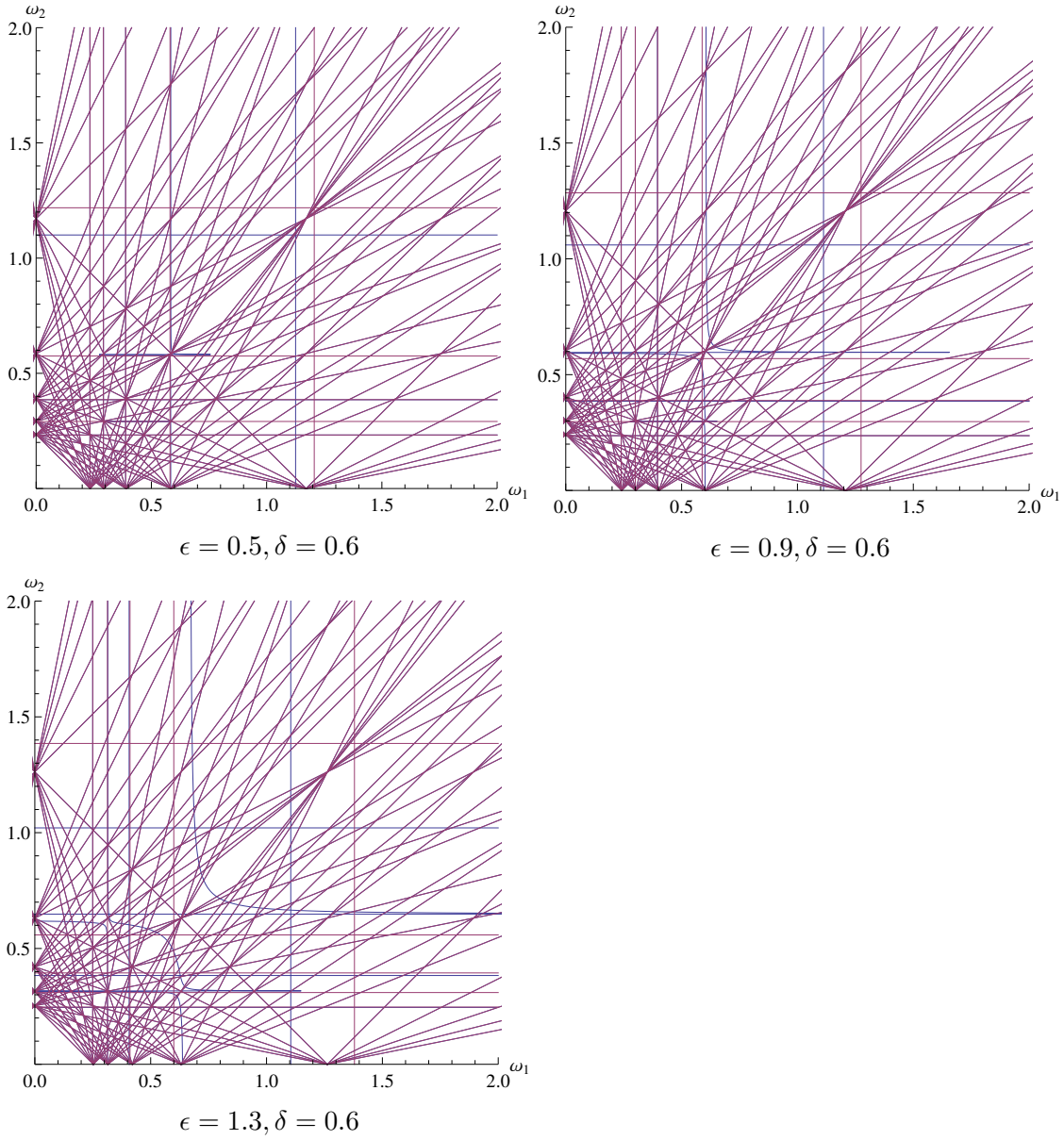

$\epsilon = 0.5, \delta = 0.6$ $\epsilon = 0.9, \delta = 0.6$

$\epsilon = 1.3, \delta = 0.6$

Figure 5.3: Transition curves predicted by harmonic balance with $-5 \leq m \leq 5$, $0 \leq n \leq 5$ for various values of ϵ

Thus the boundary of the region of instability exhibits self-similarity when we consider $\omega_1, \omega_2 \in [0, 2^{1-k}]$ for $k = 0, 1, \ldots$.

5.5 Numerical integration

In order to check the results of the harmonic balance method, we generate an approximate stability diagram by numerical integration of the linearized system (5.11).

For randomly chosen parameters $(\omega_1, \omega_2) \in [0, 2]$, we choose random initial conditions $(u(0), \dot{u}(0))$ on the unit circle - since the system is linear, the amplitude of the initial condition needs only to be consistent between trials. We then integrate the system for 1000 time steps using `ode45` in Matlab. This is an explicit Runge-Kutta (4,5) method that is recommended in the Matlab documentation for most non-stiff problems. We considered a motion to be unstable if $\max|u(t)| > 10$. The set of points (ω_1, ω_2) corresponding to unstable motions were plotted using `matplotlib.pyplot` in Python. See Figure 5.4. Each plot in Figure 5.4 contains approximately 5×10^4 points.

We note that the unstable regions given by numerical integration appear to be consistent with the transition curves predicted by harmonic balance (Figure 5.3). The regions of instability around $\omega_1 = 2/\sqrt{3}$ and $\omega_2 = 2/\sqrt{3}$ are visible for all tested values of ϵ and δ, and as ϵ increases, more tongues of the form $n\omega_1 + m\omega_2 = 2/\sqrt{3}$ become visible.

5.6 Lyapunov exponents

A second, and more informative, numerical approach for determining stability is the computation of approximate Lyapunov exponents. This is a measure of a

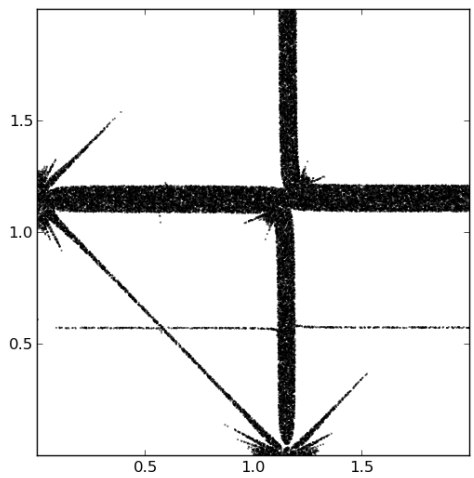

$\epsilon = 0.5, \delta = 0.6$

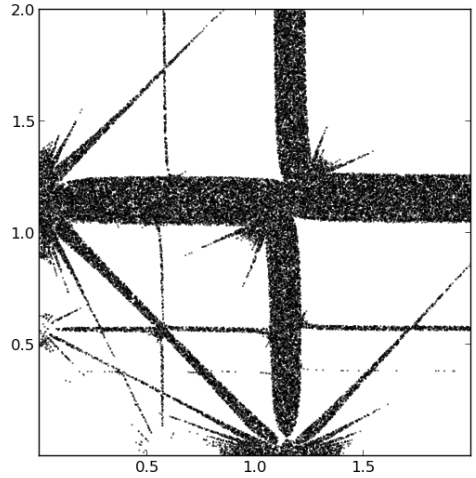

$\epsilon = 0.9, \delta = 0.6$

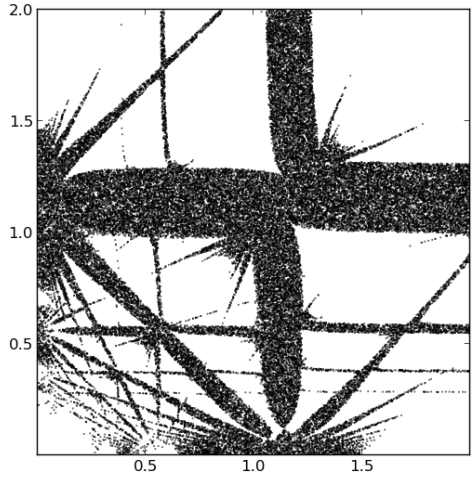

$\epsilon = 1.3, \delta = 0.6$

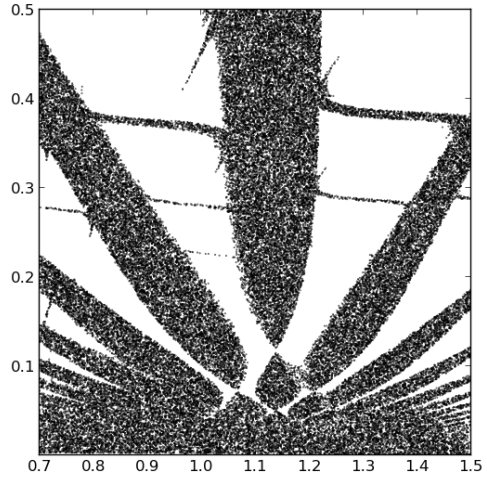

Detail view: $\epsilon = 1.3, \delta = 0.6$

Figure 5.4: Plots of unstable points in the (ω_1, ω_2) plane for various values of ϵ

solution's rate of divergence from the equilibrium point [2], and is defined as

$$\lambda = \limsup_{t\to\infty} \frac{1}{t} \ln |u(t)|. \tag{5.25}$$

If the limit is finite, then $u(t) \sim e^{\lambda t}$ or smaller as $t \to \infty$. A positive Lyapunov exponent indicates that the solution is unstable.

We do not find any negative Lyapunov exponents, but note [8] that the system (5.11) can be converted to a Hill's equation

$$\ddot{z} - z\left(\frac{4g(t)^3 + 27\dot{g}(t)^2 - 18g(t)\ddot{g}(t)}{36g(t)^2}\right) = 0 \tag{5.26}$$

by making the change of variables $u = \sqrt{g(t)}z$. Since $\sqrt{g(t)}$ is bounded, u is bounded if and only if z is bounded. And since there is no dissipation in (5.26), stable solutions correspond to $\lambda = 0$.

We approximate the Lyapunov exponents numerically by integrating as above, and taking

$$\lambda \approx \sup_{900<t<1000} \frac{1}{t} \ln |u(t)|. \tag{5.27}$$

See Figures 5.5-5.8. The shape of the unstable region is the same as in Figure 5.4, but this method allows us to see a sharp increase in unstable solutions' rate of growth along the line $\omega_1 = \omega_2$.

5.7 Conclusion

The replicator equation with quasiperiodic perturbation may be used to model biological or social systems where competition is affected by cyclical processes on different scales. We have investigated the linear stability of the interior equilibrium point for RPS systems with quasiperiodic perturbation, using Floquet

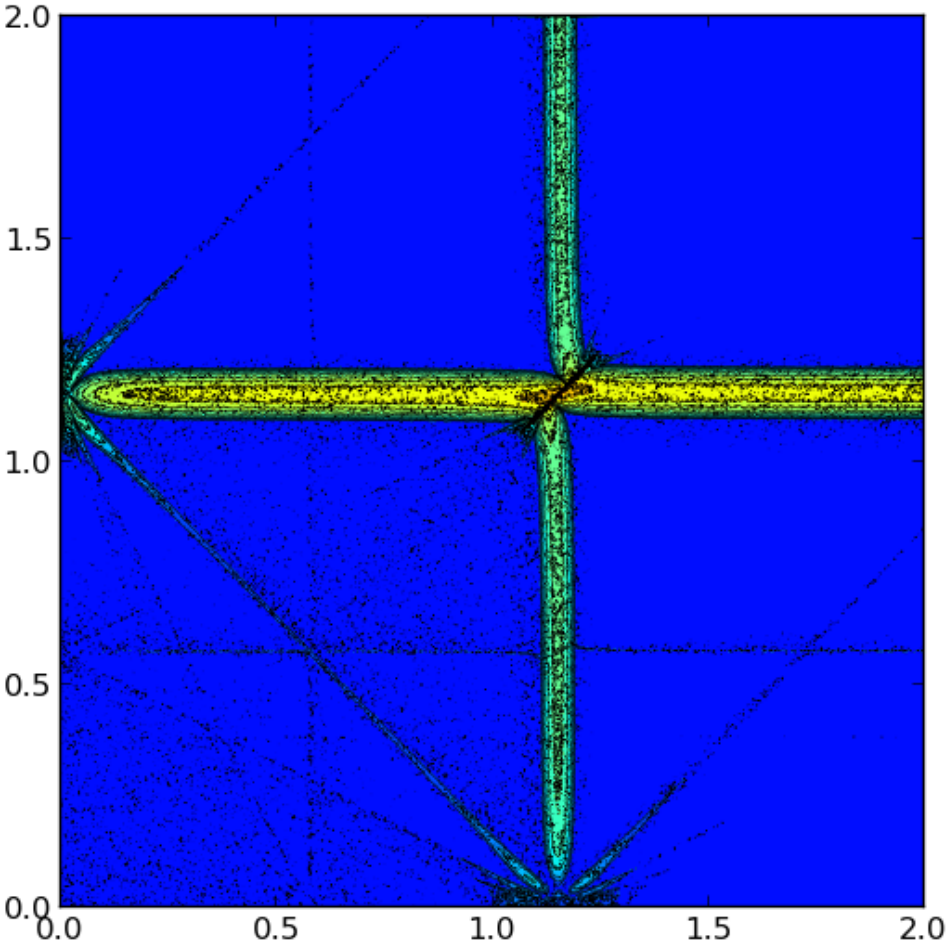

Figure 5.5: Contour plot of Lyapunov exponents in the (ω_1, ω_2) plane for $\epsilon = 0.5, \delta = 0.6$. Contours between $\lambda = 0$ and $\lambda = 0.04$.

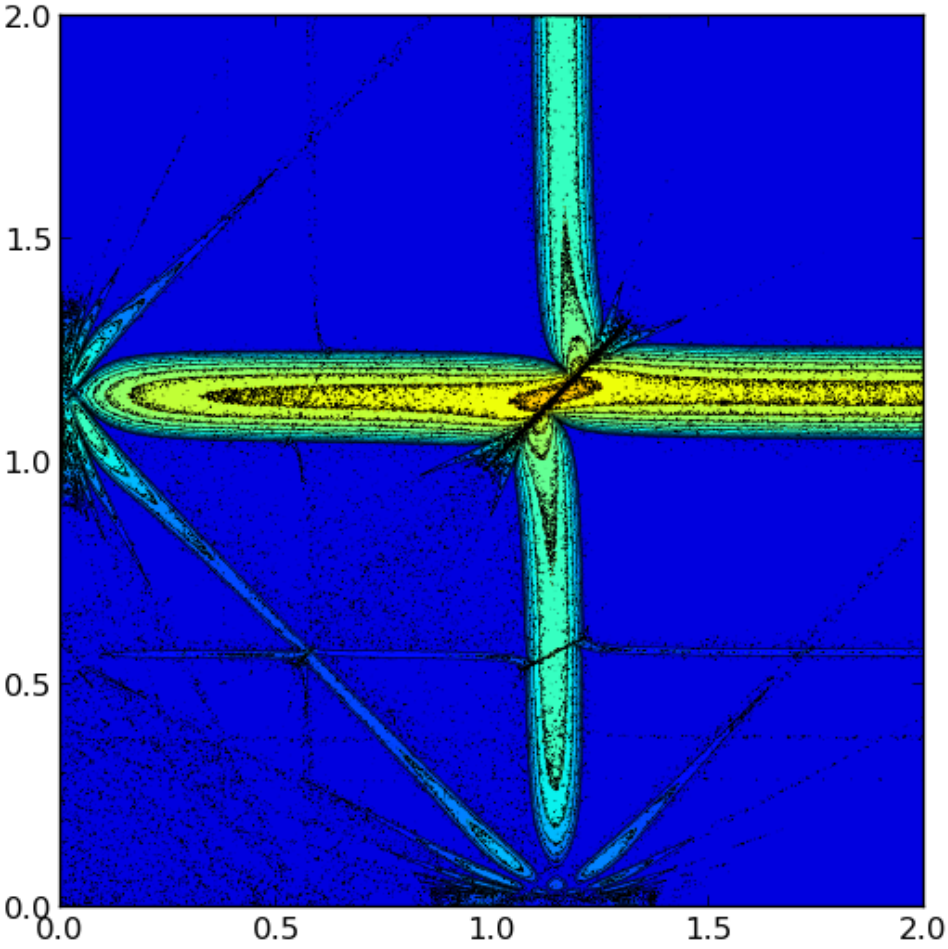

Figure 5.6: Contour plot of Lyapunov exponents in the (ω_1, ω_2) plane for $\epsilon = 0.9, \delta = 0.6$. Contours between $\lambda = 0$ and $\lambda = 0.08$.

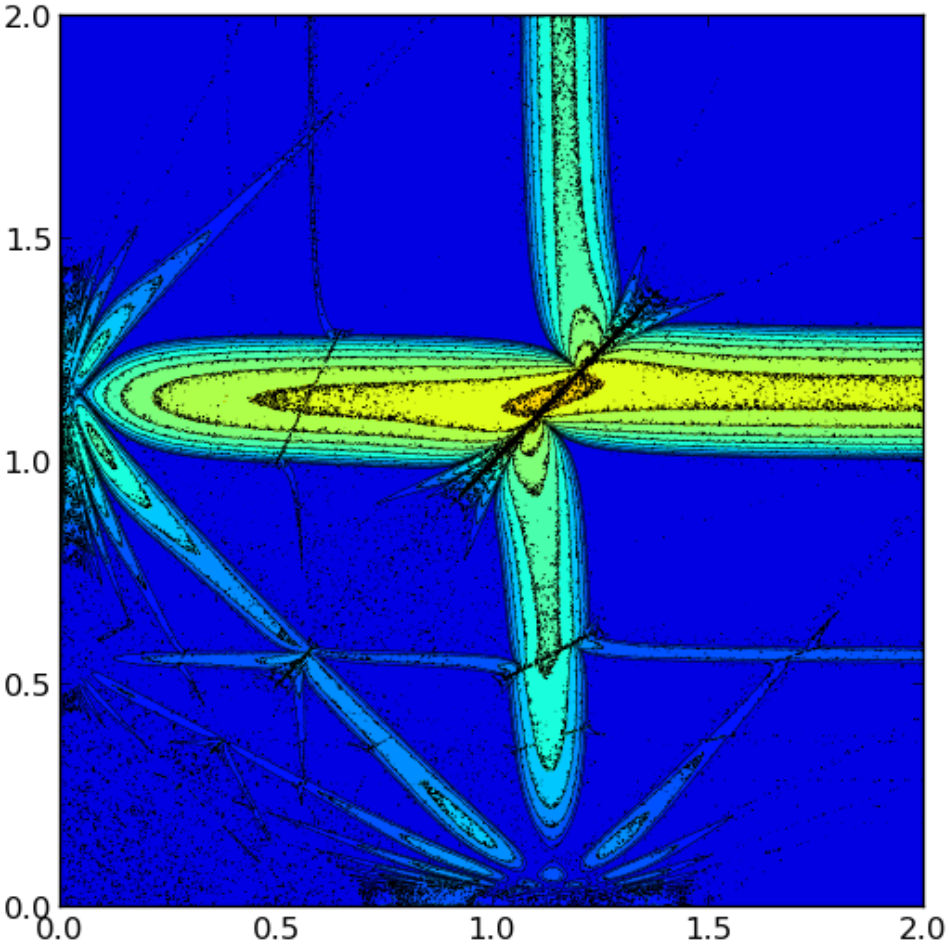

Figure 5.7: Contour plot of Lyapunov exponents in the (ω_1, ω_2) plane for $\epsilon = 1.3, \delta = 0.6$. Contours between $\lambda = 0$ and $\lambda = 0.12$.

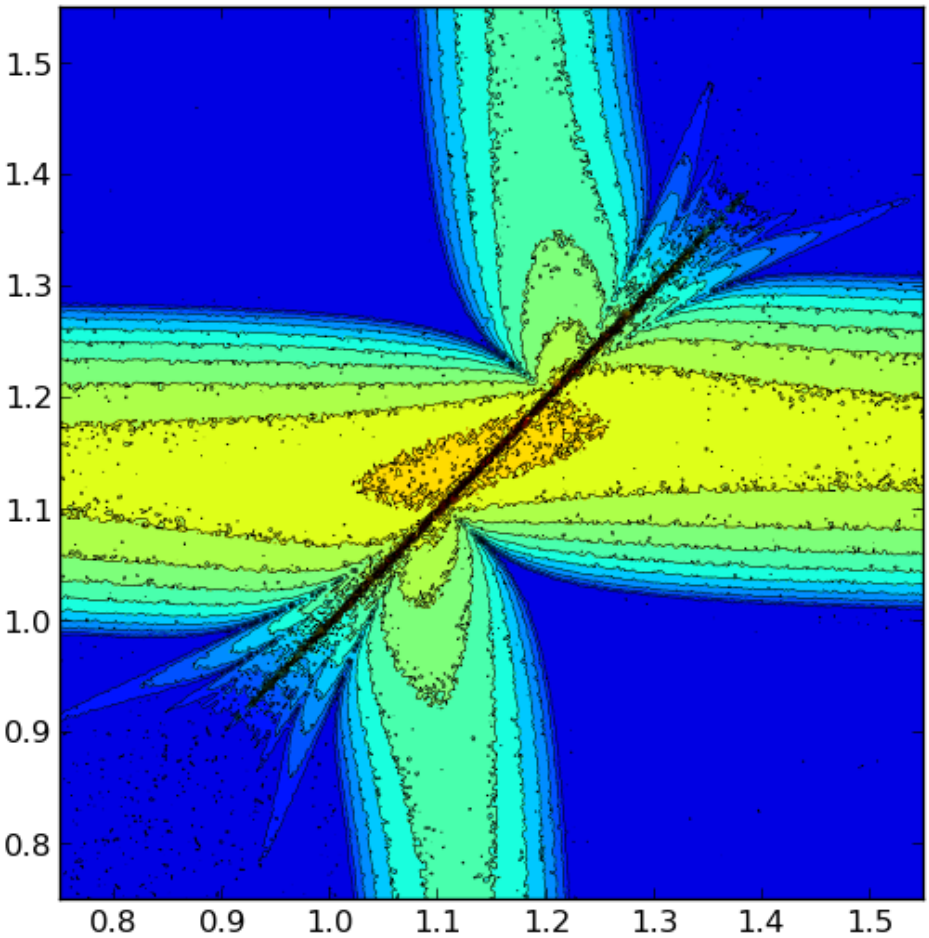

Figure 5.8: Detail view: contour plot of Lyapunov exponents in the (ω_1, ω_2) plane for $\epsilon = 0.5, \delta = 0.6$. Contours between $\lambda = 0$ and $\lambda = 0.12$.

theory and harmonic balance, as well as numerical integration and numerical computation of Lyapunov exponents. We find that stability depends sensitively on the frequencies ω_1 and ω_2, and that the region of instability in the $\omega_1 - \omega_2$ plane exhibits self-similarity.

BIBLIOGRAPHY

[1] Erneux, T., 2009. *Applied Differential Delay Equations.* Springer Science+Business Media, New York.

[2] Guckenheimer, J. and Holmes, P., 1983. *Nonlinear Oscillations, Dynamical Systems, and Bifurcations of Vector Fields.* Springer-Verlag, New York.

[3] Heckman, C., 2012. "Numerical Continuation Using DDE-Biftool." Retrieved from `http://www.math.cornell.edu/~rand/randdocs/Heckman\_DDEBiftool/` Accessed 2014-03-24.

[4] Herstein, I., 1975. *Topics in Algebra*, 2nd ed., John Wiley & Sons, New York.

[5] Hofbauer, J. and Sigmund, K., 1998. *Evolutionary Games and Population Dynamics.* Cambridge University Press, Cambridge, UK.

[6] Miekisz, J., 2008. "Evolutionary game theory and population dynamics." In *Multiscale Problems in the Life Sciences*, 269-316. Lecture Notes in Math. 1940, Springer, Berlin.

[7] Nowak, M., 2006. *Evolutionary Dynamics.* Belknap Press of Harvard Univ. Press, Cambridge, MA.

[8] Rand, R., 2012. *Lecture Notes on Nonlinear Vibrations*. Published online by The Internet-First University Press, `http://ecommons.library.cornell.edu/handle/1813/28989`

[9] Rand, R. and Verdugo, A., 2007. "Hopf bifurcation formula for first order differential-delay equations." Commun Nonlinear Sci Numer Simulat 12 (2007) 859-864.

[10] Rand, R., Yazhbin, M., and Rand, D., 2011. "Evolutionary dynamics of a system with periodic coefficients." *Comm Nonlinear Sci Numer Simulat*, 16:3887-3895.

[11] Ruelas, R., Rand, D., and Rand, R., 2012. "Nonlinear parametric excitation of an evolutionary dynamical system." *J. Mechanical Engineering science (Proceedings Inst. Mech. Eng., Part C)*, 226:1912-1920.

[12] Ruelas, R., Rand, D., and Rand, R., 2013. "Parametric Excitation and Evolutionary Dynamics." *J. Applied Mechanics* 80, 051013

[13] Sigmund, K., 2011. "Introduction to Evolutionary Game Theory." In *Evolutionary Game Dynamics*, K. Sigmund, ed., Vol. 69 of *Proceedings of Symposia in Applied Mathematics*. American Mathematical Society, Chap. 1, pp. 1-26.

[14] Taylor, P. and Jonker, L., 1978. "Evolutionarily Stable Strategies and Game Dynamics." *Mathematical Biosciences* **40**(1-2), pp. 145-156.

[15] Wesson, E. and Rand, R., 2014. "Hopf Bifurcations in Delayed Rock-Paper-Scissors Replicator Dynamics." Dynamic Games and Applications. DOI: 10.1007/s13235-015-0138-2.

[16] Yi, T. and Zuwang, W., 1997. "Effect of time delay and evolutionarily stable strategy." J Theor Biol. 187(1):111-116.

[17] Zounes, R. and Rand, R., 1998. "Transition Curves for the Quasi-periodic Mathieu Equation." *Siam J. Appl. Math*, **40**(4), pp. 1094-1115.